

SYNTHESIS, CHARACTERIZATION AND COMPUTATIONAL STUDIES OF 3-
ALKYLBENZOXAZABOROLES

A Thesis

Presented to

The Faculty of the Department of Chemistry

Sam Houston State University

In Partial Fulfillment

of the Requirements for the Degree of

Master of Science

by

Rathnayaka Mudiyansele Chathurika Rathnayaka

August, 2018

SYNTHESIS, CHARACTERIZATION AND COMPUTATIONAL STUDIES OF 3-
ALKYLBENZOXAZABOROLES

by

Rathnayaka Mudiyansele Chathurika Rathnayaka

APPROVED:

Dustin E. Gross, PhD
Thesis Director

Donovan C. Haines, PhD
Committee Member

Darren L. Williams, PhD
Committee Member

John B. Pascarella, PhD
Dean, College of Science and Engineering
Technology

DEDICATION

To my husband, parents, and brother.

ABSTRACT

Chathurika Rathnayaka, Rathnayaka Mudiyansele, *Synthesis, Characterization and Computational Studies of 3-Alkylbenzoxazaboroles*. Master of Science (Chemistry), August, 2018, Sam Houston State University, Huntsville, Texas.

Dioxaboroles, or boronate esters, are widely used to construct organic molecular architectures, such as covalent organic frameworks, due to their dynamic covalent nature. Oxazaboroles are structurally similar to dioxaboroles in which one oxygen atom is replaced by a nitrogen atom. This motif is expected to have overlapping properties of dioxaboroles, but they have yet to be incorporated into molecular architectures. Therefore, there may exist the potential for benzoxazaboroles to be used in the construction of covalent organic frameworks. With the additional valence of the nitrogen atom there is also the possibility of further functionalization and tuning of electronic properties.

Previously, our research group has explored the preliminary synthesis and characterization of several benzoxazaboroles. In the current work we have synthesized several new benzoxazaboroles using 2-(alkylamino)phenols and phenylboronic acid derivatives. bis(Benzoxazaborole)s were synthesized using 2-aminophenol or 2-(alkylamino)phenols and diboronic acids. Characterization of benzoxazaboroles and bis(benzoxazaborole)s was carried out using ^1H NMR, ^{13}C NMR, UV-visible, and fluorescence spectroscopic methods. X-ray crystallographic analysis was also used for structural identification.

Furthermore, dynamic covalent exchange reactions were conducted with 3-(alkyl)benzoxazaboroles and benzodioxaboroles to determine equilibrium constants and Gibbs free energy values for the benzoxazaborole exchange reactions.

Finally, computational calculations of benzoxazaboroles and bis(benzoxazaborole)s were utilized to support and add to the experimental results. This includes calculations of bond lengths, HOMO-LUMO energies, and Gibbs free energy values for benzoxazaborole exchange reactions.

KEY WORDS: Dioxaborole, Boronate ester, Benzoxazaborole, Covalent organic frameworks, Bis(benzoxazaborole).

ACKNOWLEDGEMENTS

This thesis has become a reality with the kind support and help of many individuals. I would like to extend my sincere thanks to all of them.

Foremost, I would like to express special gratitude to my advisor, Dr. Dustin E. Gross, for his guidance, advice, and encouragement toward the completion of this research. Without his guidance and persistent help this thesis would not have been possible.

I would also like to express my gratitude towards committee members, Dr. Donovan C. Haines and Dr. Darren L. Williams for their suggestions toward completing this thesis and for their valuable time. Additionally, I would like to thank Dr. Darren L. Williams for his help with computational chemistry and Dr. Benny E. Arney for his assistance with the NMR spectrometer. I would also like to thank all of the faculty members of the chemistry department for contributing to my success at SHSU and to Mrs. Rachell Haines for her day-to-day help.

In addition, I would like to thank all Gross group members, specifically former group member Sobiya George who initiated preliminary studies related to my research. I would also like to acknowledge the ACS PRF for financial support for this research.

Finally, I would like to thank my beloved and supportive husband, Sanjaya for his advice, guidance, and encouragement through the duration of this work. I would also like to express my gratitude, to my parents for their encouragement and support.

TABLE OF CONTENTS

	Page
DEDICATION	iii
ABSTRACT	iv
ACKNOWLEDGEMENTS	vi
TABLE OF CONTENTS	vii
LIST OF TABLES	ix
LIST OF FIGURES	xi
CHAPTER	
I INTRODUCTION	1
1.1 Nanoporous Polymers	1
1.2 Porous Organic Frameworks	1
1.3 Covalent Organic Frameworks	2
1.4 Dynamic Covalent Chemistry (DC _v C)	5
1.5 Benzoboroles	8
1.6 Aims of this Work	11
II SYNTHESIS AND CHARACTERIZATION OF 3- ALKYLBENZOXAZABOROLES AND BIS(BENZOXAZABOROLE)S	12
2.1 Introduction	12
2.2 Objectives	12
2.3 Results and Discussion	13
2.4 Conclusions	50
2.5 Experimental Section	51

III DYNAMIC COVALENT EXCHANGE: BENZOXAZABOROLES	62
3.1 Introduction.....	62
3.2 Objectives	62
3.3 Results and Discussion	62
3.4 Conclusions.....	78
3.5 Experimental Section	79
IV SUMMARY	84
REFERENCES	86
APPENDIX A – NMR spectra for the synthesized compounds.....	91
APPENDIX B – UV-vis spectra for the synthesized compounds	117
APPENDIX C – Emission spectra for the synthesized compounds	122
APPENDIX D – X-ray crystallographic data.	128
VITA.....	141

LIST OF TABLES

Table	Page
1 ΔG calculation of benzoxazaboroles in gaseous phase.....	30
2 Bond lengths of the center borole ring of 3-(ethyl)benzoxazaborole.	35
3 Bond lengths of the borole ring of bis(benzoxazaborole)s.	38
4 Conformational analysis of benzoxazaboroles 6a , 9a and 10a	39
5 Conformational analysis of bis(benzoxazaborole)s	39
6 Absorption and emission data for benzoxazaboroles in CHCl_3	44
7 Absorption and emission data for bis(benzoxazaborole)s in CHCl_3	46
8 HOMO and LUMO energy values of benzoxazaboroles and bis(benzoxazaborole)s.....	49
9 Equilibrium constants, calculated using the integral values for protons H_a and H_b of 6c and 22	70
10 Equilibrium constants, calculated using the integral values for protons H_c and H_d of 6c and 4c	70
11 Equilibrium constants, calculated using the integral values for protons H_a and H_b of 9b and 23	73
12 Equilibrium constants, calculated using the integral values for protons H_c and H_d of 9b and 4b	74
13 Equilibrium constants, calculated using the integral values for protons H_a and H_b of 22 and 6b	77
14 Equilibrium constants, calculated using the integral values for protons H_c and H_d of 6b and 4b	77

15	Amount of 3-decyl-2-phenyl-1,3,2-benzoxazaborole (6c) and catechol (21) used in each experiment.....	81
16	Amount of 2-(4-bromophenyl)-3-butyl-1,3,2-benzoxazaborole (9b) and catechol (21) used in each experiment.....	82
17	Amount of 2-phenyl-1,3,2-benzodioxaborole (22) and 2- (butylamino)phenol (4b) used in each experiment.	83

LIST OF FIGURES

Figure	Page
1 Formation of COF-1 via the self-condensation reaction of BDBA.	2
2 Formation of COF-5 via the co-condensation reaction of BDBA and HHTP.	3
3 Formation of DBLP via the condensation of 1,3,5-benzenetris-(4-phenylboronic acid) (BTPA) and HATT.	4
4 Dynamic combinatorial library.	5
5 Dynamic covalent a) olefin and b) alkyne metathesis reaction.	6
6 Dynamic covalent a) imine formation, b) transimination, and c) imine metathesis.	7
7 Dynamic covalent disulfide exchange reaction.	7
8 Formation of a) dioxaborole and b) diazaborole.	8
9 Types of phenyl benzoboroles.	8
10 Formation of oxazaborole from a 2-aminoalcohol and boronic acid.	9
11 Synthesis of 2-phenyl-1,3,2-benzoxazaborole.	9
12 The potential formation of a) oxazoline and b) imine.	9
13 Formation of benzoxazaborole from diisopropyl phenylboronate.	10
14 Formation of <i>N,N'</i> -[1,3-propane-bis-[2-phenyl-(benzoxazaborolidine)]].	10
15 Synthesis of 3-(alkyl)benzoxazaboroles.	11
16 Structure of 3-(alkyl)benzoxazaborole.	12
17 Synthesis of benzoxazaborole 3 using 2-aminophenol (2) and phenylboronic acid (1).	13
18 ¹ H NMR spectrum of benzoxazaborole 3 obtained from toluene reflux.	13

19	¹ H NMR spectrum of the formation of benzoxazaborole 3 in THF.	14
20	Formation of boroxine 1a	14
21	Partial ¹ H NMR spectra for the synthesis of benzoxazaborole in THF.	15
22	Synthesis of benzoxazaborole 3 in THF.	16
23	Percent formation of benzoxazaborole 3 over time.	17
24	Partial ¹ H NMR spectra for the synthesis of benzoxazaborole in THF- <i>d</i> ₈	18
25	Percent formation of benzoxazaborole 3 over time.	19
26	¹ H NMR spectra of a) 1:1 mixture of 2-aminophenol (2) and phenylboronic acid (1), and b) benzoxazaborole 3 in DMSO- <i>d</i> ₆	20
27	Synthesis of 2-(alkylamino)phenols 4a-c	21
28	¹ H NMR spectrum of the crude reaction mixture containing 4a and 5a in CDCl ₃	21
29	¹ H NMR spectrum of purified 2-(ethylamino)phenol (4a) in CDCl ₃	22
30	Formation of 3-alkyl-2-phenyl-1,3,2-benzoxazaboroles (6a-c).	22
31	¹ H NMR spectra of a) 2-(ethylamino)phenol (4a), b) phenylboronic acid/boroxine (1/1a), and c) 3-ethyl-2-phenyl-1,3,2-benzoxazaborole (6a) in CDCl ₃	23
32	Synthesis of benzoxazaboroles 9 and 10 using 4-bromophenylboronic acid (7) and 4-methoxyphenylboronic acid (8).	24
33	¹ H NMR of 2-(4-bromophenyl)-3-butyl-1,3,2-benzoxazaborole (9b).	25
34	Formation of bis(benzoxazaborole) 12	26
35	Synthesis of bis(benzoxazaborole)s using arylene diboronic acids.	27
36	¹ H NMR spectrum of bis(benzoxazaborole) 17 in CDCl ₃	28

37	¹ H NMR spectra of a) 2,5-thiophenediyl-bis-[3-(ethyl)benzoxazaborole] (17a), b) 9,9-dihexylfluorene-2,7-bis-[3-(ethyl)benzoxazaborole] (19a), c) 1,4-phenylene-bis-[3-(ethyl)benzoxazaborole] (13b), and d) biphenyl-4-4'-bis-[3-(ethyl)benzoxazaborole] (15b) in CDCl ₃ .	29
38	Reaction vial containing 15a in dichloromethane and layered with pentane.	32
39	X-ray crystal structure of bis(benzoxazaborole) 13a a) single and b) packing.	33
40	X-ray crystal structure of bis(benzoxazaborole) 15a .	33
41	The structural framework of benzoxazaborole.	34
42	Electrostatic potential maps of benzoxazaboroles and bis(benzoxazaborole)s.	41
43	Absorption spectra of phenylboronic acid (1), 2-(ethylamino)phenol (4a), and benzoxazaborole 6a in CHCl ₃ .	43
44	Normalized emission spectra of phenylboronic acid (1), 2-(ethylamino)phenol (4a), and benzoxazaborole 6a in CHCl ₃ .	44
45	Top views of the highest-occupied and lowest-unoccupied molecular orbitals of 6a , 9b , and 10b .	47
46	Top views of the highest-occupied and lowest-unoccupied molecular orbitals of 12 , 15 , 19 , 19a , 20 , and 20a .	48
47	Reaction of benzoxazaborole 6b and 2-(ethylamino)phenol (4a).	62
48	¹ H NMR spectra of a) the reaction mixture of 3-butyl-2-phenyl-1,3,2-benzoxazaborole (6b) and 2-(ethylamino)phenol (4a), b) pure 3-butyl-2-phenyl-1,3,2-benzoxazaborole (6b), c) pure 3-ethyl-2-phenyl-1,3,2-benzoxazaborole (6a), d) pure 2-(butylamino)phenol (4b), and e) pure 2-(ethylamino)phenol (4a) in CDCl ₃ .	64

49	Reaction of 3-decyl-2-phenyl-1,3,2-benzoxazaborole (6c) with catechol (21). ...	65
50	¹ H NMR spectra of a) the 1:1 reaction mixture of 6c and 21 , b) benzodioxaborole 22 , c) 3-decyl-1,3,2-benzoxazaborole (6c), d) 2-(decylamino)phenol (4c), and e) catechol (21) in CDCl ₃	66
51	¹ H NMR spectra the for reaction of 3-decyl-2-phenyl-1,3,2-benzoxazaborole (6c) and catechol (21).	67
52	Exchange reaction of 2-(4-bromophenyl)-3-butyl-1,3,2-benzoxazaborole (9b) and catechol (21).....	71
53	¹ H NMR spectra for the reaction of 2-(4-bromophenyl)-3-butyl-1,3,2-benzoxazaborole (9b) and catechol (21) in a 2:1, 1:1, and 1:2 ratio.	72
54	Exchange reaction of benzodioxaborole (22) and 2-(butylamino)phenol (4b). ...	75
55	¹ H NMR spectra for the reaction of benzodioxaborole (22) and 2-(butylamino)phenol (4b) in a 2:1, 1:1, and 1:2 ratio.....	76

CHAPTER I

Introduction

1.1 Nanoporous Polymers

Nanoporous materials are composed of regular inorganic or organic structures with 0.2 nm to 50 nm range pores. Three subcategories of these solids are zeolites, metal organic frameworks (MOFs), and porous organic frameworks (POFs). Zeolites are inorganic, crystalline aluminosilicates with uniform sized pores.¹ MOFs are often rigid crystalline porous coordination polymers (PCPs), containing metal ions or clusters and organic bridging units.^{1,2} Zeolites and MOFs are used as adsorbents, storage/separation materials, catalysts, in optical/magnetic devices, and in chemical sensors due to their specific properties such as well-defined pores, high surface areas, unique surface properties, and adsorption affinity.^{3,4}

1.2 Porous Organic Frameworks

POFs are rigid structures with distinctive properties such as ordered uniform pores with high surface area, high π -electron density, exceptionally high thermal stability (up to 600 °C), and low framework density. These materials are connected via strong covalent bonds such as C-C, C-N, and B-O.^{3,5} The void space or the porosity is formed through and affected by the polymerization of monomers. These properties have opened doors in areas of inclusion, host-guest, molecular manipulation, and reaction chemistry.³ They also have led to functional applications such as adsorption,⁶ catalysis, and sensing.^{3,5,7-10}

1.3 Covalent Organic Frameworks

In contrast to inorganic nanoporous solids, such as zeolites and MOFs, it is difficult to synthesize POFs with homogeneous, permanent porosity. Covalent organic frameworks (COFs) are types of POFs that are highly crystalline materials with regioregularity. Depending on the molecular arrangement, COFs are classified as two or three-dimensional.

2D COFs are obtained by linking linear, triangle, or square-shaped planar segments, which assemble into periodic layered networks via π -electron interactions. In 2005, Yaghi and coworkers reported the first 2D COF materials, COF-1 (Figure 1) and COF-5 (Figure 2).⁵ Boroxine formation is the foundation for the synthesis of COF-1, which is constructed through the self-condensation reaction of benzene diboronic acid (BDDBA).⁵ Boronate ester based COF-5 was synthesized by the co-condensation reaction of BDDBA and hexahydroxy triphenylene (HHTP).

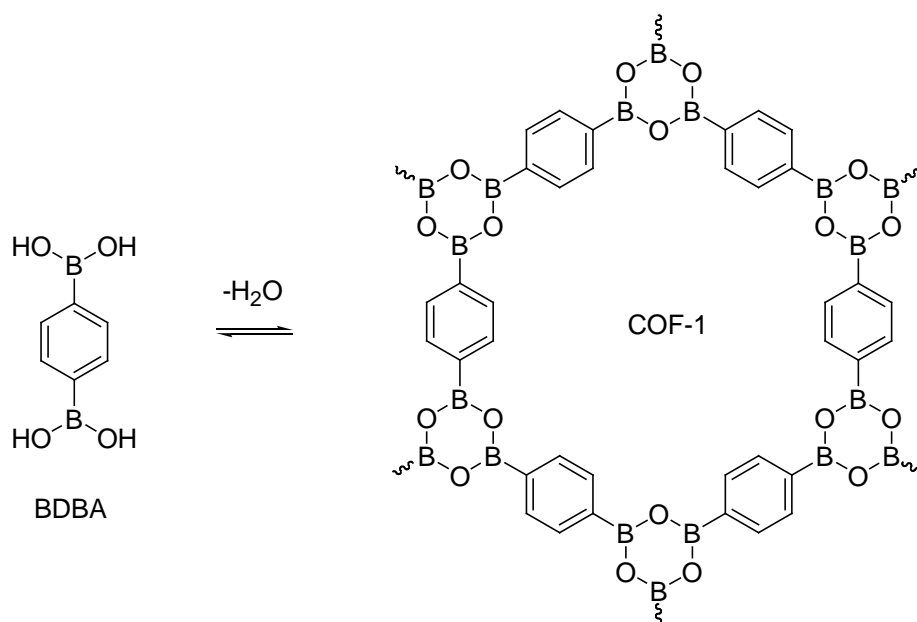


Figure 1. Formation of COF-1 via the self-condensation reaction of BDDBA.

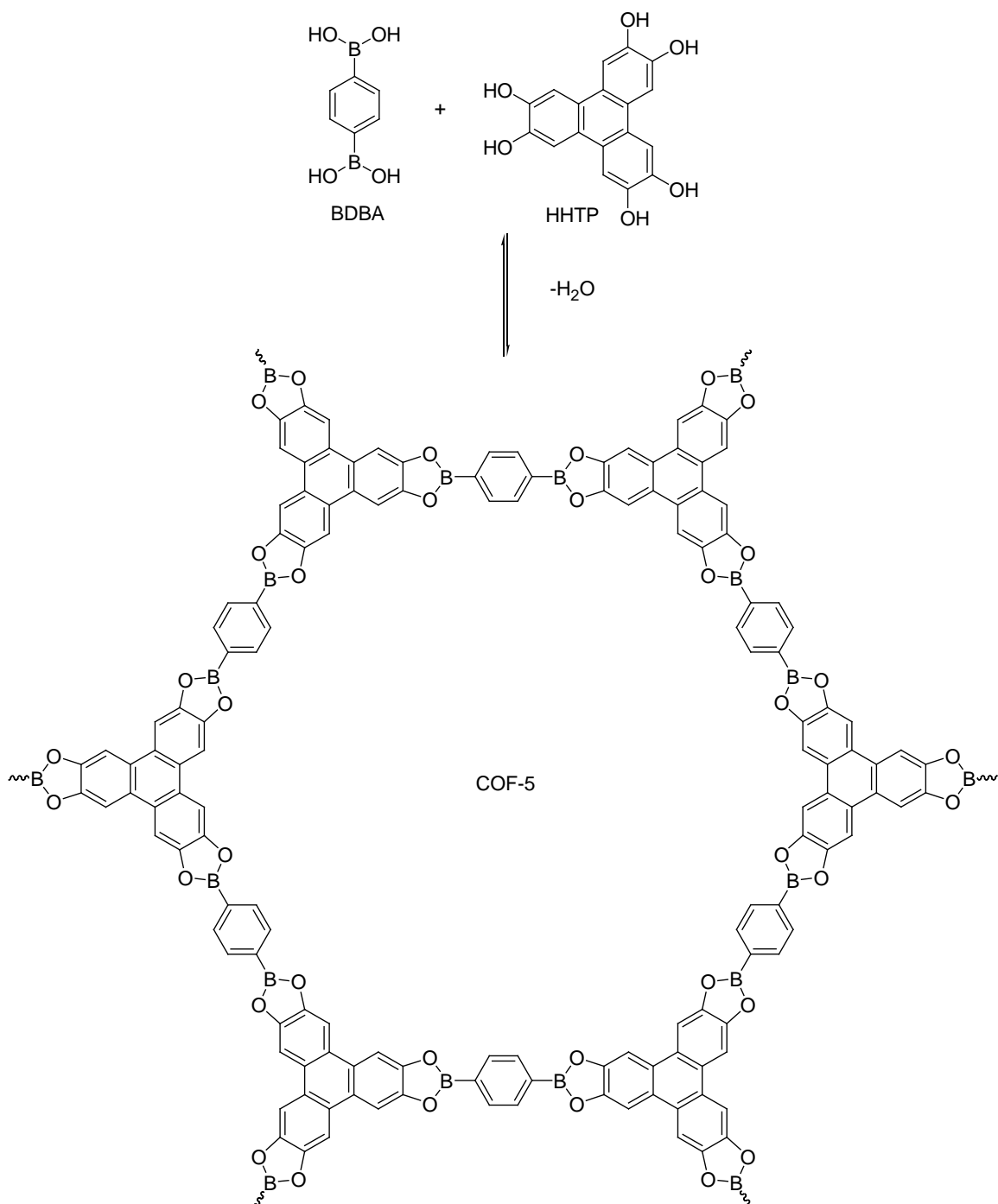


Figure 2. Formation of COF-5 via the co-condensation reaction of BDBA and HHTP.

3D frameworks are constructed by connecting tetrahedral or square shaped building units geometries with planar, triangular, or square shaped secondary building

units. The pioneering work on the design and synthesis of 3D COFs has also been achieved by Yaghi and coworkers.¹¹

The synthesis of B-N bond containing polymers is becoming an interesting area of research. To date, there are only few examples of B-N linked polymers. Recently three diazaborole-linked polymers (DBLPs) were formed through the condensation reactions using 2,3,6,7,14,15-hexaaminotriptycene (HATT) and aryl boronic acids (Figure 3). They have shown promising optical properties and potential for gas storage/separation.¹²

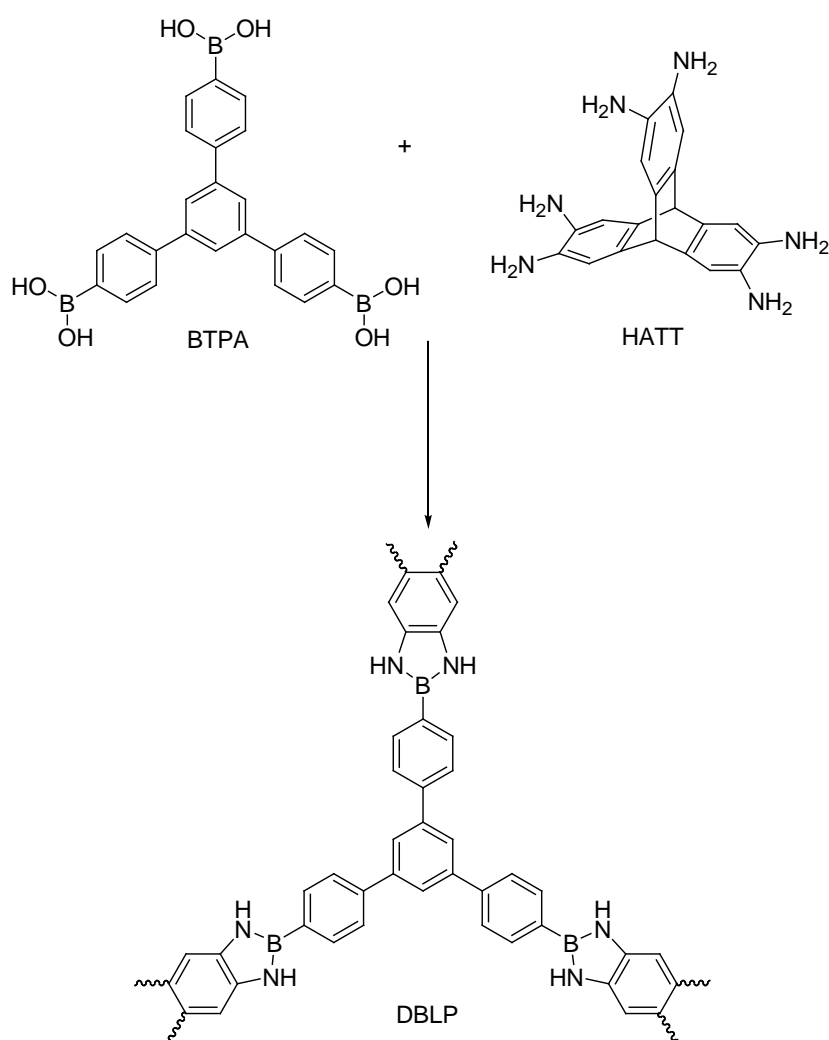


Figure 3. Formation of DBLP via the condensation of 1,3,5-benzenetris-(4-phenylboronic acid) (BTPA) and HATT.

1.4 Dynamic Covalent Chemistry (DC_vC)

The synthesis of regioregular COFs has required reversible reactions, which are related to dynamic covalent chemistry (DC_vC).¹³ A library of reversibly exchanging building blocks generated through dynamic combinatorial chemistry (DCC) is called a dynamic combinatorial library (DCL) (Figure 4). The exchange of building blocks can involve covalent bonds (DC_vC) or noncovalent bonds (supramolecular).^{14,15}

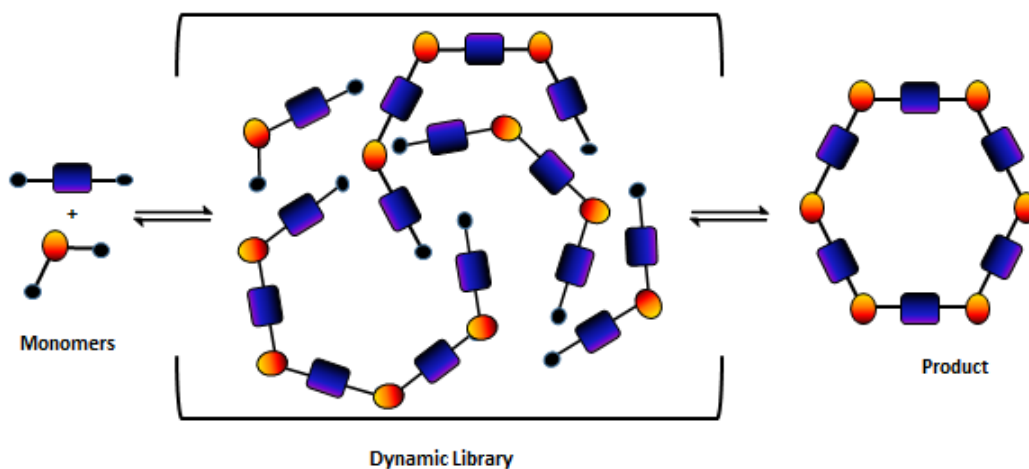


Figure 4. Dynamic combinatorial library.

DC_vC involves reversible covalent reactions that allow free exchange of molecules to form thermodynamically stable products at equilibrium.^{13,16} This reversible formation and breaking of strong covalent bonds results in the capability of “error-checking” and “proofreading”.¹⁷ DC_vC has been widely explored in useful applications such as drug discovery, biotechnology, molecular separation, light harvesting, gas adsorption/separation, host-guest chemistry, and nanocomposite fabrication.

Dynamic covalent reactions (DCR) involve covalent bonds such as C-C, C-N, C-O, C-S, S-S, and B-O. There are two principle classes of DCR. There are reactions that involve the formation of new bonds,¹⁴ and there are exchange reactions, where reaction partners exchange groups and result in the same type of bond. Directional unsymmetrical dynamic bonds such as C=N and B-O need to combine two different functional groups while symmetric bonds such as carbon-carbon double and triple bonds involve self exchange.¹⁶

Transition metal catalyzed metathesis reactions such as alkyne metathesis and olefin metathesis exhibit dynamic covalent nature. These reactions have been used to obtain high yields of shape-persistent arylene ethynylene macrocycles. In olefin metathesis, reaction partners on C=C double bonds are subjected to exchange in the presence of a transition metal catalyst (Figure 5a).¹⁸ Alkyne metathesis involves the dynamic exchange of alkylidyne units between two acetylenes (Figure 5b).¹⁹ Eventhough alkyne metathesis is a reversible process, its use is limited due to the lack of availability of catalysts that do not require stringent air and moisture free conditions.

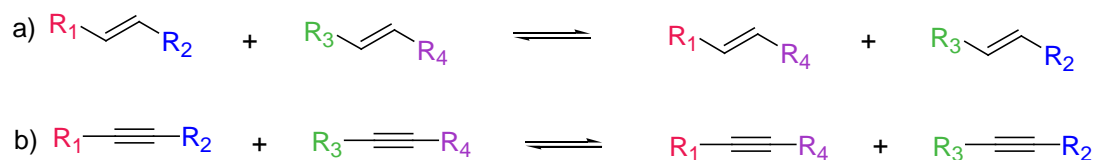


Figure 5. Dynamic covalent a) olefin and b) alkyne metathesis reaction.

Dynamic covalent C-N bonds, present in imines, hydrazones, and oximes, are widely used in the synthesis of 2D and 3D molecular architectures including covalent organic frameworks (Figure 6).^{20,21}

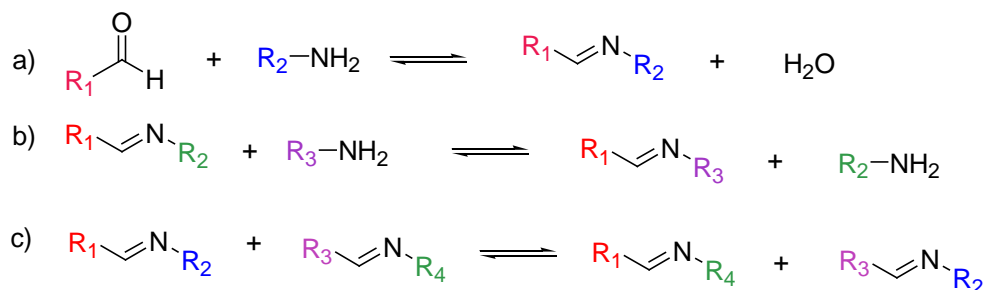


Figure 6. Dynamic covalent a) imine formation, b) transimination, and c) imine metathesis.

Dynamic covalent disulfide exchange reactions are among earliest reactions that have been investigated in DC_vC research (Figure 7).²²



Figure 7. Dynamic covalent disulfide exchange reaction.

Of interest for this thesis are dynamic covalent bonds based on boron. Boronic acids undergo esterification reactions with diols to form boronic esters or boronates (Figure 8a). Generally, boron forms compounds with an sp^2 hybridized B atom and trigonal planar geometry due to the presence of six valence electrons and deficiency of two electrons. Boronic acids are trivalent boron containing organic compounds that have two hydroxyl groups and one aryl on B-C bond. The reactivity and properties of boronic acids depends upon the type of carbon group directly bonded to the boron atom and they are classified as alkyl-, alkynyl-, and aryl- boronic acids. Boronic acids are considered as mild organic Lewis acids due to presence of vacant P orbital in boron atom. Moreover, they are considered “green” compounds due to lower toxicity than most organoboranes and their ultimate degradation to environmentally friendly boric acid.²³

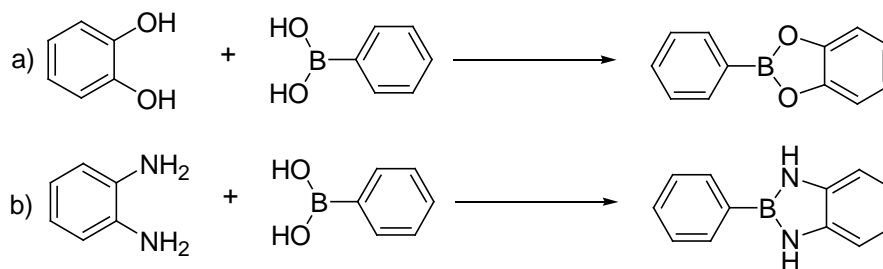


Figure 8. Formation of a) dioxaborole and b) diazaborole.

1.5 Benzoboroles

Diazaboroles (Figure 8b) are formed by reacting a 1,2-diamine with a boronic acid. Most of COF syntheses have relied on dioxaborole linkages,⁵ and there has been one example having diazaborole linkages (Figure 3).¹² Oxazaboroles are structurally analogous to dioxaboroles and diazaboroles, yet there is a lack of research regarding benzoxazaborole materials (Figure 9).

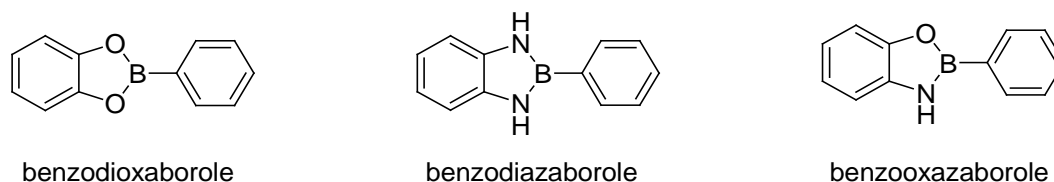


Figure 9. Types of phenyl benzoboroles.

Oxazaboroles may also possess dynamic covalent nature similar to diazaboroles and dioxaboroles, which may allow them to be used in synthesis of shape persistent macrocycles or covalent organic frameworks. It is believed that oxazaborole based COFs would exhibit similar properties as diazaboroles and dioxaborole based COFs.

Oxazaboroles can be synthesized via a condensation reaction between a boronic acid and an unsaturated 2-aminoalcohol (Figure 10). Successful formation of the product is achieved by the elimination of water.

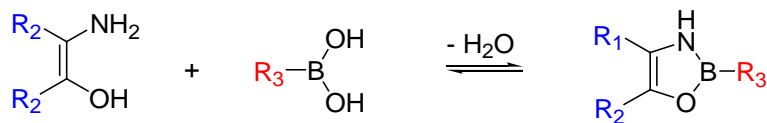


Figure 10. Formation of oxazaborole from a 2-aminoalcohol and boronic acid.

The synthesis of 2-phenyl-1,3,2-benzoxazaborole was first reported in 1958 by Dewar and coworkers.²⁴ Benzoxazaborole was obtained by heating a solution of *o*-aminophenol with phenylboron dichloride (Figure 11). They obtained a good yield of crystalline product that was soluble in benzene, ether, and chloroform.²⁴

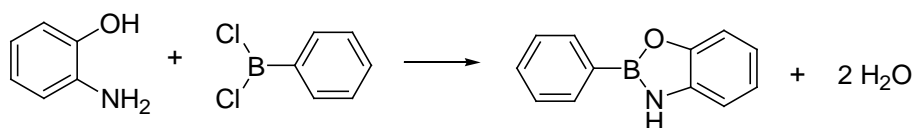


Figure 11. Synthesis of 2-phenyl-1,3,2-benzoxazaborole.

In 1958, the synthesis of oxazaborole was attempted by Sugihara and coworkers.²⁵ An aminoalcohol or aminophenol and benzene boronic acid were refluxed for 4 hours in anhydrous acetone to obtain the product. Thereafter, acetone was removed under reduced pressure on a steambath. The product formation was not successful, and it was reported to be unstable. It is likely that acetone reacted with the aminophenol to form imines or oxazoline compounds (Figure 12).

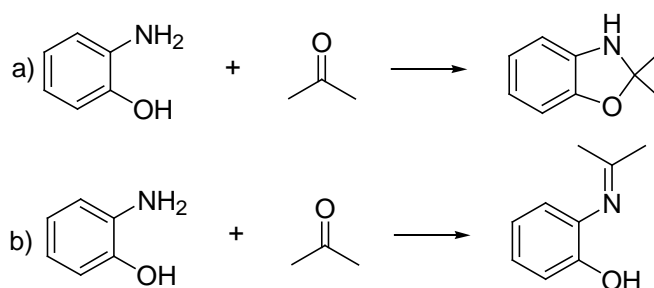


Figure 12. The potential formation of a) oxazoline and b) imine.

Brotherton and Steinberg reported a separate study in 1961, which resulted in a good yield of 2-phenyl-1,3,2-benzoxazaborole from refluxing 2-aminophenol and diisopropyl phenylboronate (Figure 13).²⁶

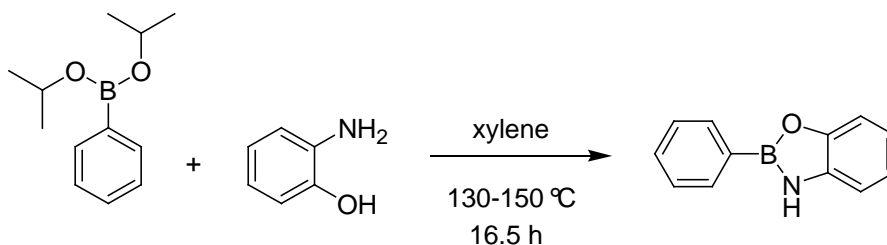


Figure 13. Formation of benzoxazaborole from diisopropyl phenylboronate.

A few years back the synthesis and characterization of an alkyl-linked bisoxazaborole was accomplished by Barba and coworkers.²⁷ The formation of product was achieved by refluxing 2,2-(1,3-propanediamine)bisphenol with two equiv of phenylboronic acid in xylene (Figure 14).

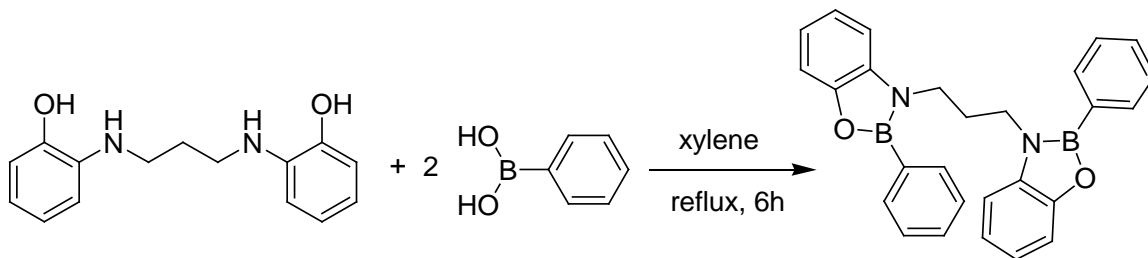


Figure 14. Formation of *N,N'*-[1,3-propane-bis-[2-phenyl-(benzoxazaborolidine)]].

Recently, Sobiya George, a former research group member synthesized and characterized several benzoxazaboroles, including several alkyl benzoxazaboroles from 2-(alkylamino)phenols (Figure 15).²⁸

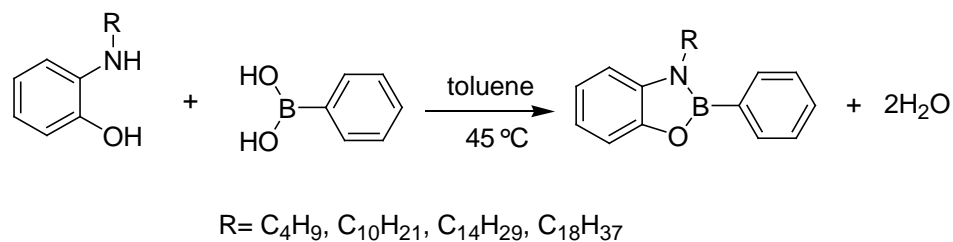


Figure 15. Synthesis of 3-(alkyl)benzoxazaboroles.

1.6 Aims of this Work

The overarching goal of this work is to synthesize oxazaborole based materials. First the direct synthesis of benzoxazaborole will be carried out in different solvents. Then synthesis and spectroscopic characterization of 3-(alkyl)benzoxazaborole derivatives and alkyl bis(benzoxazaborole)s will be carried out. A computational study of benzoxazaboroles and bis(benzoxazaborole)s will be carried out to obtain optimum geometries, electrostatic potential maps, HOMO-LUMO energies, and thermodynamics of the formation of benzoxazaboroles. The dynamic covalent nature of benzoxazaboroles and benzodioxaboroles will be investigated. Finally, equilibrium constant values and Gibbs free energy values of benzoborole exchange reactions will be calculated both experimentally and computationally.

CHAPTER II

Synthesis and Characterization of 3-alkylbenzoxazaboroles and bis(benzoxazaborole)s

2.1 Introduction

The direct synthesis of benzodioxaboroles²⁹ and benzodiazaboroles³⁰ in CDCl₃ has been reported. The synthesis of benzoxazaborole in CDCl₃ was attempted by former group member, Sobiya George which was not successful due to the low solubility of 2-aminophenol. The solubility problem of 2-aminophenol can be overcome by alkylation of N atom, and the synthesis of benzoxazaboroles with 2-(alkyl)aminophenols is possible (Figure 16).

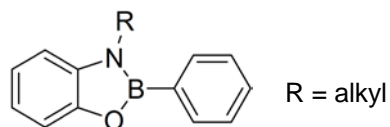


Figure 16. Structure of 3-(alkyl)benzoxazaborole.

Benzodioxaborole and benzodiazaborole based polymers or macrocycles are synthesized by condensation reaction between diboronic acid with a tetraol or tetraamine.^{5,12} For the synthesis of bis(benzoxazaborole)s, aminophenols may be reacted with diboronic acids.

2.2 Objectives

The objectives of this study were to i) synthesize benzoxazaborole and bis(benzoxazaborole) derivatives using condensation reactions of various phenylboronic acids or arylene diboronic acids and 2-(alkylamino)phenols and ii) characterize the new compounds using ¹H NMR, ¹³C NMR, fluorescence, and UV-vis spectroscopic methods, X-ray crystallography, and computational methods.

phenylboronic acid (**1**) were dissolved in THF, and the solvent was removed under reduced pressure at room temperature. The ^1H NMR spectrum of the product indicated that the reaction did not go to completion (Figure 19).

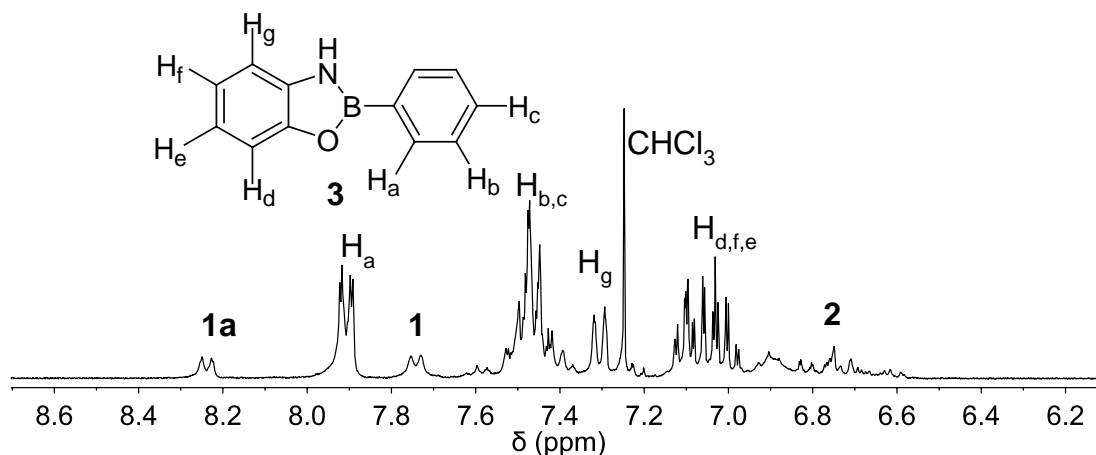


Figure 19. ^1H NMR spectrum of the formation of benzoxazaborole **3** in THF. ^1H NMR in CDCl_3 .

The spectrum showed evidence of formation of the product, along with remaining starting materials, 2-aminophenol (**2**), phenylboronic acid (**1**), and boroxine **1a**, the self condensation product of phenylboronic acid **1** (Figure 20). This result indicates that THF might be a suitable method to synthesize benzoxazaborole **3** under mild conditions.

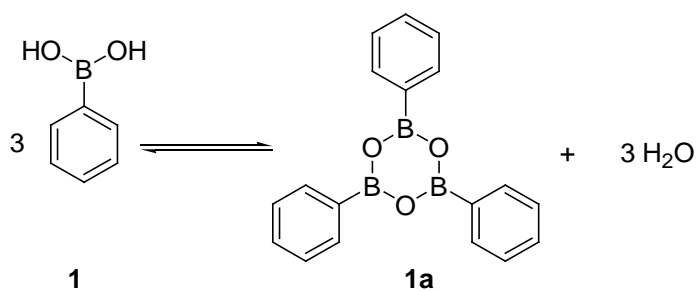


Figure 20. Formation of boroxine **1a**.

Next, the direct synthesis of benzoxazaborole **3** was attempted in deuterated THF ($\text{THF-}d_8$) for direct analysis by NMR. Initially, phenylboronic acid (**1**) was dissolved in

THF- d_8 in an NMR tube. ^1H NMR analysis showed the major component was boroxine **1a** ~8.2 ppm (Figure 21).

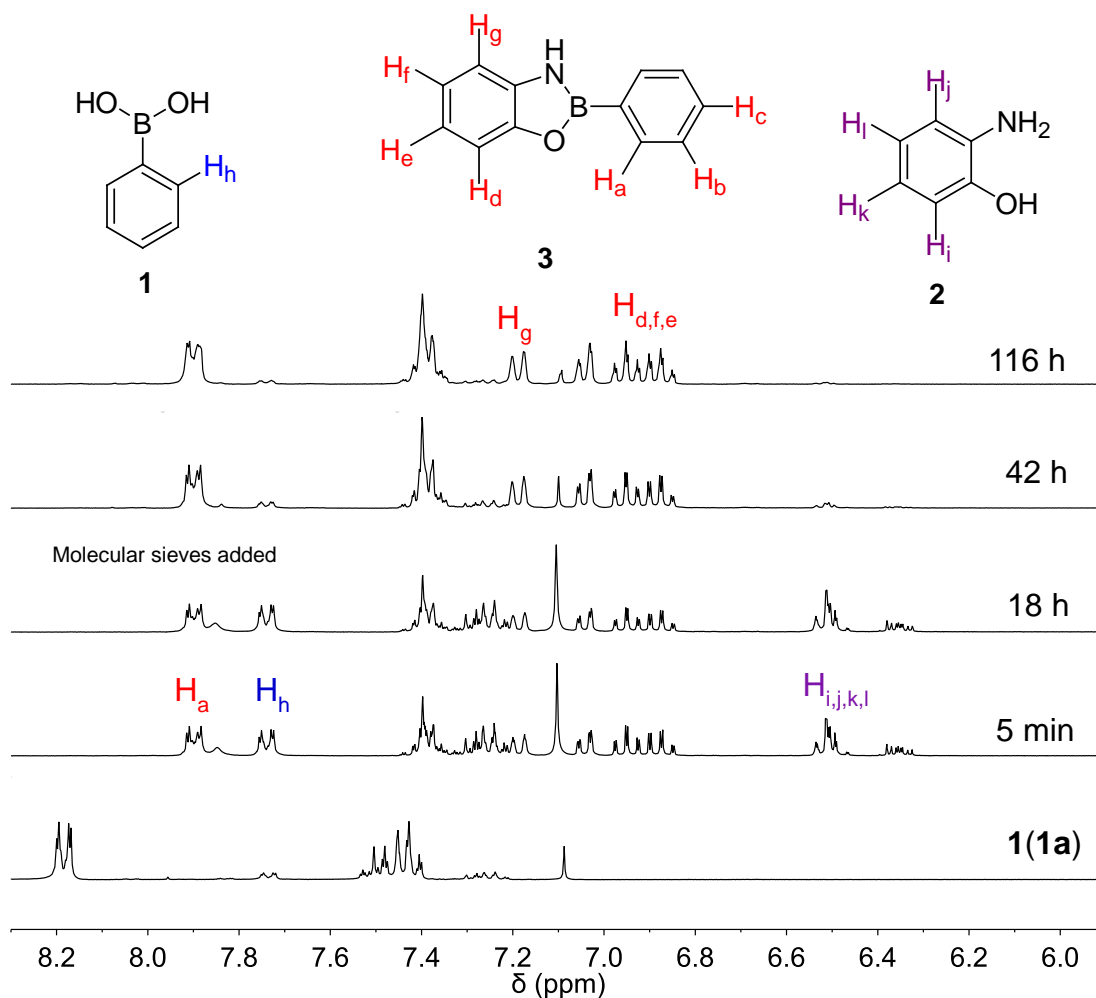


Figure 21. Partial ^1H NMR spectra for the synthesis of benzoxazaborole in THF.

After adding 1 equiv of 2-aminophenol (**2**), ^1H NMR analysis provided evidence of formation of benzoxazaborole **3**. However the starting materials were only partially converted to benzoxazaborole **3**. After analysis of the ^1H NMR and the corresponding signal integrals, the following scheme is proposed (Figure 22).

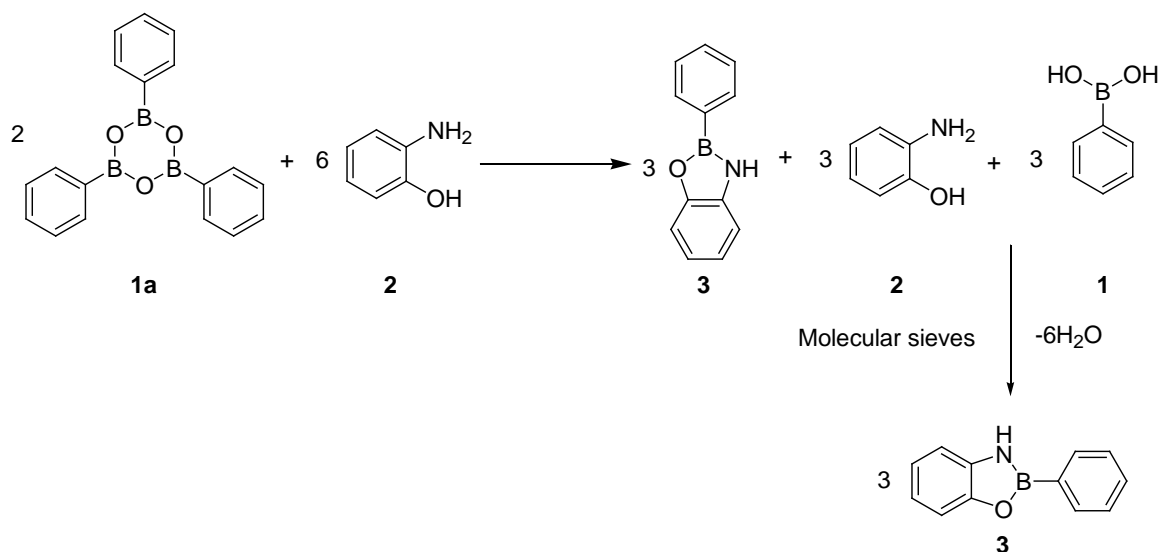


Figure 22. Synthesis of benzoxazaborole **3** in THF.

Initially, 2 equiv of boroxine **1a** react with 3 equiv of the 2-aminophenol (**2**) to form 3 equiv of benzoxazaborole **3** and 3 equiv of phenylboronic acid (**1**) (Figure 22a). After 18 hours, there was no change and two beads of molecular sieves were added (Figure 22). The purpose of adding molecular sieves is to shift the equilibrium of reaction towards formation of benzoxazaborole **3** by removing water from the system. ¹H NMR spectra were obtained over time and the remaining aminophenol **2** and phenyl boronic acid (**1**) were converted to benzoxazaborole **3** (Figure 23).

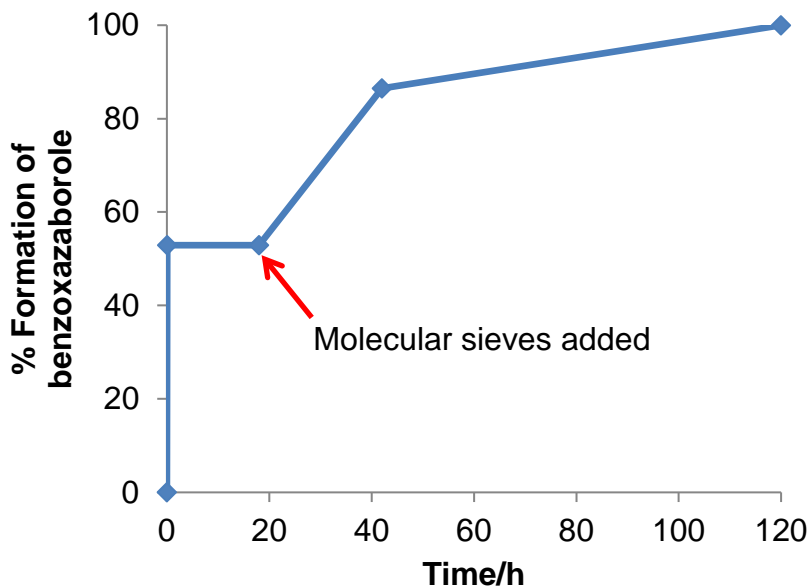


Figure 23. Percent formation of benzoxazaborole **3** over time.

Next, the direct synthesis of benzoxazaborole **3** was carried out in THF- d_8 with adding the molecular sieves at the beginning. The phenylboronic acid (**1**) used for this experiment, was obtained from another commercial source and it did not contain boroxine **1a** only phenylboronic acid **1** was present. This was determined by the presence of signals at ~ 7.7 ppm (Figure 24). After adding 1 equiv of 2-aminophenol (**2**) 50% conversion was achieved. Molecular sieves were added and the reaction progress was monitored over time by NMR.

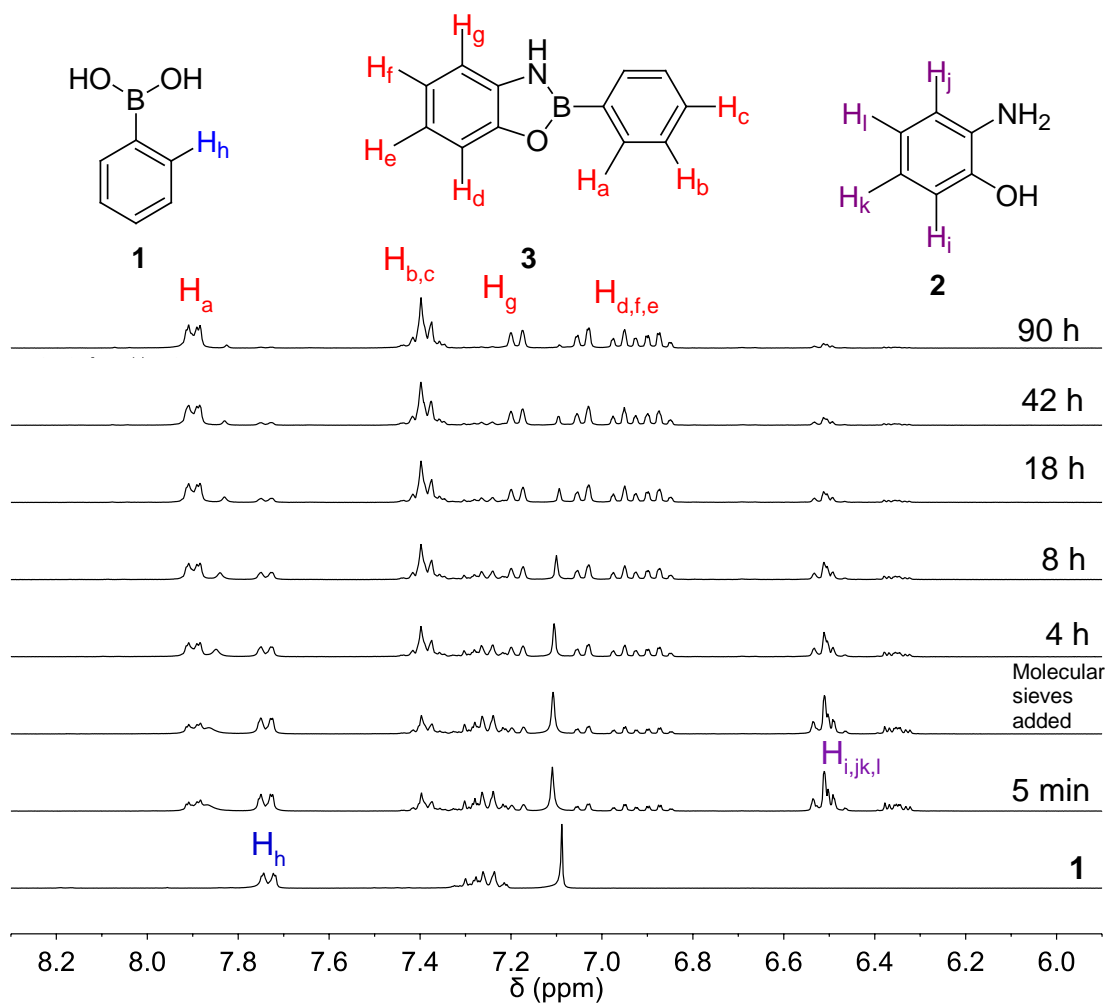


Figure 24. Partial ^1H NMR spectra for the synthesis of benzoxazaborole in $\text{THF-}d_8$.

The complete conversion of starting materials, phenylboronic acid (**1**) and 2-aminophenol (**2**), to benzoxazaborole **3** was achieved after 90 h (Figure 25). Interestingly, when the sample was checked after 10 days (240 h) ^1H NMR analysis showed an increase phenylboronic acid (**1**) and 2-aminophenol (**2**). This is likely due to absorption of moisture from the atmosphere and subsequent hydrolysis of benzoxazaborole **3**. Although the formation of **3** was successful the long reaction time forced us to look into other solvents.

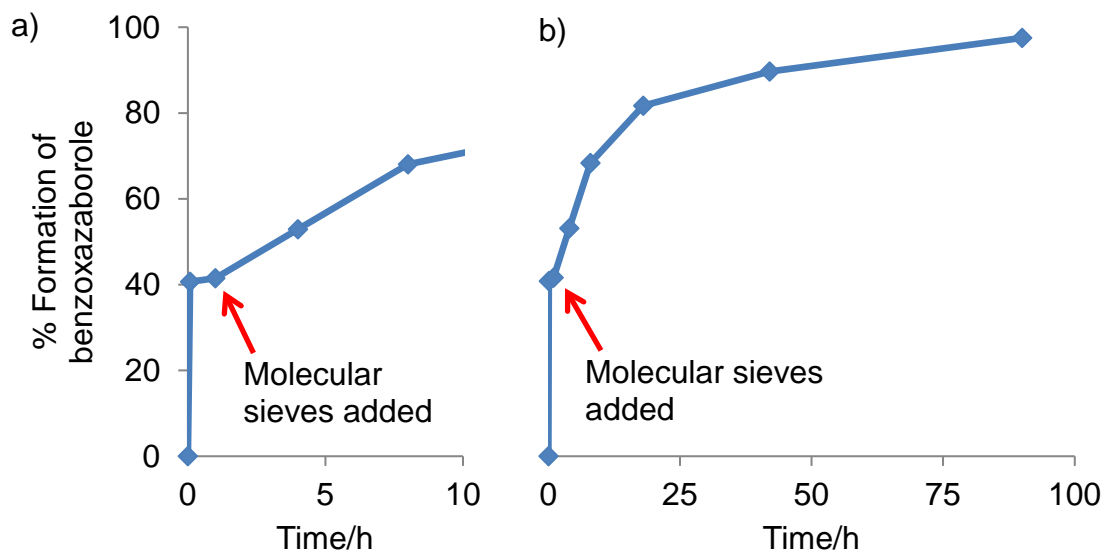


Figure 25. Percent formation of benzoxazaborole **3** over time. a) 0-10 min and b) 0-100 min.

Next, the direct mixing 2-aminophenol (**2**) and phenylboronic acid (**1**) in DMSO- d_6 at room temperature was attempted (Figure 26a). The ^1H NMR spectrum was compared to an ^1H NMR spectrum of pure benzoxazaborole **3** (Figure 26b). The direct synthesis of benzoxazaboroles showed evidence of product formation; however, the reaction did not go to completion even after one week. Additionally, in the ^1H NMR spectrum of benzoxazaborole **3** hydrolysis products (**1** and **2**) were present. We also hypothesize the presence of **3a** (Figure 26b). The changes in each of the NMR spectra were caused by the presence of water in DMSO- d_6 . This provides further evidence of the effect of water on the characterization and synthesis of benzoxazaborole in polar hygroscopic solvents.

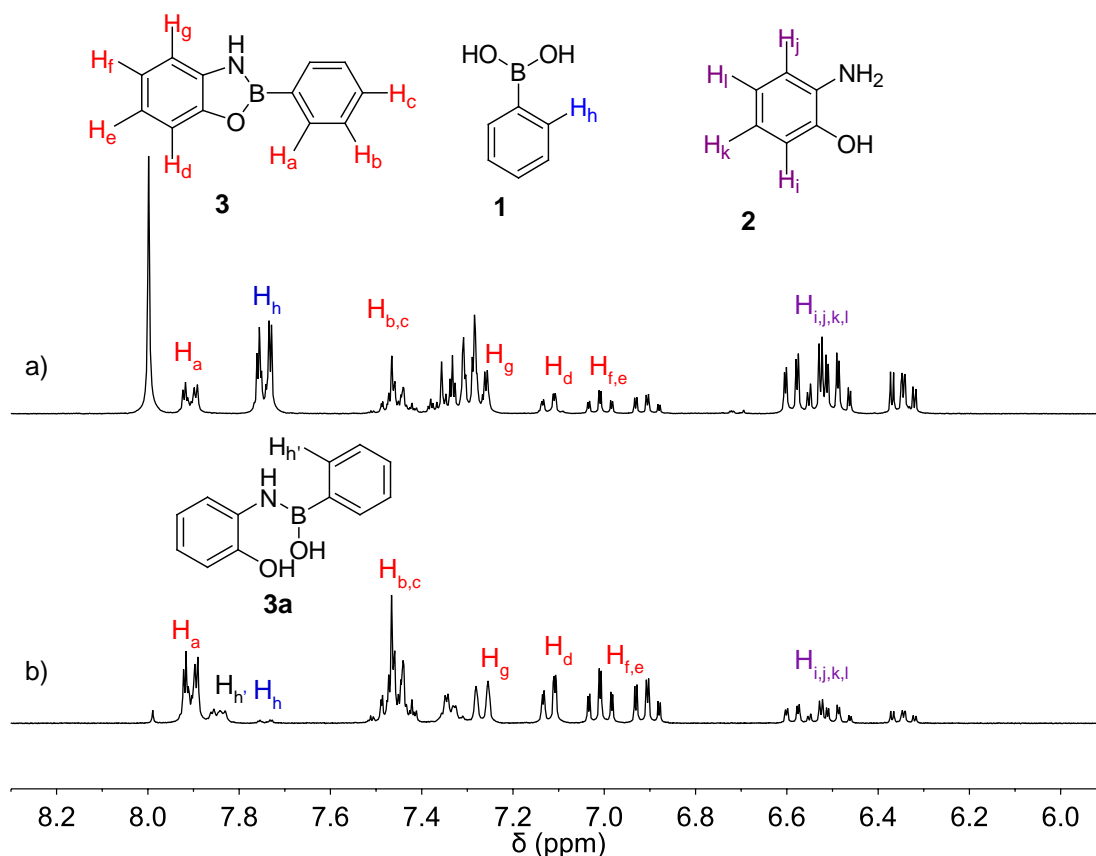


Figure 26. ^1H NMR spectra of a) 1:1 mixture of 2-aminophenol (**2**) and phenylboronic acid (**1**), and b) benzoxazaborole **3** in $\text{DMSO-}d_6$.

After synthesizing benzoxazaborole **3** in several solvents the synthesis of 3-(alkyl)benzoxazaboroles was carried out in CDCl_3 , which seems to be the best solvent for benzoxazaborole formation.

2.3.2 Synthesis of 2-(alkylamino)phenols (4a-c). Similar to our previous work²⁸ and literature methods^{27,31} 2-(alkylamino)phenols (**4a-c**) were synthesized via the reaction of 2-aminophenol (**2**) and an alkyl halide. Three different 2-(alkylamino)phenols (**4a-c**) were synthesized using iodoethane, 1-bromobutane, and 1-bromodecane (Figure 27). All three reaction mixtures contained two major products, (monoalkylamino)phenol **4** and (dialkylamino)phenol **5** as observed by ^1H NMR and TLC (Figure 28).

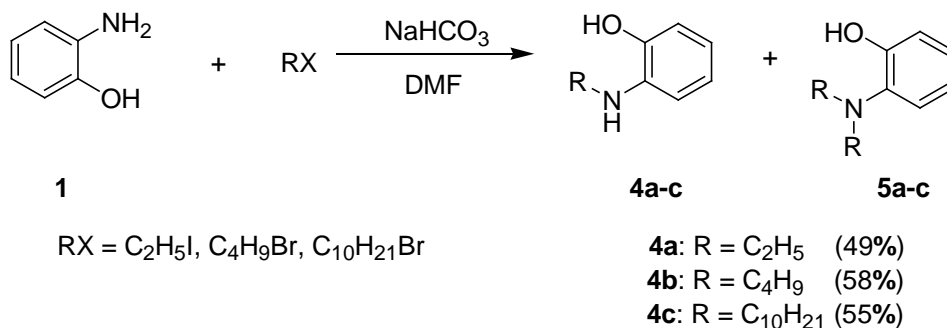


Figure 27. Synthesis of 2-(alkylamino)phenols **4a-c**.

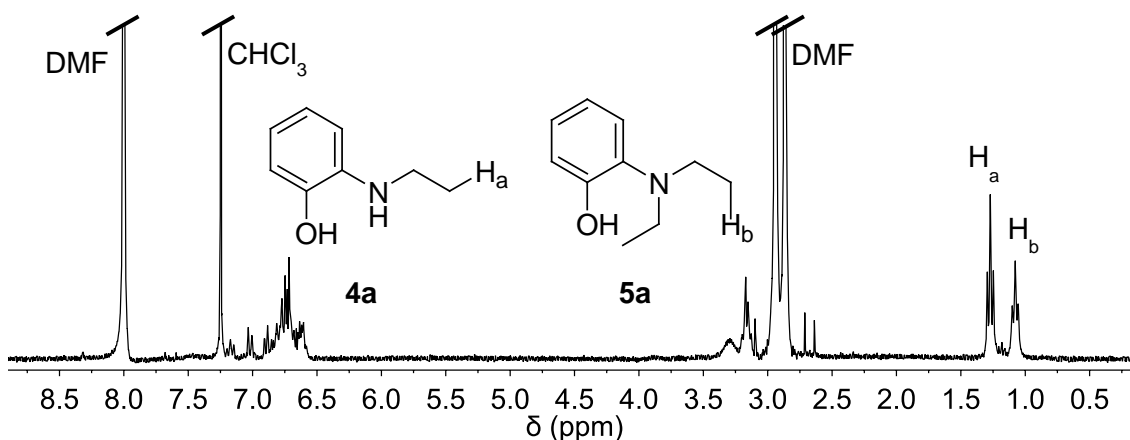


Figure 28. ¹H NMR spectrum of the crude reaction mixture containing **4a** and **5a** in CDCl₃.

The target 2-(alkylamino)phenols (**4a-c**) were purified and isolated (50-60% yield) using silica gel column chromatography with EtOAc:hexanes as the eluent. ¹H NMR spectroscopy was used to confirm the identity and purity of the products (Figure 29). All three 2-(alkylamino)phenols (**4a-c**) were readily soluble in CDCl₃. This is in contrast to 2-aminophenol (**2**), which is sparingly soluble in chloroform. There was not an attempt to isolate the 2-(dialkylamino)phenol.

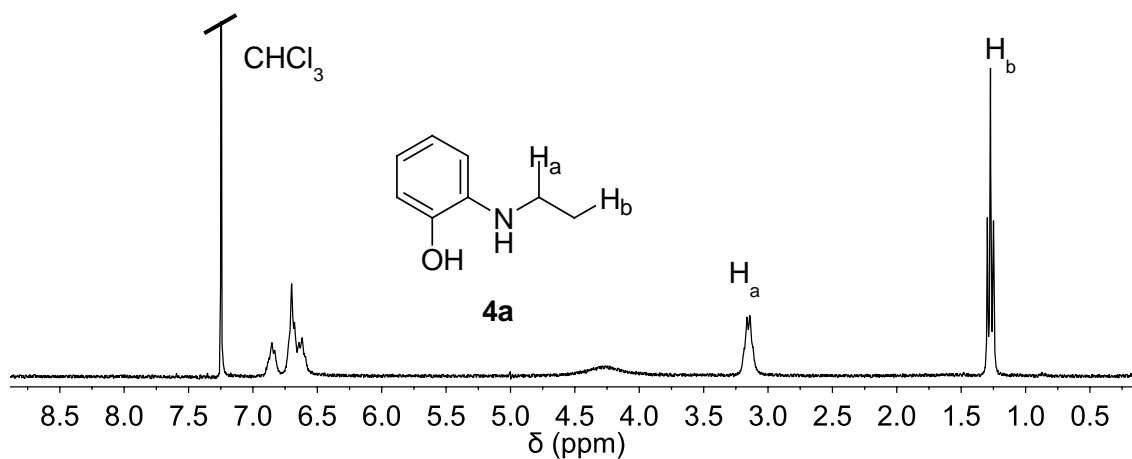


Figure 29. ^1H NMR spectrum of purified 2-(ethylamino)phenol (**4a**) in CDCl_3 .

2.3.3 Synthesis of 3-alkyl-2-phenyl-1,3,2-benzoxazaboroles. Following a synthetic method developed in our research group for benzodioxaborole and benzoxazaborole, the synthesis of 3-(alkyl)benzoxazaboroles **6a-c** was attempted by mixing a 1:1 ratio of 2-(alkylamino)phenols **4a-c** with phenylboronic acid (**1**) in EtOAc or CDCl_3 (Figure 30).³² The reaction was complete within 5 minutes and the formation of product was confirmed by ^1H NMR (Figure 31).

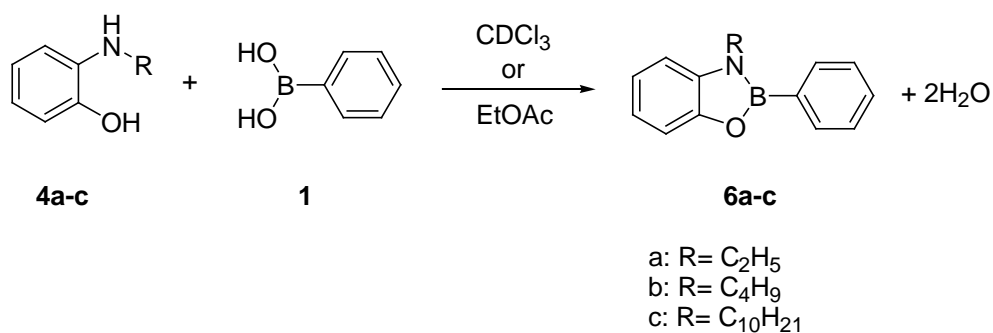


Figure 30. Formation of 3-alkyl-2-phenyl-1,3,2-benzoxazaboroles (**6a-c**).

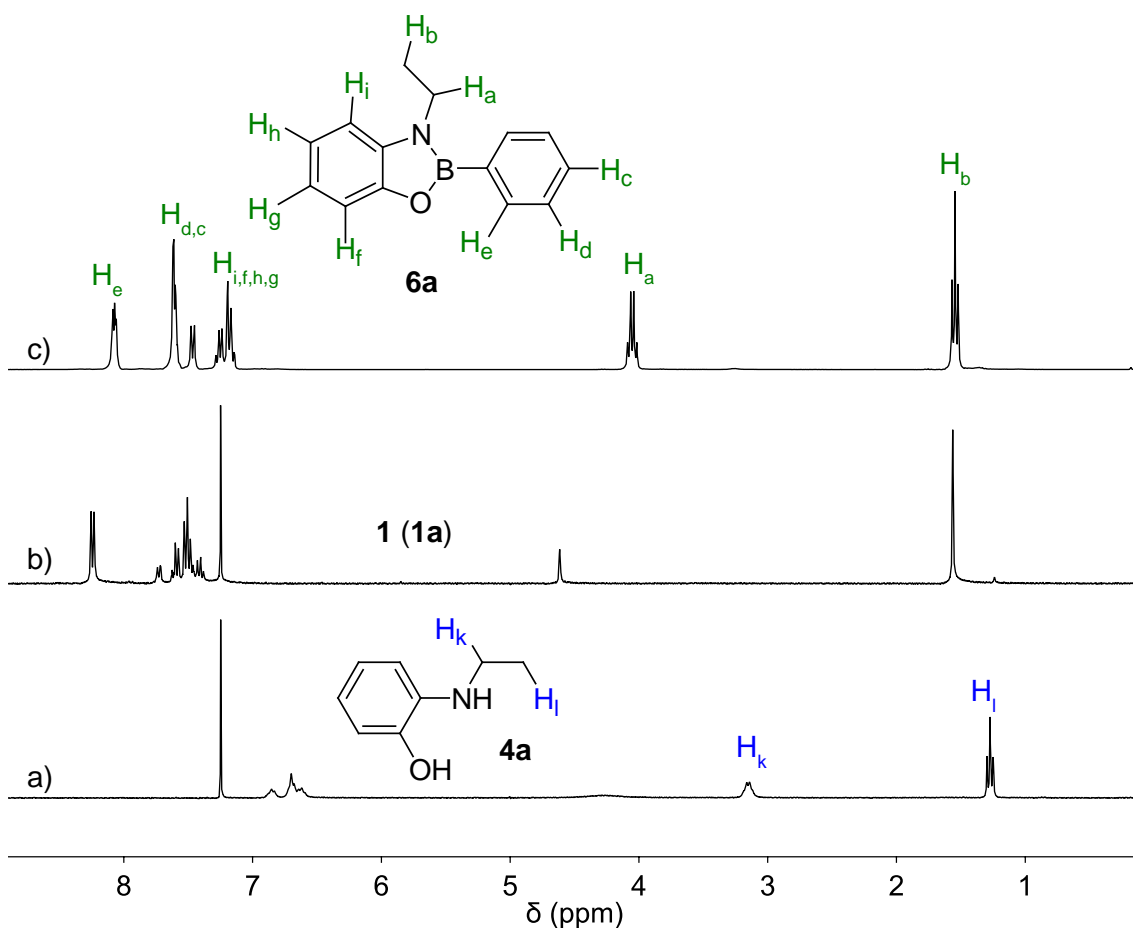


Figure 31. ¹H NMR spectra of a) 2-(ethylamino)phenol (**4a**), b) phenylboronic acid/boroxine (**1/1a**), and c) 3-ethyl-2-phenyl-1,3,2-benzoxazaborole (**6a**) in CDCl₃.

2.3.4 Synthesis of 3-alkyl-2-phenyl-1,3,2-benzoxazaborole derivatives. All of the above synthesized 3-(alkyl)benzoxazaboroles are oils, which limits further characterization such as X-ray crystallography. Therefore, the synthesis of benzoxazaborole derivatives was carried out to obtain derivatives with higher melting points. Specifically, benzoxazaborole derivatives were synthesized by reacting 4-bromophenylboronic acid (**7**) or 4-methoxyphenylboronic acid (**8**) and 2-(alkylamino)phenols **4a-c** (Figure 32).

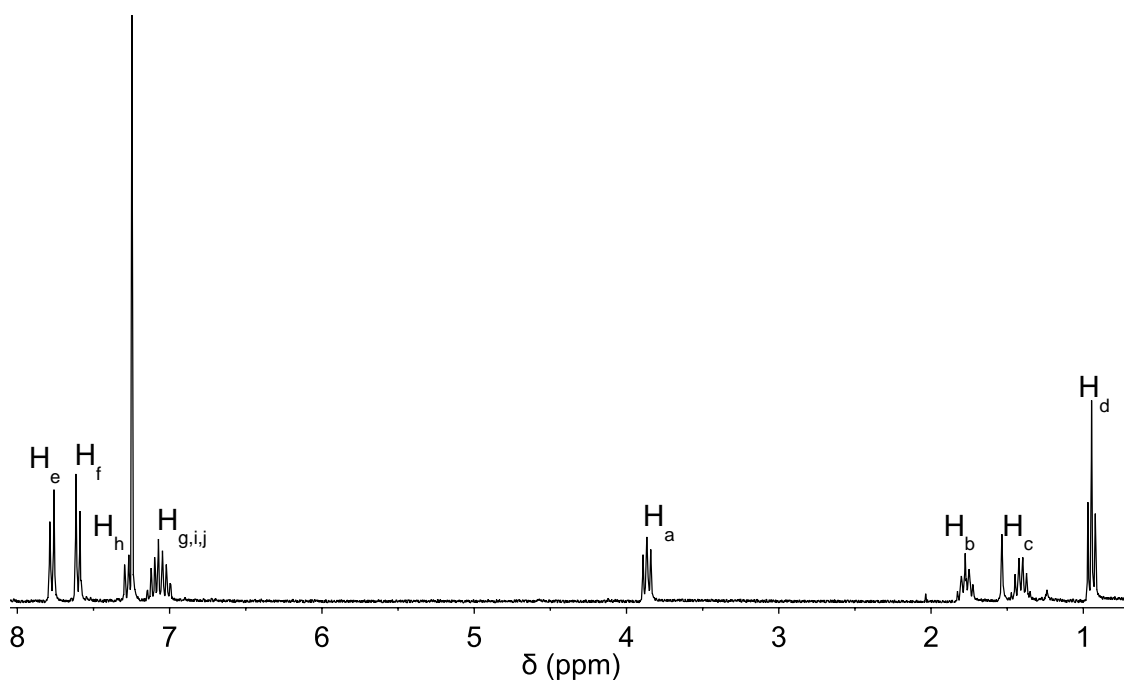
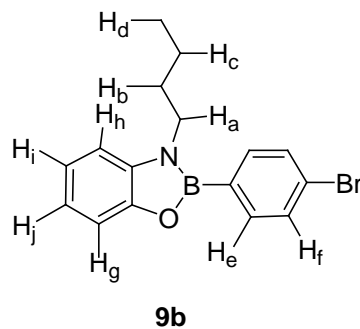


Figure 33. ^1H NMR of 2-(4-bromophenyl)-3-butyl-1,3,2-benzoxazaborole (**9b**).

All of the above synthesized benzoxazaboroles were solids except 3-butyl-2-(4-methoxyphenyl)-1,3,2-benzoxazaborole (**10b**). To date, attempts at obtaining X-ray quality crystals have not been successful.

2.3.5 Synthesis of bis(benzoxazaborole)s. Initial studies regarding the synthesis of bis(benzoxazaborole)s were carried out by former group member Sobiya George.²⁸

Bis(benzoxazaborole) **12** was synthesized by a condensation reaction of commercially available 2-aminophenol (**2**) and 1,4-benzene diboronic acid (**11**) (Figure 34).

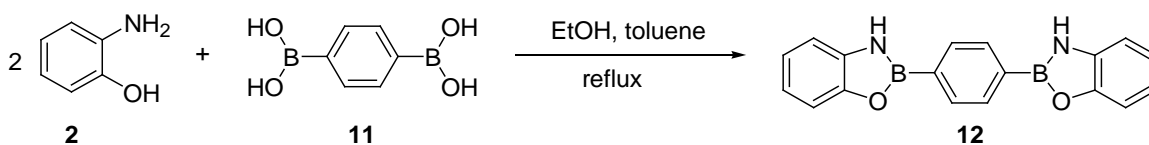


Figure 34. Formation of bis(benzoxazaborole) **12**.

Characterization of bis(benzoxazaborole) using ^1H NMR and ^{13}C NMR was not fruitful due to poor solubility of bis(benzoxazaborole) in CDCl_3 . When using $\text{DMSO-}d_6$ as the NMR solvent, the product hydrolyzed back to the starting materials. This was likely due to presence of water in the DMSO as described earlier in this chapter.

The solubility of bis(benzoxazaborole)s was overcome in part by synthesizing alkyl bis(benzoxazaborole)s (**13a-c**, **15a**, **17a** and **21a**) using 2-(alkylamino)phenols **4a-c**. The condensation reaction of 2-(alkylamino)phenols **4a-c** and 1,4-benzene diboronic acid (**11**) was carried out to synthesize bis(benzoxazaborole)s **13a-c** using a similar method used by former group member, Sobiya George (Figure 35). The poor solubility of 1,4-diboronic acids in toluene was overcome by adding ethanol. After refluxing overnight with a Dean-Stark trap, and removal of solvent under vacuum, the products were isolated in greater than 90% yield.

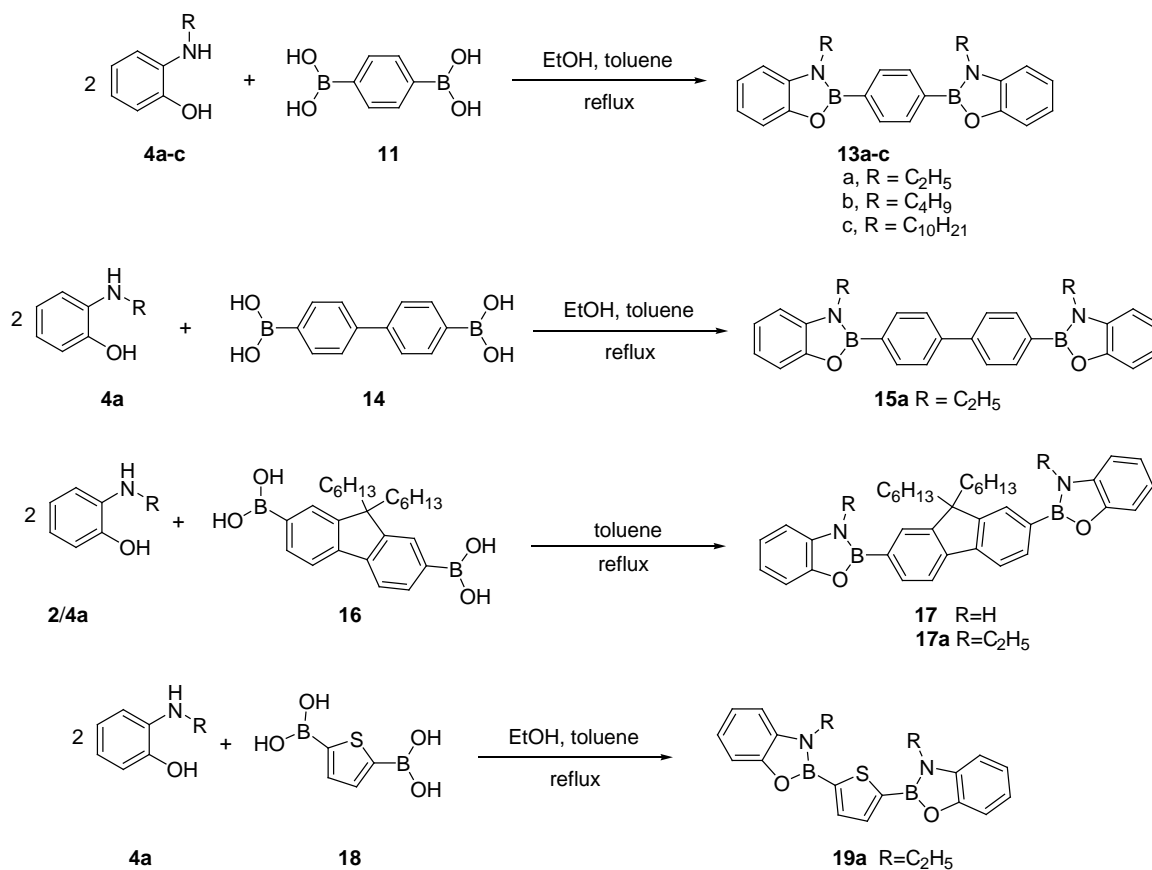


Figure 35. Synthesis of bis(benzoxazaborole)s using arylene diboronic acids.

All synthesized non-alkyl bis(benzoxazaborole)s, except for the fluorene derivative **17** (Figure 36), were not soluble in CDCl₃. Other solvents such as DMSO-*d*₆ cannot be used for the NMR analysis of benzoxazaboroles and bis(benzoxazaborole)s due to hydrolysis back to the starting materials.

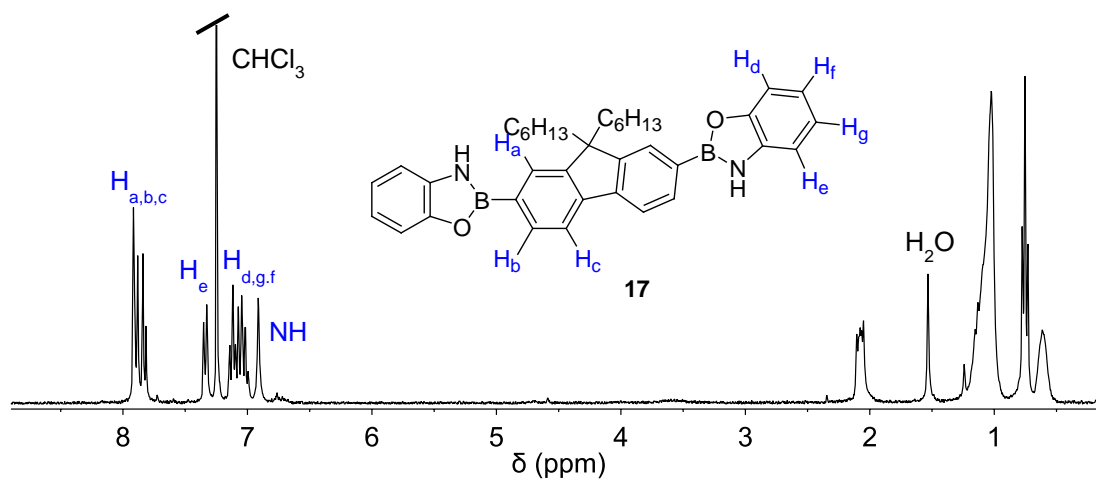


Figure 36. ^1H NMR spectrum of bis(benzoxazaborole) **17** in CDCl_3 .

All alkyl bis(benzoxazaborole)s (**13a-c**, **15a**, **17a**, and **19a**) were readily soluble in CDCl_3 . ^1H NMR and ^{13}C NMR analysis supported the formation of the product by the appearance of signals corresponding to the product and disappearance of signals corresponding to the starting materials (Figure 37). Complete product formation was not observed with **19a** in which 10% of starting materials were left in the reaction mixture. The complete conversion of starting materials to product may be possible by adding molecular sieves.

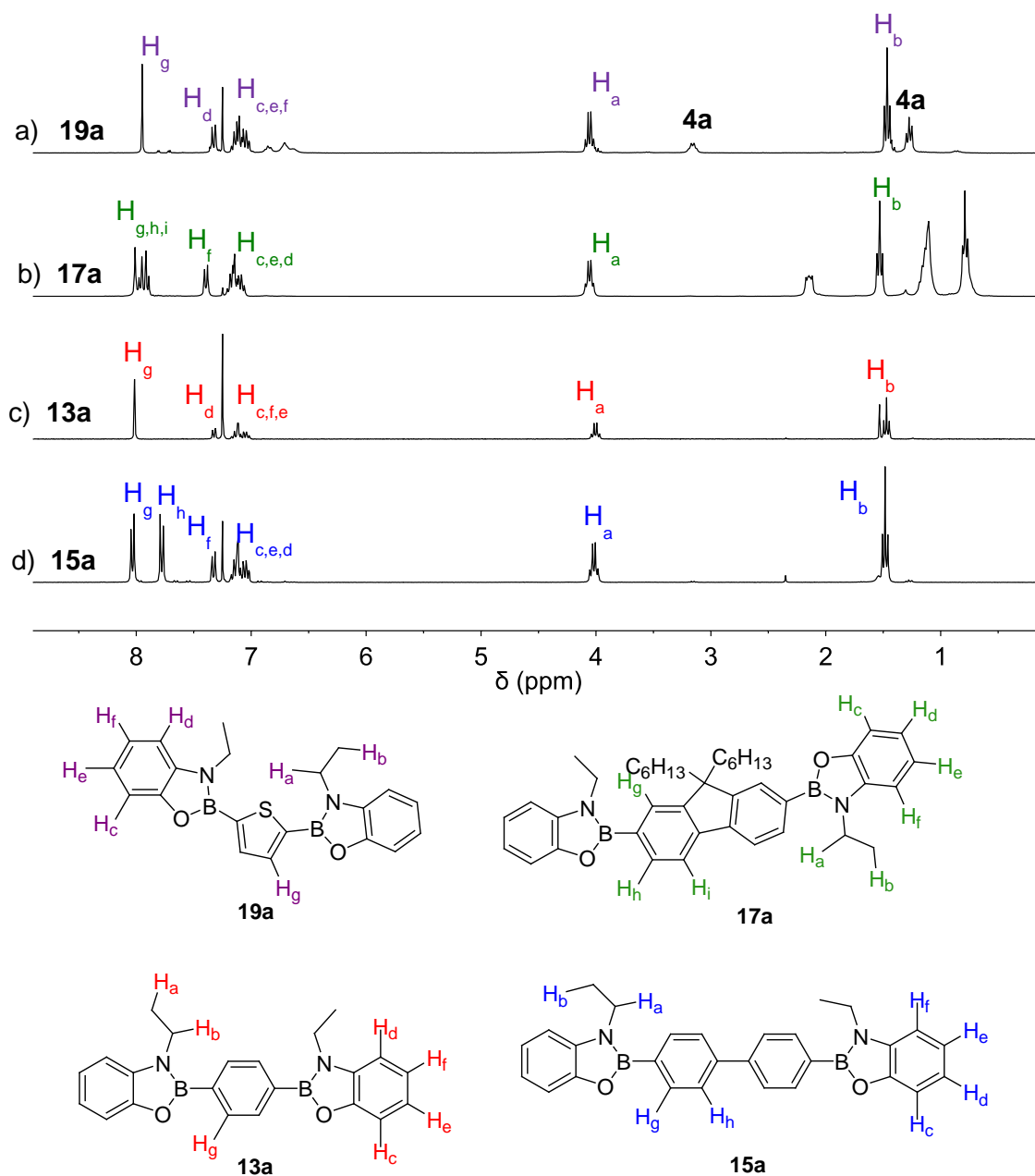


Figure 37. ^1H NMR spectra of a) 2,5-thiophenediyl-bis-[3-(ethyl)benzoxazaborole] (**17a**), b) 9,9-dihexylfluorene-2,7-bis-[3-(ethyl)benzoxazaborole] (**19a**), c) 1,4-phenylene-bis-[3-(ethyl)benzoxazaborole] (**13b**), and d) biphenyl-4-4'-bis-[3-(ethyl)benzoxazaborole] (**15b**) in CDCl_3 .

2.3.6. Thermodynamic calculations. Recently, Northrop and Goldberg investigated thermodynamics of several boroles using computational calculations and compared them with experimental results.³³ In our research, former group member Janaka Abeysinghe performed Gibbs free energy calculations of several diazaborole derivatives and two oxazaboroles.³⁴ Besides those calculations, the computational calculations for thermochemistry of benzoxazaboroles in the gaseous phase are not yet reported. Therefore, the Gibbs free energies of formation ($\Delta G_{\text{formation}}$) of benzoxazaboroles in the gas phase at room temperature (298K) were calculated using the equation $\Delta G_{\text{formation}} = E_{\text{products}} - E_{\text{reactants}}$ (Table 1). Initially, the optimal geometries were obtained using a computationally inexpensive Hartree-Fork (HF) method and minimal basis set (3-21G). Then optimized geometries were subjected to full convergence geometry optimization using density functional theory (DFT) and the B3LYP function with the basis set 6-311++G(d,p). The molecules were then subjected to frequency calculations at the same level of theory.³⁵

Table 1

ΔG calculation of benzoxazaboroles in gaseous phase.

	Products			Reactants		
	Benzoxazaborole (Hartrees)	2 H ₂ O (Hartrees)	PBA derivative (Hartrees)	aminophenol (Hartrees)	ΔG (P-R) (Hartrees)	ΔG (kJ/mol)
6a	-696.827	-152.91	-408.300	-441.434	-0.003	-7.88
6b	-775.423	-152.91	-408.300	-520.030	-0.003	-7.88
6c	-1011.213	-152.91	-408.300	-755.820	-0.003	-7.88
9a	-3270.383	-152.91	-2981.857	-441.434	-0.002	-5.25

(continued)

	Products			Reactants		
9b	-3348.980	-152.91	-2981.857	-520.030	-0.002	-5.25
9c	-3584.770	-152.91	-2981.857	-755.820	-0.002	-5.25
10a	-811.356	-152.91	-522.824	-441.434	-0.008	-21.77
10b	-889.953	-152.91	-522.824	-520.030	-0.008	-21.77
10c	-1125.742	-152.91	-522.824	-755.820	-0.008	-21.77

The Gibbs free energy of formation (ΔG) of benzoxazaboroles in the gas phase display a favorability for formation of methoxy substituted benzoxazaboroles over bromo and un-substituted benzoxazaboroles. The formation of benzoxazaborole is also independent of alkyl chain length.

2.3.7 X-ray crystallographic studies of bis(benzoxazaborole)s. Additional support for benzoxazaborole formation comes from single crystal X-ray crystallographic characterization. Crystals of bis(benzoxazaborole)s (**13a** and **15a**) were grown using solvent diffusion followed by solvent evaporation.

The solvents were selected according to their boiling points and sample dissolution. The solvent in which the sample is readily soluble was used to dissolve the sample, which is known as the good solvent. The solvent in which the sample is insoluble or sparingly soluble, (the bad solvent, 1-pentane) was placed at the top of the good solvent (dichloromethane). In this technique, 1-pentane penetrates into dichloromethane and the volume of solvent decreases due to slow evaporation of solvents (Figure 38). Eventually, crystal formation resulted upon saturation of the bis(benzoxazaborole) solution. Colorless crystals of bis(benzoxazaborole)s (**13a** and **15a**) were obtained after 7 days.

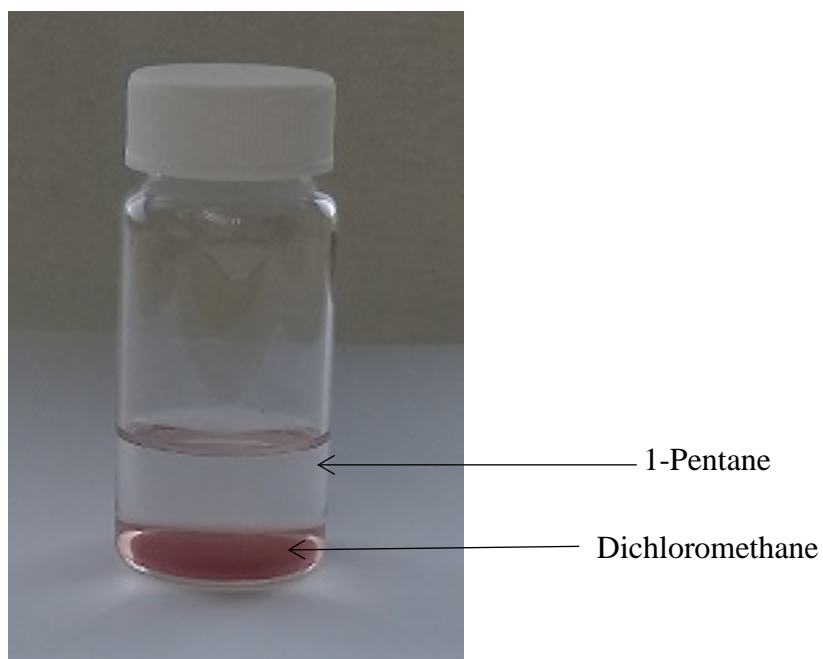


Figure 38. Reaction vial containing **15a** in dichloromethane and layered with pentane.

X-ray diffraction analysis of the crystals was conducted and structures of each bis(benzoxazaborole) (**13a** and **15a**) was obtained (Figure 39 and 40). The dihedral angle between N-B-C-C of bis(benzoxazaborole) **13a** was 25° and the dihedral angle between O-B-C-C was 25° (see appendix for the relevant data). The π - π stacking distance in bis(benzoxazaborole) **13a** was 4.05 \AA . X-ray crystal structure packing of bis(benzoxazaborole)s was hindered by the ethyl group attached to the nitrogen atom (Figure 41).

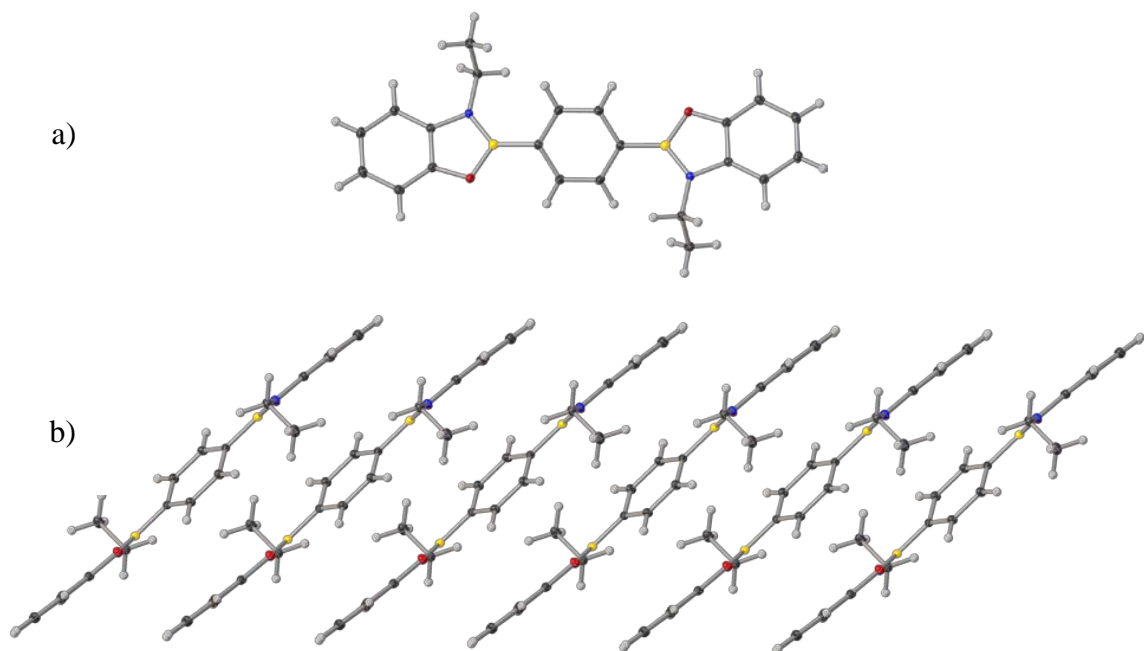


Figure 39. X-ray crystal structure of bis(benzoxazaborole) **13a** a) single and b) packing.

The crystal structure of bis(benzoxazaborole) **15a** contained a disordered end having two different dihedral angles of 6° and 14° for O-B-C-C and 3° and 36° for N-B-C-C. The other half of bis(benzoxazaborole) **15a** had dihedral angles of 9° for N-B-C-C and 8° for O-B-C-C. The dihedral angle between two phenyl rings of the biphenyl moiety was 43° . The π - π stacking distance in bis(benzoxazaborole) **15a** was 3.39 \AA .

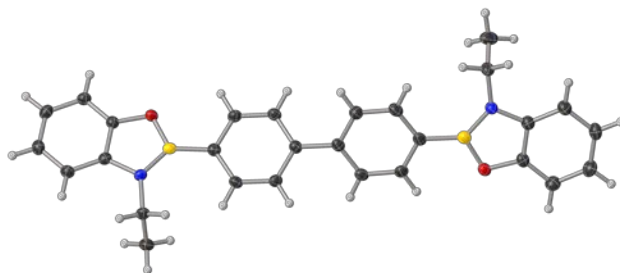


Figure 40. X-ray crystal structure of bis(benzoxazaborole) **15a**.

Bond lengths and bond angles were also obtained from the crystal structures and compared with the computationally calculated bond lengths and bond angles (see section 2.3.7).

2.3.8 Geometry Optimization using computational chemistry. Initially, the optimal geometries were obtained using a computationally inexpensive Hartree-Fock (HF) method and minimal basis set (3-21G). Then optimized geometries were subjected to full convergence geometry optimization using density functional theory (DFT) and the B3LYP function with the basis set 6-311++G(d,p). The calculated bond lengths (see Figure 41) are summarized in Tables 2 and 3.

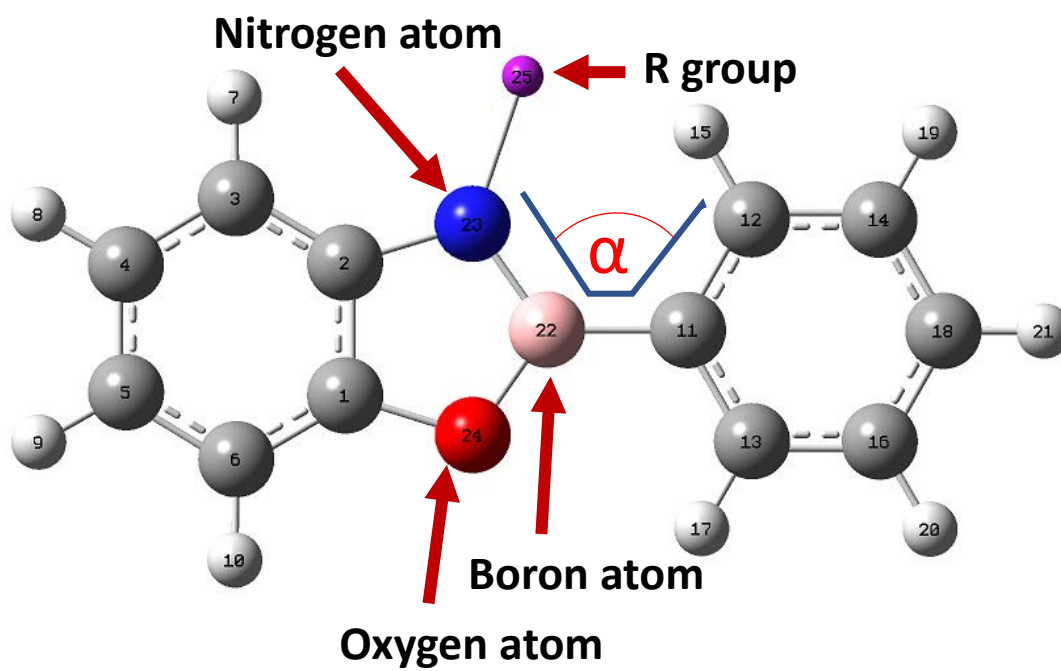
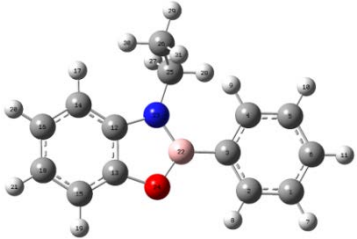
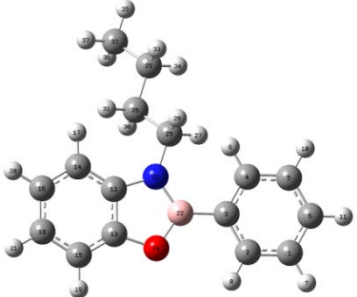
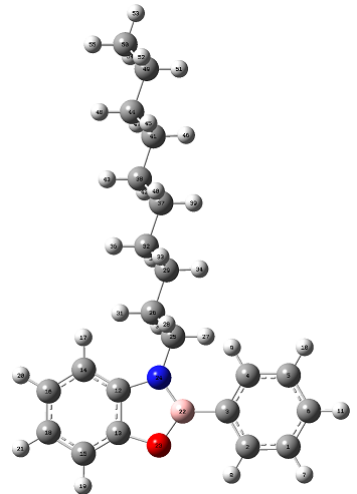


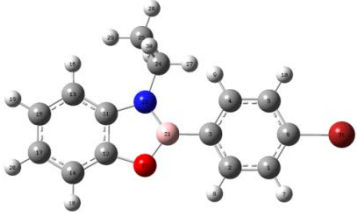
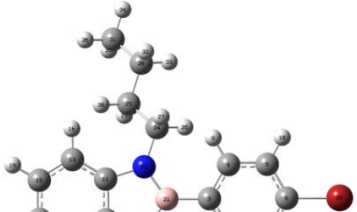
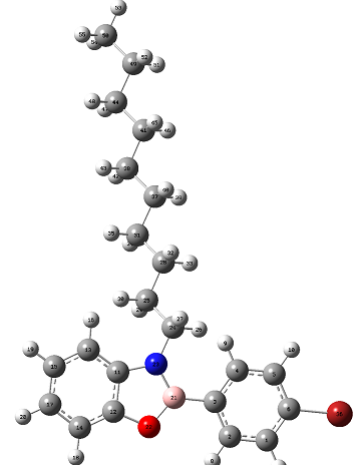
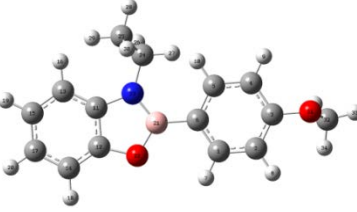
Figure 41. The structural framework of benzoxazaborole.

Table 2

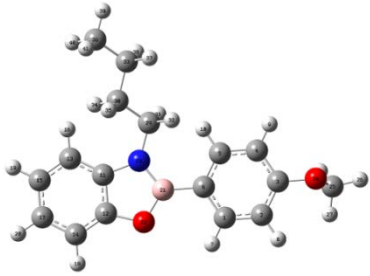
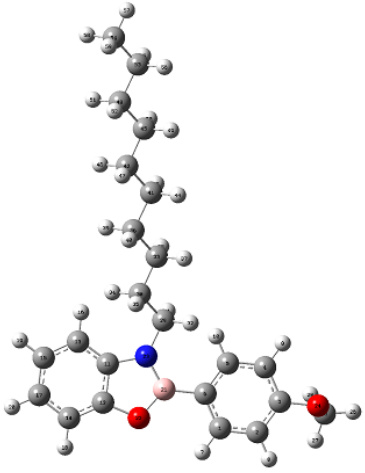
Bond lengths of the center borole ring of 3-(ethyl)benzoxazaborole.

Molecule	Bond lengths (Å)				
	C-B	N-B	O-B	N-C	O-C
 6a	1.55	1.43	1.40	1.40	1.37
 6b	1.55	1.43	1.40	1.40	1.37
 6c	1.55	1.43	1.40	1.40	1.37

(continued)

Molecule	Bond lengths (Å)				
	C-B	N-B	O-B	N-C	O-C
 9a	1.55	1.43	1.40	1.40	1.37
 9b	1.55	1.43	1.40	1.40	1.37
 9c	1.55	1.43	1.40	1.40	1.37
 10a	1.55	1.44	1.41	1.40	1.37

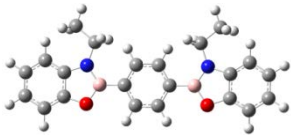
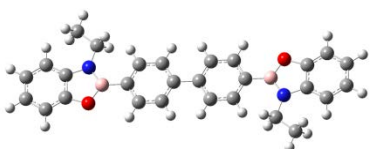
(continued)

Molecule	Bond lengths (Å)				
	C-B	N-B	O-B	N-C	O-C
 <p style="text-align: center;">10b</p>	1.55	1.44	1.41	1.40	1.37
 <p style="text-align: center;">10c</p>	1.55	1.44	1.41	1.40	1.37

As expected when varying the alkyl chain there was minimal variation in the structure of the benzoxazaborole core. Benzoxazaboroles with electron donating, (methoxy) are found to exhibit longer O-B, N-B bond lengths relative to benzoxazaboroles with an electron withdrawing group (bromo), which exhibits shorter O-B, N-B bond lengths, though the difference is small. This trend is observed because para donating substituents are able to increase the electron density around the boron atom, while para withdrawing groups decrease electron density at the boron atom.

Table 3

Bond lengths of the borole ring of bis(benzoxazaborole)s.

Molecule	Bond lengths (Å)					
	C-B	N-B	O-B	N-C	O-C	
	12	1.56	1.42	1.38	1.39	1.36
	13a	1.55 (1.55) ^a	1.43 (1.42) ^a	1.40 (1.40) ^a	1.40 (1.39) ^a	1.37 (1.37) ^a
	15	1.55	1.43	1.40	1.40	1.37
	15a	1.56 (1.56) ^a	1.42 (1.40) ^a	1.39 (1.40) ^a	1.40 (1.41) ^a	1.35 (1.33) ^a
	19	1.55	1.43	1.40	1.40	1.37
	19a	1.54	1.43	1.40	1.41	1.37
	20	1.54	1.43	1.40	1.40	1.37
	20a	1.55	1.44	1.37	1.40	1.37

^aBond lengths obtained from X-ray crystallographic analysis.

The bond lengths of the borole rings in bis(benzoxazaborole)s were the same as that of benzoxazaboroles. The computationally calculated bond lengths of

bis(benzoxazaborole)s **13a** and **15a** were also compared with the bond lengths obtained from X-ray crystal structures and were found to be similar (Table 3).

The C-C-B-N dihedral angles (see Figure 41) of all benzoxazaboroles are observed to be around 22 which is likely due to the alkyl chain on the nitrogen atom of benzoxazaborole. However, the energy differences between optimized geometries and coplanar geometries of benzoxazaboroles are very low (Table 4).

Table 4

Conformational analysis of benzoxazaboroles 6a, 9a and 10a.

Molecule	Dihedral angle	G _{Actual}	G _{Planar}	$\Delta G_{\text{Difference}}$	$\Delta G_{\text{Difference}}$
	α	(Hartrees)	(Hartrees)	(Hartrees)	(kJ/mol)
6a	24	-696.827	-696.824	0.003	8
9a	22	-3270.383	-3270.381	0.002	5
10a	20	-811.356	-811.354	0.002	5

Table 5

Conformational analysis of bis(benzoxazaborole)s

Molecule	Dihedral angle	G _{Actual}	G _{Planar}	$\Delta G_{\text{Difference}}$	$\Delta G_{\text{Difference}}$
	α	(Hartrees)	(Hartrees)	(Hartrees)	(kJ/mol)
12	0	-1004.238	-1004.238	0.000	0
13a	33	-1161.414	-1161.412	0.002	5
15	0	-1235.277	-1235.277	0.000	0
15a	26	-1392.454	-1392.450	0.004	10
19	0	-1325.045	-1325.045	0.000	0
19a	0	-1482.202	-1482.202	0.000	0

As observed with benzoxazaboroles, bis(benzoxazaborole)s **13a** and **15a** also possess a dihedral angle due to the alkyl substituent. The energy difference between the optimized geometries and coplanar geometries for non-alkyl bis(benzoxazaborole)s are zero and the bis(3-alkylbenzoxazaborole)s also had very small values.

2.3.9. Electrostatic potential maps. Electrostatic potential maps, also known as electrostatic potential energy maps or molecular electrical potential surfaces, are three dimensional diagrams of molecules that aid in visualize atom of the charge distributions on molecules. Electrostatic potential maps of a molecule can be used to identify the electron rich and electron deficient regions, which have direct correlation with electron donation and accepting ability The red colored regions, which are rich in electron density, donate electrons while blue colored regions with low electron density, accept electrons. Recently, Northrop and Goldberg investigated electron density maps of boronate esters.³³ Moreover, electrostatic potential maps of diazaboroles were reported by Davies and coworkers.³⁶ Former group member Janaka Abeysinghe also utilized computational chemistry to investigate electrostatic potential maps of several diazaborole derivatives.³⁴ The electrostatic potential maps (EPMs) of benzoxazaboroles and bis(benzoxazaborole)s (isovalues: -0.02 to 0.02) were obtained using DFT methods at the B3LYP/6-311++G(d,p) level (Figure 42).

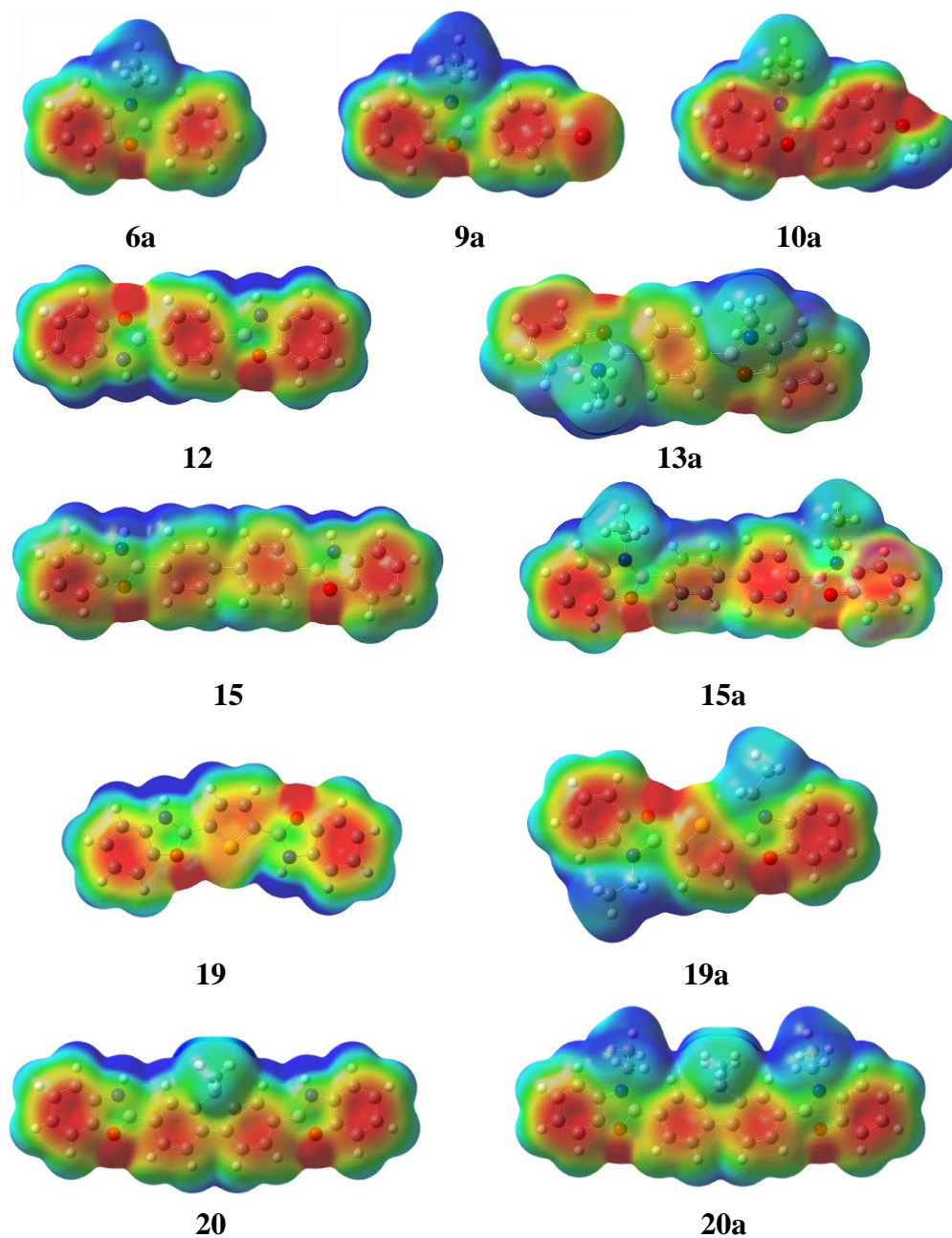


Figure 42. Electrostatic potential maps of benzoxazaboroles and bis(benzoxazaborole)s.

The EPMs reveal that all benzoxazaboroles and bis(benzoxazaborole)s have electron accumulation on the aminophenol moiety rather than the phenylboronic acid moiety. In the bromo-substituted benzoxazaborole (**9a**), the electron density around the phenylboronic acid moiety is reduced due to the electron withdrawing bromine atom. In

the methoxy substituted benzoxazaborole **10a**, which has electron donating ability, high electron density is observed in the phenylboronic acid moiety when compared to bromo and un-substituted benzoxazaboroles. All calculations of bis(benzoxazaborole)s predict less electron density around phenylene diboronic acid moiety compared to the aminophenol moiety. The electron density around borole ring was also observed to be low as indicated by electrostatic potential maps.

2.3.10 UV-vis spectroscopic characterization.

Benzodioxaboroles and benzodiazaboroles are known to be blue emissive materials.^{33,37} Benzoxazaboroles are expected to exhibit similar properties, since they are structurally analogous. To gain more insight in their optoelectronic character, benzoxazaboroles and bis(benzoxazaborole)s were characterized using UV-vis and fluorescence spectroscopies.

Initially, the collection of absorption and emission spectra of benzoxazaboroles and bis(benzoxazaborole)s was attempted in DMF. The absorption λ_{max} obtained for benzoxazaborole **3** (295 nm) and 2-aminophenol (**2**, 294 nm) were similar. After comparing molar absorption coefficients (ϵ) of benzoxazaborole **6a** and 2-(ethylamino)phenol **4a**, which were also similar, it was determined that hydrolysis of benzoxazaborole occurs readily in DMF. Therefore, chloroform (CHCl_3) was used for UV-visible and fluorescence spectroscopic studies.

The absorption spectrum of benzoxazaborole **6a** (λ_{max} , 289 nm) was obtained in CHCl_3 and compared with the absorption spectra of the starting materials (concentration of 1 mM) phenylboronic acid (λ_{max} , 269 nm) and 2-(ethylamino)phenol (λ_{max} , 275 nm) at a concentration of 0.1 mM (Figure 43).

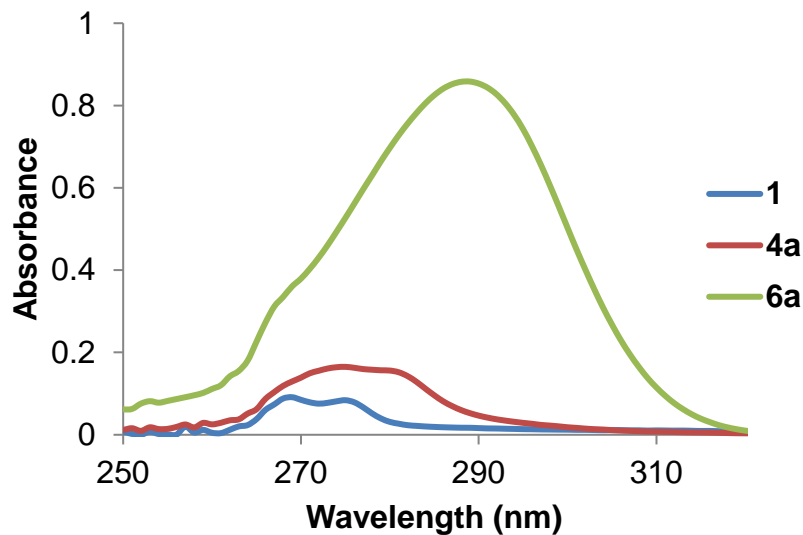


Figure 43. Absorption spectra of phenylboronic acid (**1**), 2-(ethylamino)phenol (**4a**), and benzoxazaborole **6a** in CHCl_3 .

The emission spectra of benzoxazaborole **6a** (λ_{max} , 366 nm), phenylboronic acid (**1**) (λ_{max} , 293 nm), and 2-(ethylamino)phenol (**4a**) (λ_{max} , 316 nm), were obtained in CHCl_3 by irradiating at the absorption λ_{max} of each compound (Figure 44). In addition to the difference in emission wavelength, an increase in emission intensity was observed for benzoxazaborole **6a** compared to the starting materials. This supports the presence of benzoxazaboroles.

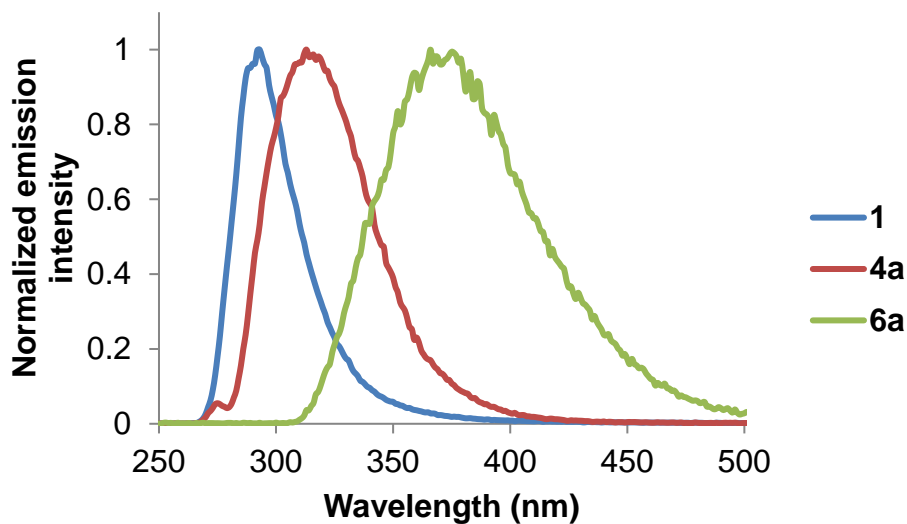


Figure 44. Normalized emission spectra of phenylboronic acid (**1**), 2-(ethylamino)phenol (**4a**), and benzoxazaborole **6a** in CHCl_3 .

Table 6

Absorption and emission data for benzoxazaboroles in CHCl_3

Compound	λ_{abs} (nm)	λ_{em} (nm)	$\lambda_{\text{em}} - \lambda_{\text{abs}}$ (nm)	ΔE (kJ/mol)
6a	289	366	77	1.39×10^3
6b	289	375	86	1.41×10^3
6c	289	365	76	1.57×10^3
9a	291	376	85	1.41×10^3
9b	291	384	93	1.16×10^3
9c	291	382	91	1.41×10^3
10a	290	346	56	1.96×10^3
10b	290	349	59	2.06×10^3
10c	290	347	57	2.26×10^3

The spectra for all benzoxazaboroles show emission in the blue region. Wavelengths for both absorption and emission spectra were red shifted in alkyl benzoxazaboroles compared to non-alkyl benzoxazaborole (**3**). According to the absorption and emission spectra of alkyl benzoxazaboroles, it indicates that there is no significant influence of length of alkyl chain on the absorption or emission.

Next, the effect of para-substitution on the alkyl benzoxazaboroles was studied using absorption and emission spectra. The λ_{max} of bromo substituted benzoxazaboroles **9a-c** was observed to be red shifted compared to the methoxy and unsubstituted benzoxazaboroles. Methoxy substituted benzoxazaboroles **10a-c** are also observed to be red shifted compared to the unsubstituted benzoxazaboroles **6a-c**. This may be due to charge transfer between the methoxy group and the boron atom. A similar increase in red shift for methoxy-substituted diazaboroles was reported by Maruyama and Kawanishi in 2002.³⁸

Characterization of bis(benzoxazaborole)s **12** and **15** was not possible in CHCl_3 , due to poor solubility. The absorption or emission wavelengths of bis(benzoxazaborole)s **13a-c** are independent of alkyl chain length. The λ_{max} of biphenyl bis(benzoxazaborole) **15a** was observed to be red shifted, which is likely due to presence of additional phenyl ring. The observed stokes shift for all alkyl bis(benzoxazaborole)s (**13a-c** and **15a**) ranged from 90-96 nm in CHCl_3 (Table 6).

Table 7

Absorption and emission data for bis(benzoxazaborole)s in CHCl₃

Compound	λ_{abs} (nm)	λ_{em} (nm)	$\lambda_{\text{em}}-\lambda_{\text{abs}}$ (nm)	ΔE (kJ/mol)
13a	300	393	93	1.29×10^3
13b	301	393	92	1.25×10^3
13c	302	392	90	1.33×10^3
15a	308	405	97	1.23×10^3

2.3.11. HOMO and LUMO energy diagrams.

The optimized geometries of benzoxazaboroles and bis(benzoxazaborole)s were utilized to obtain the HOMO and LUMO for each of the benzoxazaboroles and bis(benzoxazaborole)s (Figures 45 and 46).

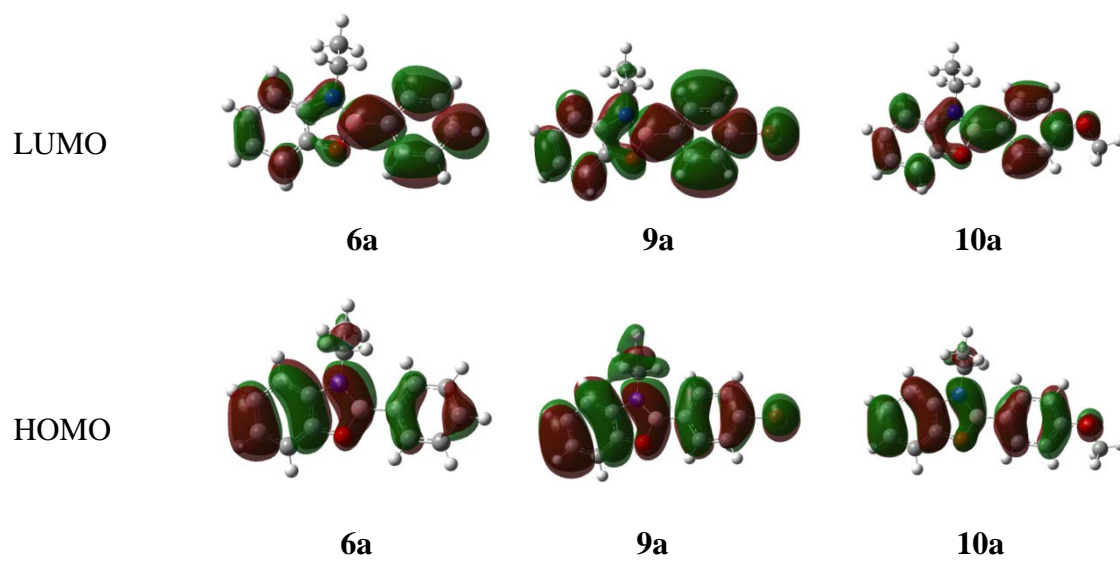


Figure 45. Top views of the highest-occupied and lowest-unoccupied molecular orbitals of **6a**, **9b**, and **10b**.

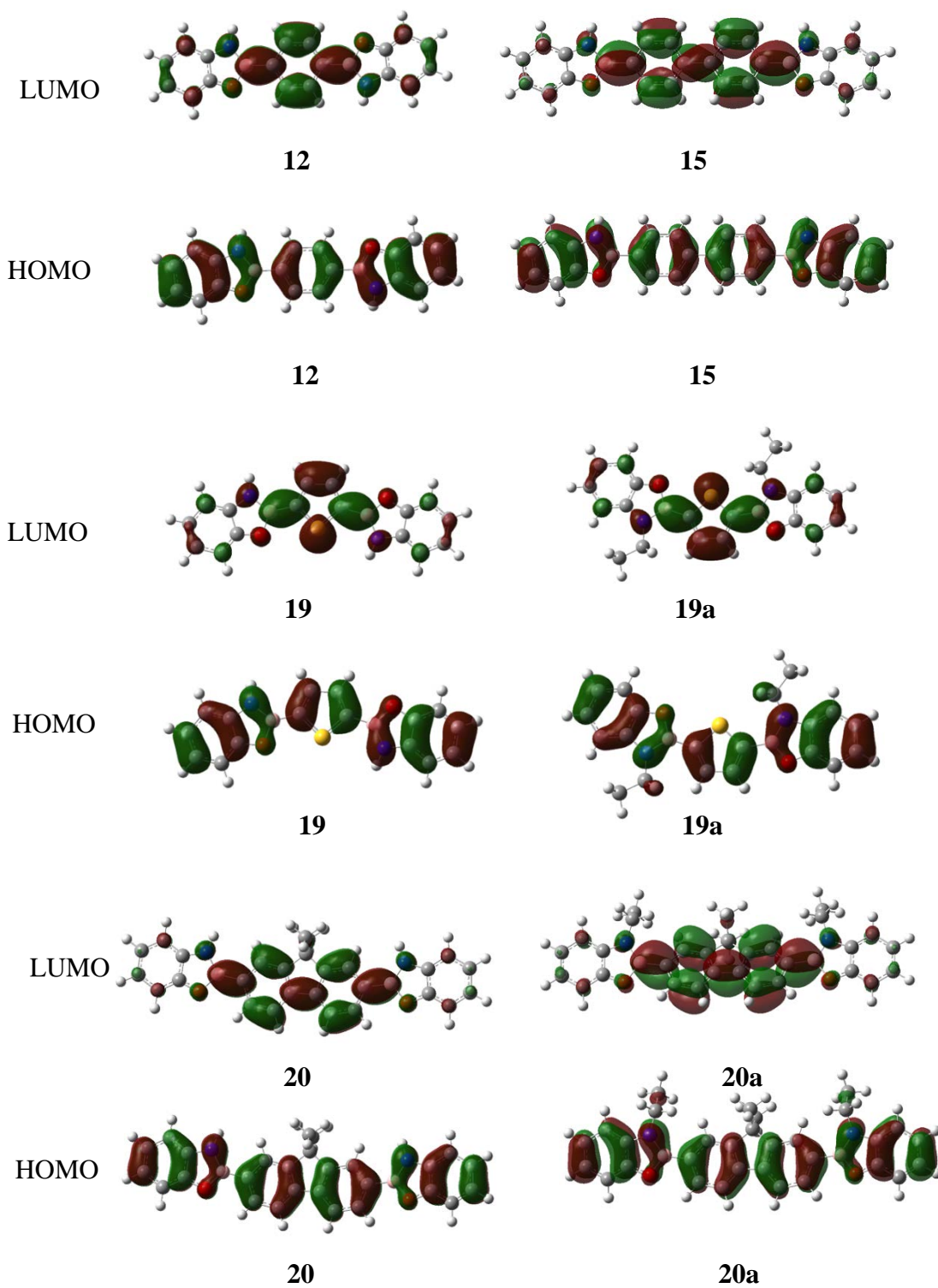


Figure 46. Top views of the highest-occupied and lowest-unoccupied molecular orbitals of 12, 15, 19, 19a, 20, and 20a.

Computational analysis reveals that the HOMO orbitals of all unsubstituted benzoxazaboroles and bromo-substituted benzoxazaboroles are quite similar; all localized to their more electron-rich aminophenol-based units while methoxy substituted benzoxazaboroles are delocalized across the π -conjugated aminophenol, phenylboronic acid and borole moieties. The LUMOs of all benzoxazaboroles are localized on their electron poor boronic acid moieties.

The computational investigations predicted that the HOMOs of all bis(benzoxazaborole)s are completely delocalized across the π -conjugated system, while the LUMOs are localized on their central, electron-poor diboronic acid moieties.

Table 8

HOMO and LUMO energy values of benzoxazaboroles and bis(benzoxazaborole)s.

Compound	E_{HOMO} (Hartrees)	E_{LUMO} (Hartrees)	ΔE (Hartrees)	$\bar{\nu}$ (cm^{-1})	λ_{cal} (nm)	λ_{obs} in CHCl_3 (nm)
6a	-0.21862	-0.04249	0.17613	38656.4	258.7	289
9a	-0.22272	-0.05252	0.17020	37354.9	267.7	291
10a	-0.21128	-0.03295	0.178233	39117.9	255.6	290
12	-0.21926	-0.06276	0.15650	34348.0	291.1	-
13a	-0.21594	-0.05486	0.16108	35353.2	282.9	300
15	-0.21779	-0.06650	0.15129	33204.6	301.2	-
15a	-0.21125	-0.06379	0.14746	32364.0	309.0	308
19	-0.21662	-0.06694	0.14968	32851.2	304.4	-
19a	-0.20900	-0.06264	0.14636	32122.5	311.3	-
20	-0.21321	-0.06885	0.14436	31683.6	315.6	-
20a	-0.21054	-0.06518	0.14536	31903.1	313.4	-

HOMO- LUMO energy calculations of benzoxazaboroles predict that methoxy substituted benzoxazaboroles have higher HOMO-LUMO energy gap compared to bromo substituted and un-substituted benzoxazaboroles while bromo substituted benzoxazaboroles have the lowest HOMO-LUMO energy gap. Increased conjugation of bis(benzoxazaborole)s were also reflected in the larger calculated HOMO-LUMO energy gaps of bis(benzoxazaborole)s and benzoxazaboroles. Electron transition occurs from π - π^* or n - π^* , which correlates with absorption and emission properties of benzoxazaboroles and bis(benzoxazaborole)s. Low HOMO-LUMO energy gap predicted higher λ_{max} values for absorption and emission wavelengths of benzoxazaboroles and bis(benzoxazaborole)s. The computational calculations supported experimental data by predicting higher λ_{max} values of bis(benzoxazaborole)s for both absorption and emission wavelengths than benzoxazaboroles. This is likely due to their extended π conjugation.

2.4 Conclusions

The synthesis or characterization of benzoxazaborole in DMSO-*d*₆ was limited due to the concurrent hydrolysis. Removal of water from the reaction medium using molecular sieves increased the formation of benzoxazaborole **3** in THF. Synthesis of 3-(alkyl)benzoxazaboroles using para-substituted phenylboronic acid is possible under mild reaction conditions. bis(Benzoxazaborole)s were successfully synthesized using arylene diboronic acids and 2-(alkylamino)phenols.

Computational calculations of benzoxazaboroles and bis(benzoxazaborole)s supported the experimental data. Thermodynamic calculations predicted that formation of all benzoxazaboroles require similar energy. X-ray diffraction analysis of bis(benzoxazaborole) **13a** and **15a** provided additional structural characterization. Bond

length calculations for bis(benzoxazaborole) **13a** and **15a** gave similar values for both X-ray structural analysis and computational calculations.

The UV-vis and fluorescence spectroscopic analysis proved that benzoxazaboroles and bis(benzoxazaborole)s are blue emissive materials. HOMO-LUMO energy gaps from computational calculations supported this observation.

2.5 Experimental Section

Chromatography. All thin-layer chromatography (TLC) analyses were performed on silica gel 60 F₂₅₄ aluminium sheets and corresponding visualizations were carried out either with UV light (254 nm) or using visualization aides, KMnO₄ or iodine stains. Column chromatographic separations were conducted using 60 Å silica gel. All glassware was oven dried before use.

Chemicals and reagents. All starting materials and reagents were purchased from commercial sources (Alfa Aesar) and used without further purification, unless otherwise mentioned. Compounds **3**, **4b**, **4c**, **6b**, **6c**, and **13c** were synthesized using the method reported by Sobiya George.²⁸ The NMR solvents CDCl₃ and DMSO-*d*₆, were stored over 4 Å molecular sieves. The molecular sieves were activated by drying in an oven at 105 °C for 24 hours.

NMR spectroscopy. The ¹H and ¹³C NMR spectra were collected on a JEOL Eclipse 300+ spectrometer. Chemical shifts are reported in δ (ppm) relative to the solvent signal for ¹H and ¹³C {(CHCl₃: 7.26 for ¹H, CDCl₃: 77.23 for ¹³C) or (DMSO-*d*₆: 2.50 for ¹H, DMSO-*d*₆: 39.52 for ¹³C) or (THF: 3.55 and 1.70 for ¹H)}. The splitting patterns are designated as s (singlet); d (doublet); t (triplet); dd (doublet of doublets); dt (doublet of triplets); (quartet); quint (quintet); m (multiplet); br s (broad singlet).

X-ray crystallography. A sample of bis(benzoxazaborole)s **13a** and **15a** were dissolved in a minimal amount of dichloromethane in a reaction vial. Pentane was placed carefully at the top of the dichloromethane layer. Colorless x-ray quality crystals were obtained after 7 days. Samples of crystals were sent to the University of Texas at Austin for X-ray crystallographic analysis. See appendix for details.

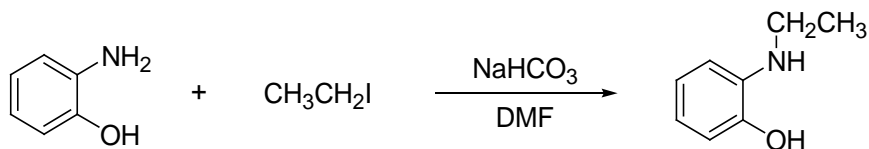
UV-vis spectroscopy. UV-vis spectra were collected using a JASCO V-750 spectrophotometer. The samples were dissolved in CHCl_3 or DMF and the transmittance was recorded. The spectra of absorbance vs wavelength (nm) were plotted.

Fluorescence spectroscopy Fluorescence spectra were collected using an F-4500 FL spectrophotometer (Slit width-5.0 nm). Samples (0.0125 mM-1 mM) were prepared in CHCl_3 and DMF. For each compound the λ_{max} from absorption spectra was selected as the excitation wavelength.

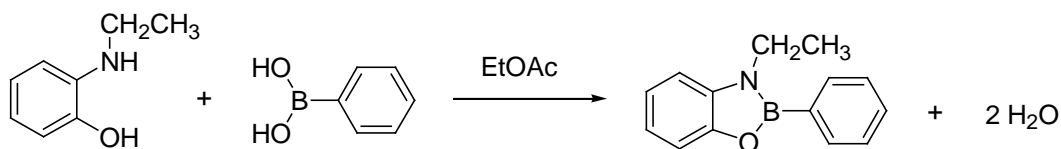
Computational calculations. All computational calculations of benzoxazaboroles and bis(benzoxazaborole)s were performed with the Gaussian G09W suite of programs. Originally, the molecular structures were built within the GaussView 5.0 interface and the geometric optimization in the gas phase was carried out to obtain geometries with lowest energy by utilizing computationally low cost, Hartree-Fock (HF) level with a minimum basis set (3-21G). Then the optimized geometries were subjected to full convergence geometry optimization using density functional theory (DFT) and B3LYP function with the 6-311++G(d,p) basis set to obtain a more accurate geometry. The molecules were then subjected to frequency calculations at the same level of theory.³⁵

Electrostatic potential maps and HOMO-LUMO energy diagrams were obtained utilizing optimized geometries. The isovalue used to obtain electrostatic potential maps and HOMO-LUMO energy diagrams is -0.02 to 0.02.

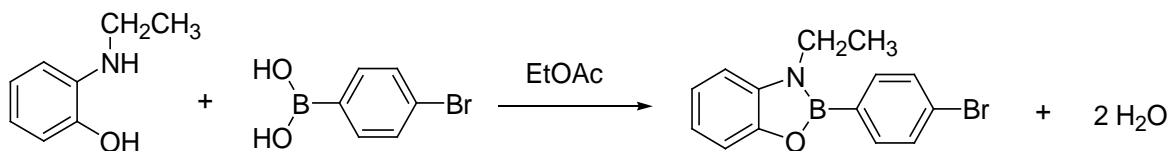
2-(Ethylamino)phenol (4a)



In a 100 ml round bottom flask 2-aminophenol (2.73 g, 25.0 mmol, 1.0 equiv), iodoethane (2.00 ml, 25.0 mmol, 1.0 equiv), NaHCO₃ (2.31 g, 27.5 mmol, 1.1 equiv), and DMF (12.5 ml) were combined and the mixture was stirred for 24h at room temperature. The reaction mixture was diluted with ethyl acetate (150 ml) and washed with H₂O (3×20 ml), dried over MgSO₄, and concentrated in vacuum at room temperature. The resulting dark red solid was purified by column chromatography [silica gel, ethyl acetate:hexanes (1:5)] to obtain yellow needle shaped crystals. The yellow crystalline solid was further purified by recrystallization with a mixture of hexanes and benzene to give colorless needle shaped crystals. (1.68 g, 49% yield). TLC R_f = 0.31 [ethyl acetate:hexanes (1:5)]. ¹H NMR (301 MHz, CDCl₃, δ): 6.84 (d, *J* = 7.8 Hz, 1H, ArH), 6.76–6.56 (m, 3H, ArH), 4.26 (br s, 1H, NH), 3.15 (q, *J* = 7.4 Hz, 2H, NH-CH₂), 1.27 (t, *J* = 7.1 Hz, 3H, CH₃). ¹³C NMR (76 MHz, CDCl₃, δ) 144.0 (1C, ArC), 137.4 (1C, ArC), 121.7 (1C, ArC), 118.0 (1C, ArC), 114.6 (1C, ArC), 112.8 (1C, ArC), 39.1 (1C), 15.0 (1C); UV (CHCl₃) λ_{max}, nm (log ε):275 (6.43).

3-Ethyl-2-phenyl-1,3,2-benzoxazaborole (6a).

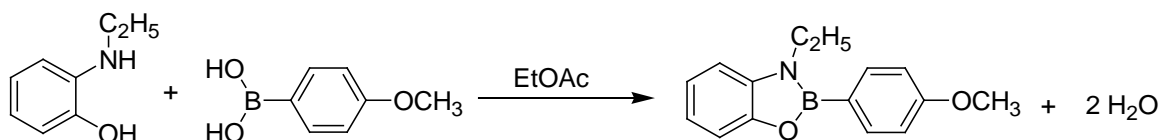
In a 100 ml round bottom flask 2-(ethylamino)phenol (343 mg, 2.5 mmol, 1 equiv) and phenylboronic acid (305 mg, 2.5 mmol, 1 equiv) were mixed in ethyl acetate (25 ml). The solvent was removed under vacuum at room temperature to give a dark brown, viscous oil (53 mg, 95% yield). ¹H NMR (301 MHz, CDCl₃, δ): 8.08 (d, 2H, Ar H), 7.65–7.56 (m, 3H, ArH), 7.47 (d, *J* = 7.7 Hz, 1H, ArH), 7.26–7.15 (m, 3H, ArH), 4.05 (q, *J* = 7.2 Hz, 2H, NH-CH₂), 1.53 (t, *J* = 7.2 Hz, 3H, CH₃). ¹³C NMR (76 MHz, CDCl₃, δ): 149.7 (1C, ArC), 138.6 (1C, ArC), 134.2 (2C, ArC), 130.8 (1C, ArC), 128.5 (2C, ArC), 122.0 (1C, ArC), 120.2 (1C, ArC), 112.5 (1C, ArC), 109.5 (1C, ArC), 37.8 (1C), 15.7 (1C); UV (CHCl₃) λ_{max}, nm (log ε):289 (6.46).

2-(4-Bromophenyl)-3-ethyl-1,3,2-benzoxazaborole (9a).

In a 50 ml round bottom flask 2-(ethylamino)phenol (69 mg, 0.5 mmol, 1 equiv) and 4-bromophenylboronic acid (100 mg, 0.5 mmol, 1 equiv) were mixed in ethyl acetate (25 ml). The reaction mixture was heated to 60 °C for 5 min until all reactants dissolved. The solvent was removed under vacuum at room temperature to give a dark red solid (147 mg, 98% yield). ¹H NMR (301 MHz, CDCl₃, δ): 7.76 (d, 2H, ArH), 7.62 (d, *J* = 5.4 Hz, 2H, ArH), 7.33 (d, *J* = 7.6 Hz, 1H, ArH), 7.21–6.99 (m, 3H, ArH), 3.95 (q, 2H, NH-CH₂), 1.43 (t, 3H, CH₃). ¹³C NMR (76 MHz, CDCl₃, δ): 149.4 (1C, ArC), 138.3 (1C, ArC), 135.6 (2C, ArC), 135.5 (2C, ArC), 131.6 (1C, ArC), 125.4 (1C, ArC), 122.0 (2C, ArC), 120.3

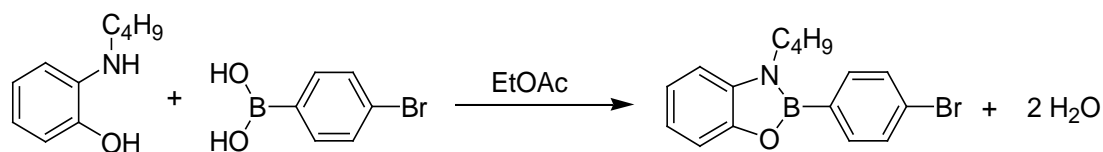
(2C, ArC), 112.4 (1C, ArC), 109.4 (1C, ArC), 37.7 (1C), 15.8 (1C); UV (CHCl₃) λ_{max} , nm (log ϵ):291 (6.76).

3-Ethyl-2-(4-methoxyphenyl)-1,3,2-benzoxazaborole (10a).



In a 20 ml reaction vial 2-(ethylamino)phenol (69 mg, 0.5 mmol, 1 equiv) and 4-methoxyphenylboronic acid (76 mg, 0.5 mmol, 1 equiv) were mixed in ethyl acetate (15 ml). The solvent was removed under vacuum at room temperature to give a yellow solid (123 mg, 97% yield). ¹H NMR (301 MHz, CDCl₃, δ): 7.88 (d, J = 8.4 Hz, 2H, ArH), 7.27 (d, J = 9.6 Hz, 1H, ArH), 7.17–6.92 (m, 5H, ArH), 3.95 (q, J = 7.2 Hz, 2H, NH-CH₂), 3.86 (s, 3H, -OCH₃), 1.44 (t, 3H, CH₃). ¹³C NMR (76 MHz, CDCl₃, δ): 161.5 (1C, ArC), 149.5 (1C, ArC), 138.6 (1C, ArC), 135.8 (2C, ArC), 121.7 (1C, ArC), 119.8 (1C, ArC), 113.9 (2C, ArC), 112.2 (1C, ArC), 109.0 (1C, ArC), 55.2 (1C), 37.6 (1C), 15.7 (1C); UV (CHCl₃) λ_{max} , nm (log ϵ):290 (6.76).

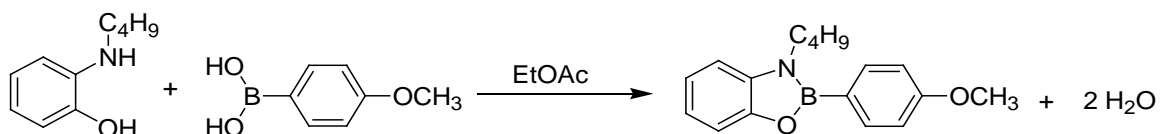
2-(4-Bromophenyl)-3-butyl-1,3,2-benzoxazaborole (9b).



In a 50 ml round bottom flask 2-(butylamino)phenol (165 mg, 1 mmol, 1 equiv) and 4-bromophenylboronic acid (200 mg, 1 mmol, 1 equiv) were mixed in ethyl acetate (25 ml). The solvent was removed under vacuum at room temperature to give a dark brown solid (303 mg, 92% yield). ¹H NMR (301 MHz, CDCl₃, δ): 7.79 (d, J = 8.1 Hz, 2H, Ar H), 7.61 (d, J = 8.1 Hz, 2H, ArH), 7.30 (d, J = 7.5 Hz, 1H, ArH), 7.19–6.97 (m, 3H, ArH), 3.88

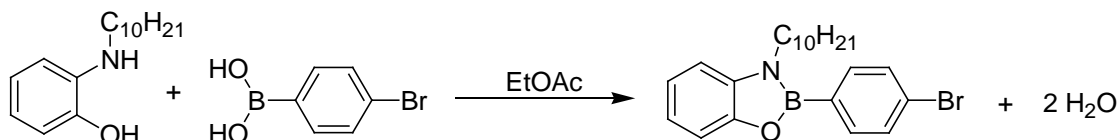
(t, $J = 7.6$ Hz, 2H, NH-CH₂), 1.85–1.70 (m, 2H, CH₂), 1.49–1.35 (m, 2H, CH₂), 0.96 (t, $J = 7.3$ Hz, 3H, CH₃). ¹³C NMR (76 MHz, CDCl₃, δ): 149.4 (1C, ArC), 138.6 (1C, ArC), 135.6 (2C, ArC), 131.6 (2C, ArC), 125.4 (1C, ArC), 122.0 (1C, ArC), 120.3 (1C, ArC), 112.4 (1C, ArC), 109.7 (1C, ArC), 43.0 (1C), 32.5 (1C), 20.5 (1C), 14.0 (1C); UV (CHCl₃) λ_{max} , nm (log ϵ):291 (6.76).

3-Butyl-2-(4-methoxyphenyl)-1,3,2-benzoxazaborole (10b).



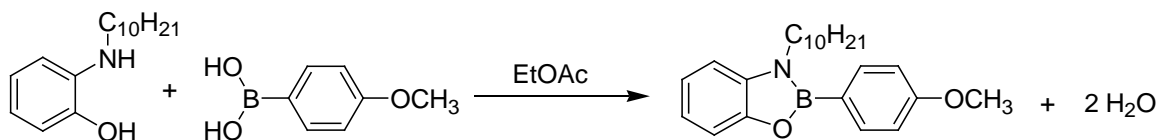
In a 50 ml round bottom flask 2-(butylamino)phenol (166 mg, 1 mmol, 1 equiv) and 4-methoxyphenylboronic acid (152 mg, 1 mmol, 1 equiv) were mixed in ethyl acetate (25 ml). The solvent was removed under vacuum at room temperature to give a dark brown semi-solid (267 mg, 94% yield). ¹H NMR (301 MHz, CDCl₃, δ): 7.91 (d, $J = 8.7$ Hz, 2H, ArH), 7.29 (dd, $J = 7.7, 1.2$ Hz, 1H, ArH), 7.18–6.95 (m, 5H, ArH), 3.96–3.78 (m, 5H, NH-CH₂ & -OCH₃), 1.90–1.73 (m, 2H, CH₂), 1.53–1.36 (m, 2H, CH₂), 0.98 (t, $J = 7.4$ Hz, 3H, CH₃). ¹³C NMR (76 MHz, CDCl₃, δ): 161.5 (1C, ArC), 149.5 (1C, ArC), 135.8 (1C, ArC), 121.6 (2C, ArC), 119.8 (1C, ArC), 114.0 (1C, ArC), 112.2 (2C, ArC), 109.3 (1C, ArC), 100.0 (1C, ArC), 55.3 (1C), 43.0 (1C), 32.5 (1C), 20.5 (1C), 14.1 (1C); UV (CHCl₃) λ_{max} , nm (log ϵ):290 (6.76).

2-(4-Bromophenyl)-3-decyl-1,3,2-benzoxazaborole (9c).



In a 20 ml reaction vial 2-(decylamino)phenol (125 mg, 0.5 mmol, 1 equiv) and 4-bromophenylboronic acid (100 mg, 0.5 mmol, 1 equiv) were mixed in ethyl acetate (15 ml). The solvent was removed under vacuum at room temperature to give a dark orange solid (203 mg, 98%). ^1H NMR (301 MHz, CDCl_3 , δ): 7.77 (d, $J = 8.1$ Hz, 2H, ArH), 7.61 (d, $J = 8.2$ Hz, 2H, ArH), 7.29 (d, $J = 7.8$ Hz, 1H, ArH), 7.19-6.97 (3H, ArH), 3.91-3.79 (t, 2H, NH- CH_2), 1.84-1.70 (m, 2H, CH_2), 1.43-1.26 (m, 14H, CH_2), 0.88 (t, $J = 6.6$ Hz, 3H, CH_3) ^{13}C NMR (76 MHz, CDCl_3) δ 149.3 (1C, ArC), 138.5 (1C, ArC), 135.6 (2C, ArC), 131.5 (2C, ArC), 125.4 (1C, ArC), 121.9 (1C, ArC), 120.2 (1C, ArC), 112.4 (1C, ArC), 109.6 (1C, ArC), 43.1 (1C), 32.0 (1C), 30.3 (1C), 29.6 (1C), 29.4 (3C), 27.2 (1C), 22.8 (1C), 14.2 (1C) UV (CHCl_3) λ_{max} , nm (log ϵ):291 (6.76).

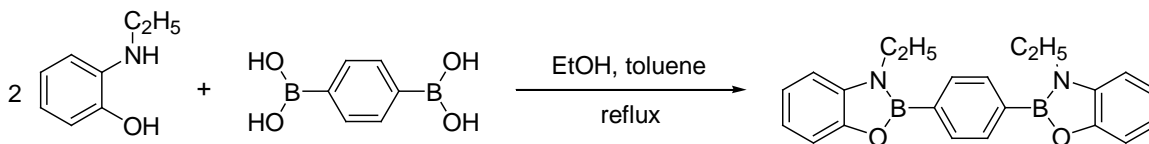
3-Decyl-2-(4-methoxyphenyl)-1,3,2-benzoxazaborole (10c).



In a 20 ml reaction vial 2-(decylamino)phenol (125 mg, 0.5 mmol, 1 equiv) and 4-methoxyphenylboronic acid (76 mg, 0.5 mmol, 1 equiv) were mixed in ethyl acetate (15 ml). The solvent was removed under vacuum at room temperature to give a dark orange solid (158 mg, 94%) ^1H NMR (301 MHz, CDCl_3 , δ): 7.89 (d, $J = 8.2$ Hz, 2H, ArH), 7.16-6.94 (m, 6H, ArH), 3.87 (t, 2H, NH- CH_2), 1.87-1.75 (m, 2H, CH_2), 1.49-1.32 (m, 14H, CH_2), 0.88 (t, $J = 6.6$ Hz, 3H, CH_3) ^{13}C NMR (76 MHz, CDCl_3 , δ): 161.5 (1C, ArC), 149.5 (1C, ArC), 138.9 (1C, ArC), 135.8 (1C, ArC), 121.6 (1C, ArC), 119.8 (1C, ArC), 113.9 (1C,

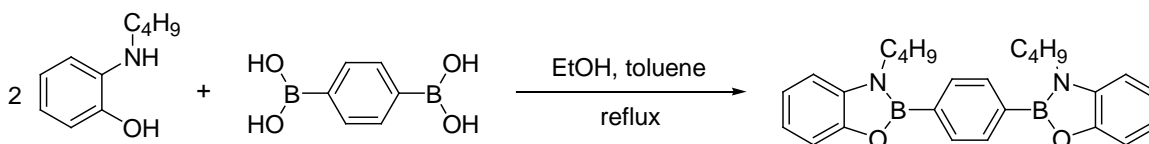
ArC), 112.1 (1C, ArC), 109.2 (1C, ArC), 55.2 (1C), 43.2 (1C), 32.0 (1C), 30.4 (1C), 29.7 (1C), 29.4 (3C), 27.2 (1C), 22.8 (1C), 14.2 (1C); UV (CHCl₃) λ_{\max} , nm (log ϵ): 290 (6.76).

1,4-Phenylene-bis-[3-(ethyl)benzoxazaborole] (13a).



In a 25 ml round bottom flask 2-(ethylamino)phenol (275 mg, 2.0 mmol, 2 equiv) and 1,4-benzenediboronic acid (166 mg, 1.0 mmol, 1 equiv) were mixed in ethanol (5 ml) and toluene (15 ml) and refluxed overnight with a Dean-Stark trap. The solvent was removed under vacuum at room temperature to give a colorless solid (378 mg, 90% yield). ¹H NMR (301 MHz, CDCl₃, δ): 8.02 (s, 4H), 7.32 (d, J = 7.7 Hz, 2H, ArH), 7.01–7.21 (m, 6H, ArH), 4.00 (q, J = 7.7 Hz, 4H, NH-CH₂), 1.48 (t, J = 7.2 Hz, 6H, CH₃), ¹³C NMR (76 MHz, CDCl₃, δ): 149.5 (2C, ArC), 138.4 (2C, ArC), 133.6 (4C, ArC), 121.9 (2C, ArC), 120.2 (2C, ArC), 112.4 (2C, ArC), 109.4 (4C, ArC), 37.7 (2C), 15.8 (2C); UV (CHCl₃) λ_{\max} , nm (log ϵ): 300.

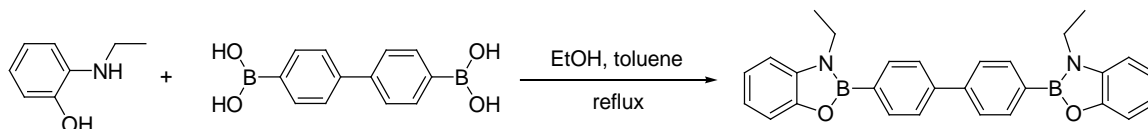
1,4-Phenylene-bis-[3-(butyl)benzoxazaborole] (13b).



In a 25 ml round bottom flask 2-(butylamino)phenol (331 mg, 2.0 mmol, 2 equiv) and 1,4-benzenediboronic acid (166 mg, 1.0 mmol, 1 equiv) were mixed in ethanol (5 ml) and toluene (15 ml) and refluxed overnight with a Dean-Stark trap. The solvent was removed under vacuum at room temperature to give a dark brown solid. (384 mg, 90% yield). ¹H NMR (301 MHz, CDCl₃, δ): 8.02 (s, 4H, ArH), 7.31 (d, J = 7.6 Hz, 2H, ArH),

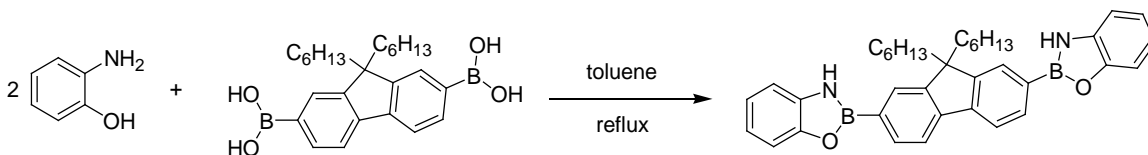
7.19–6.97 (m, 6H, ArH), 3.94 (t, 4H, NH-CH₂), 1.83 (quint, 4H, CH₂), 1.55–1.36 (m, 4H, CH₂), 0.97 (t, 6H, CH₃). ¹³C NMR (76 MHz, CDCl₃, δ): 149.5 (2C, ArC), 138.4 (2C, ArC), 133.6 (4C, ArC), 121.8 (2C, ArC), 120.1 (2C, ArC), 112.4 (2C, ArC), 109.6 (4C, ArC), 43.0 (2C), 32.5 (2C), 20.5 (2C), 14.0 (2C); UV (CHCl₃) λ_{max}, nm (log ε):301 (7.08).

Biphenyl-4-4'-bis-[3-(ethyl)benzoxazaborole] (15a).



In a 25 ml round bottom flask 2-(ethylamino)phenol (68.6 mg, 0.50 mmol, 2 equiv) and biphenyl-4-4'-diboronic acid (60.5 mg, 0.25 mmol, 1 equiv) were mixed in ethanol (5 ml) and toluene (15 ml) and refluxed for 3 days with a Dean Stark trap. The solvent was removed under vacuum at room temperature to give a off-white solid (110 mg, 99% yield). ¹H NMR (301 MHz, CDCl₃, δ): 8.03 (d, *J* = 8.0 Hz, 2H, ArH), 7.77 (d, *J* = 8.1 Hz, 2H, ArH), 7.32 (d, *J* = 7.6Hz, 2H, ArH), 7.11-7.05 (m, 6H, ArH), 4.01 (q, *J* = 7.3 Hz, 4H, NH-CH₂), 1.48 (t, *J* = 7.2 Hz, 6H, CH₃). ¹³C NMR (76 MHz, CDCl₃, δ): 149.5 (2C, ArC), 142.7 (2C, ArC), 138.5 (2C, ArC), 134.6 (4C, ArC), 127.0 (4C, ArC), 121.9 (2C, ArC), 120.1 (2C, ArC), 112.4 (2C, ArC), 109.3 (4C, ArC), 37.7 (2C), 15.8 (2C). UV (CHCl₃) λ_{max}, nm (log ε):308 (7.39).

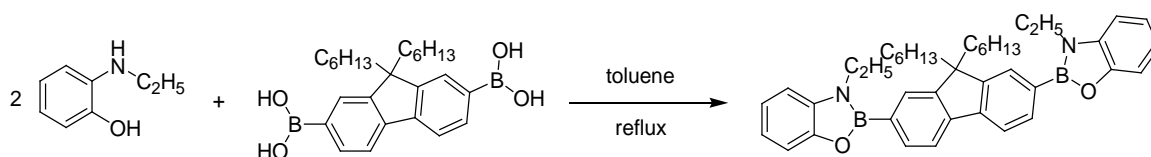
9,9-Dihexylfluorene-2,7-bis(benzoxazaborole) (17).



In a 25 ml round bottom flask 2-aminophenol (54.6 mg, 0.50 mmol, 2 equiv) and 9,9-dihexylfluorene-2,7-diboronic acid (105.5 mg, 0.25 mmol, 1 equiv) were mixed in toluene (15 ml) and refluxed for 3 days with a Dean-Stark trap. The solvent was removed

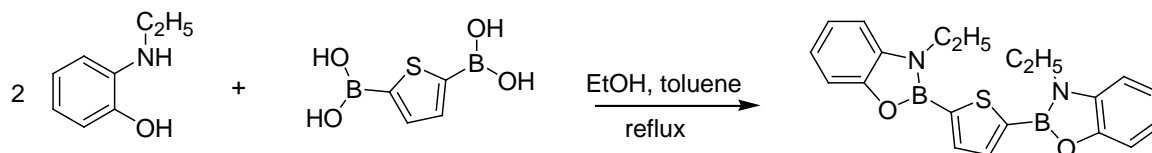
under vacuum at room temperature to give a colorless solid. (137 mg, 95% yield). ^1H NMR (301 MHz, CDCl_3 , δ): 7.96–7.79 (m, 4H, ArH), 7.34 (d, $J = 7.4$ Hz, 2H, ArH), 7.17–6.97 (m, 6H, ArH), 6.92 (br s, 2H, NH), 2.15–1.99 (m, 4H, CH_2), 1.16–0.54 (m, 22H, $(\text{CH}_2)_4\text{CH}_3$). ^{13}C NMR (76 MHz, CDCl_3) δ 150.9 (2C, ArC), 149.9 (2C, ArC), 143.6 (2C, ArC), 136.5 (2C, ArC), 132.7 (2C, ArC), 128.1 (2C, ArC), 122.1 (2C, ArC), 120.4 (2C, ArC), 120.1 (4C, ArC), 112.5 (2C, ArC), 111.3 (2C, ArC), 40.6 (2C), 31.6 (2C), 29.8 (2C), 23.9 (2C), 22.7 (2C), 14.1 (2C), 14.1 (2C).

9,9-Dihexylfluorene-2,7-bis-[3-(ethyl)benzoxazaborole] (17a).



In a 25 ml round bottom flask 2-(ethylamino)phenol (68.6 mg, 0.50 mmol, 1 equiv) and 9,9-dihexylfluorene-2,7-diboronic acid (105.5 mg, 0.25 mmol, 1 equiv) were mixed in toluene (15 ml) and refluxed for 3 days with a Dean-Stark trap. The solvent was removed under vacuum at room temperature to give a colorless solid. (148 mg, 95% yield). ^1H NMR (301 MHz, CDCl_3 , δ): 8.08–7.86 (m, 6H, ArH), 7.39 (d, $J = 7.6$ Hz, 2H, ArH), 7.23–7.02 (m, 6H, ArH), 4.06 (q, $J = 7.2$ Hz, 4H, NH- CH_2), 2.27–1.99 (m, 4H, - CH_2), 1.53 (t, $J = 7.1$ Hz, 6H, CH_3), 1.25–0.64 (m, 22H, $(\text{CH}_2)_4\text{CH}_3$). ^{13}C NMR (76 MHz, CDCl_3 , δ): 150.9 (2C, ArC), 149.57 (2C, ArC), 143.1 (2C, ArC), 138.6 (2C, ArC), 132.7 (2C, ArC), 128.6 (2C, ArC), 121.9 (2C, ArC), 120.1 (2C, ArC), 120.4 (2C, ArC), 112.3 (2C, ArC), 109.2 (4C, ArC), 55.3 (2C), 40.6 (2C), 37.8 (2C), 31.6 (2C), 29.8 (2C), 24.0 (2C), 22.7 (2C), 15.8 (2C), 14.1 (2C).

2,5-Thiophenediyl-bis-[3-(ethyl)benzoxaborole] (19a).



In a 25 ml round bottom flask 2-(ethylamino)phenol (137 mg, 1 mmol, 1 equiv) and 2,5-thiophenediylbisboronic acid (85.9 mg, 1 mmol, 2 equiv) were mixed in ethanol (1 ml) and toluene (15 ml) and refluxed for 3 days with a Dean-Stark trap. The solvent was removed under vacuum at room temperature to give a colorless solid. (190 mg, 90% yield). ¹H NMR (301 MHz, CDCl₃, δ): 7.95 (s, 2H, ArH), 7.33 (d, *J* = 7.8 Hz, 2H, ArH), 7.22–7.00 (m, 6H, ArH), 4.06 (q, *J* = 7.2 Hz, 4H, NH-CH₂), 1.47 (t, *J* = 7.2 Hz, 6H, CH₃). ¹³C NMR (76 MHz, CDCl₃, δ): 149.5 (2C, ArC), 138.1 (2C, ArC), 137.1 (2C, ArC), 129.1 (2C, ArC), 121.9 (2C, ArC), 120.1 (2C, ArC), 112.4 (2C, ArC), 109.1 (4C, ArC), 37.9 (2C), 15.7 (2C).

CHAPTER III

Dynamic Covalent Exchange: Benzoxazaboroles

3.1 Introduction

Dynamic covalent reversibility is an important feature during the synthesis of boron-based covalent organic frameworks. Benzodioxaboroles, or boronate esters, are well known species that are capable of dynamic self repair.³⁹ More recently, the dynamic covalent nature of diazaboroles was shown by our research group.^{28,34} At the same time, we found that benzoxazaboroles and benzodioxaboroles have the ability to undergo exchange reactions.

3.2 Objectives

The goal of this project was to study dynamic covalent nature of 3-(alkyl)benzoxazaboroles under mild reaction conditions. This was accomplished experimentally by reacting 3-(alkyl)benzoxazaboroles with benzodioxaboroles in different ratios. Equilibrium constant and Gibbs free energy values of exchange reactions will be determined experimentally and calculated computationally.

3.3 Results and Discussion

3.3.1 Dynamic covalent exchange of benzoxazaboroles. To analyze capability of dynamic covalent exchange a 1:1 ratio of 3-butyl-2-phenyl-1,3,2-benzoxazaborole (**6b**) and 2-(ethylamino)phenol (**4a**) were mixed in CDCl₃ (Figure 47).

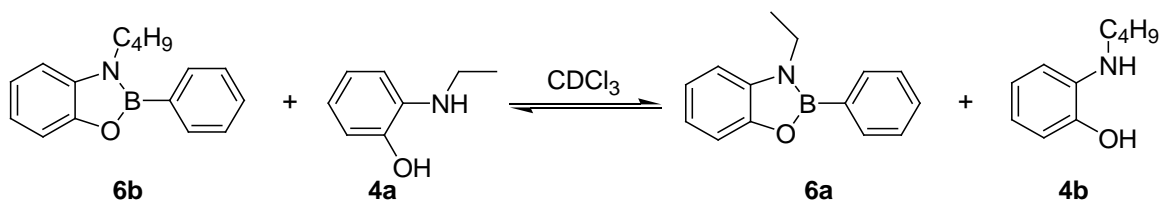


Figure 47. Reaction of benzoxazaborole **6b** and 2-(ethylamino)phenol (**4a**).

Apparent equilibrium was achieved soon after mixing the reactants, and ^1H NMR analysis was used to identify the presence of 3-ethyl-2-phenyl-1,3,2-benzoxazaborole (**6a**), 3-butyl-2-phenyl-1,3,2-benzoxazaborole (**6b**), 2-(ethylamino)phenol (**4a**) and 2-(butylamino)phenol (**4b**) (Figure 48). In the ^1H NMR spectrum of the reaction mixture, a quartet and triplet were observed at the chemical shift (~ 4 ppm) corresponding to the *N*-methylene protons of benzoxazaboroles **6a** and **6b**. This confirms the dynamic covalent exchange of **6b** and **6a**. When comparing the integral values of the two *N*-methylene signals, a nearly 1:1 ratio of **6a** and **6b** is observed. This indicates that each of the 3-(alkyl)benzoxazaboroles have similar stabilities and their stability is not affected by the length of the alkyl chain.

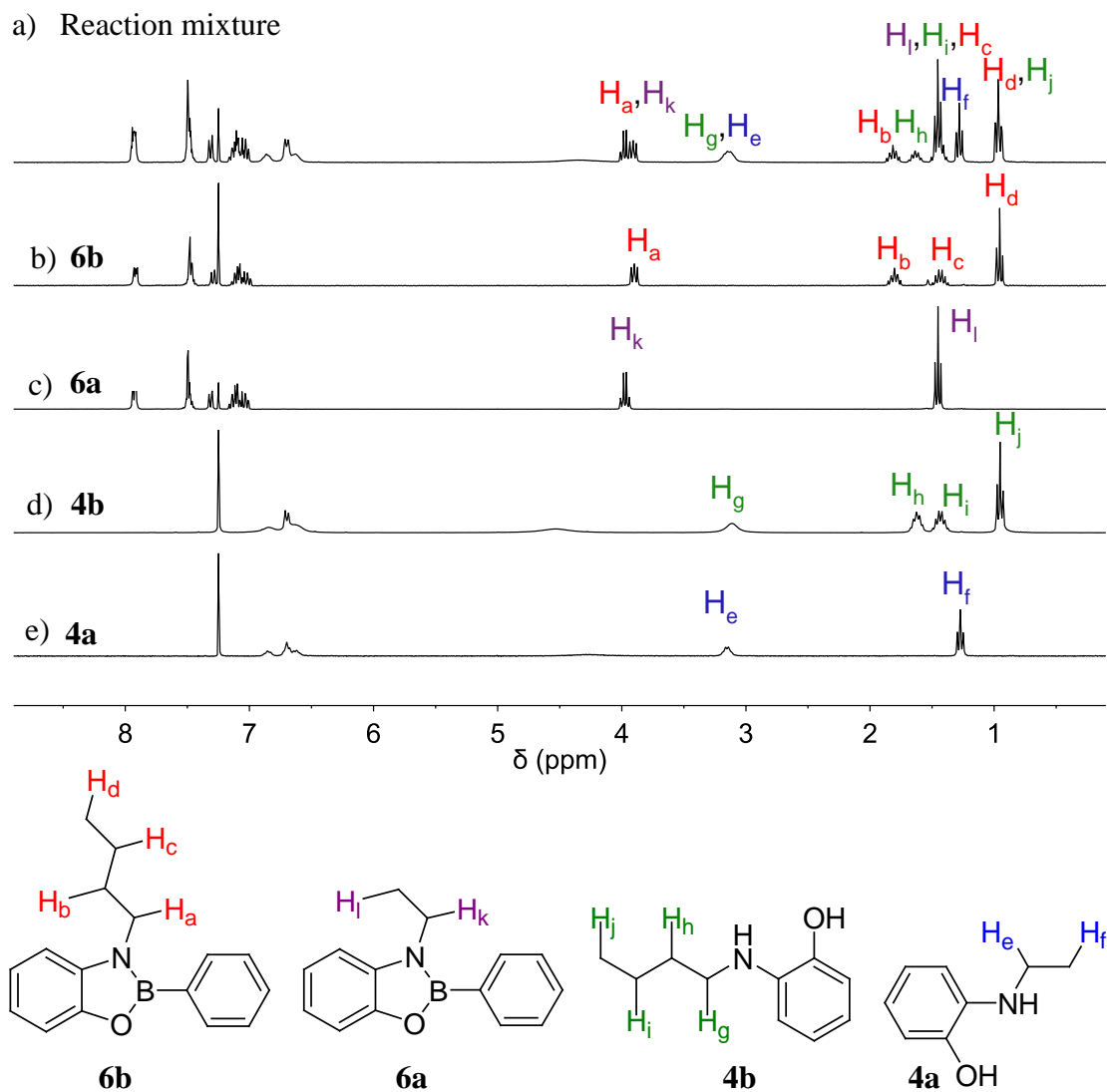


Figure 48. ^1H NMR spectra of a) the reaction mixture of 3-butyl-2-phenyl-1,3,2-benzoxazaborole (**6b**) and 2-(ethylamino)phenol (**4a**), b) pure 3-butyl-2-phenyl-1,3,2-benzoxazaborole (**6b**), c) pure 3-ethyl-2-phenyl-1,3,2-benzoxazaborole (**6a**), d) pure 2-(butylamino)phenol (**4b**), and e) pure 2-(ethylamino)phenol (**4a**) in CDCl_3 .

The Gibbs free energy of the above reaction was calculated computationally using DFT and B3LYP function with the 6-311++G(d,p) method in the gas phase at room temperature.

$$\Delta G^\circ = (\text{Energy } \mathbf{6a} + \text{Energy } \mathbf{4b}) - (\text{Energy } \mathbf{6b} + \text{Energy } \mathbf{4a})$$

$$\Delta G^\circ = [(-696.827) + (-520.030)] - [(-775.423) + (-441.434)]$$

$$\Delta G^\circ = 0 \text{ Hartrees}$$

$$\Delta G^\circ = 0 \text{ kJ/mol}$$

The ΔG° was found to be 0 kJ/mol. This supports the experimental observation that both **6a** and **6b** have similar energy and stabilities.

3.3.2 Dynamic covalent exchange: the reaction of benzoxazaboroles with catechol. To investigate the relative stabilities of benzoboroles direct mixing experiments were carried out. Benzoxazaborole **6c** and catechol **21** were mixed in a 1:1 ratio in CDCl₃ (Figure 49). The mixture reached apparent steady state conditions within five minutes and there was no change in the ¹H NMR spectrum over 24 h.



Figure 49. Reaction of 3-decyl-2-phenyl-1,3,2-benzoxazaborole (**6c**) with catechol (**21**).

In the ¹H NMR spectrum of the reaction mixture, signals corresponding to both starting materials and products were observed (Figure 50). When mixing a 1:1 ratio of **6c:21** nearly 1:1 ratio of **6c:22** was observed. This indicates dynamic covalent exchange between **6c** and **22**.

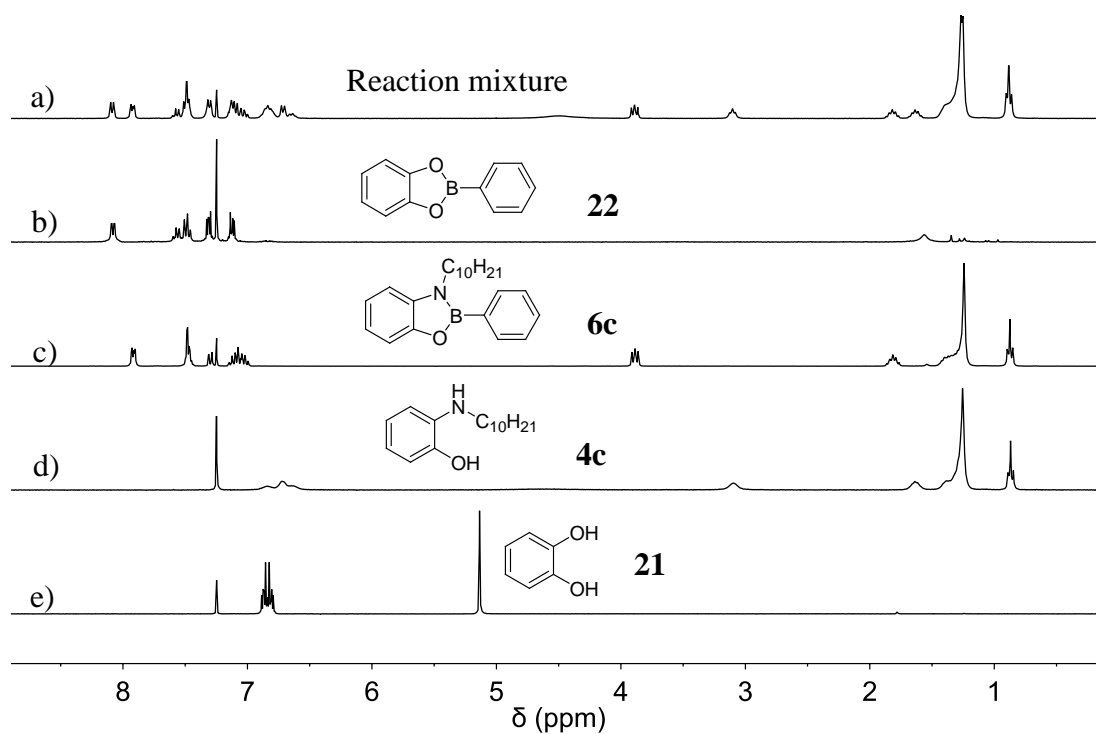


Figure 50. ^1H NMR spectra of a) the 1:1 reaction mixture of **6c** and **21**, b) benzodioxaborole **22**, c) 3-decyl-1,3,2-benzoxazaborole (**6c**), d) 2-(decylamino)phenol (**4c**), and e) catechol (**21**) in CDCl_3 .

The reaction was also run at a 2:1 and 1:2 ratio of **6c**:**21**, respectively (Figure 51). The ratio of **6c**:**21** was determined by integrating the protons ortho to the boron atom of **6c** (H_b) and **21** (H_a) and the methylene protons **6c** (H_c) and **4c** (H_d).

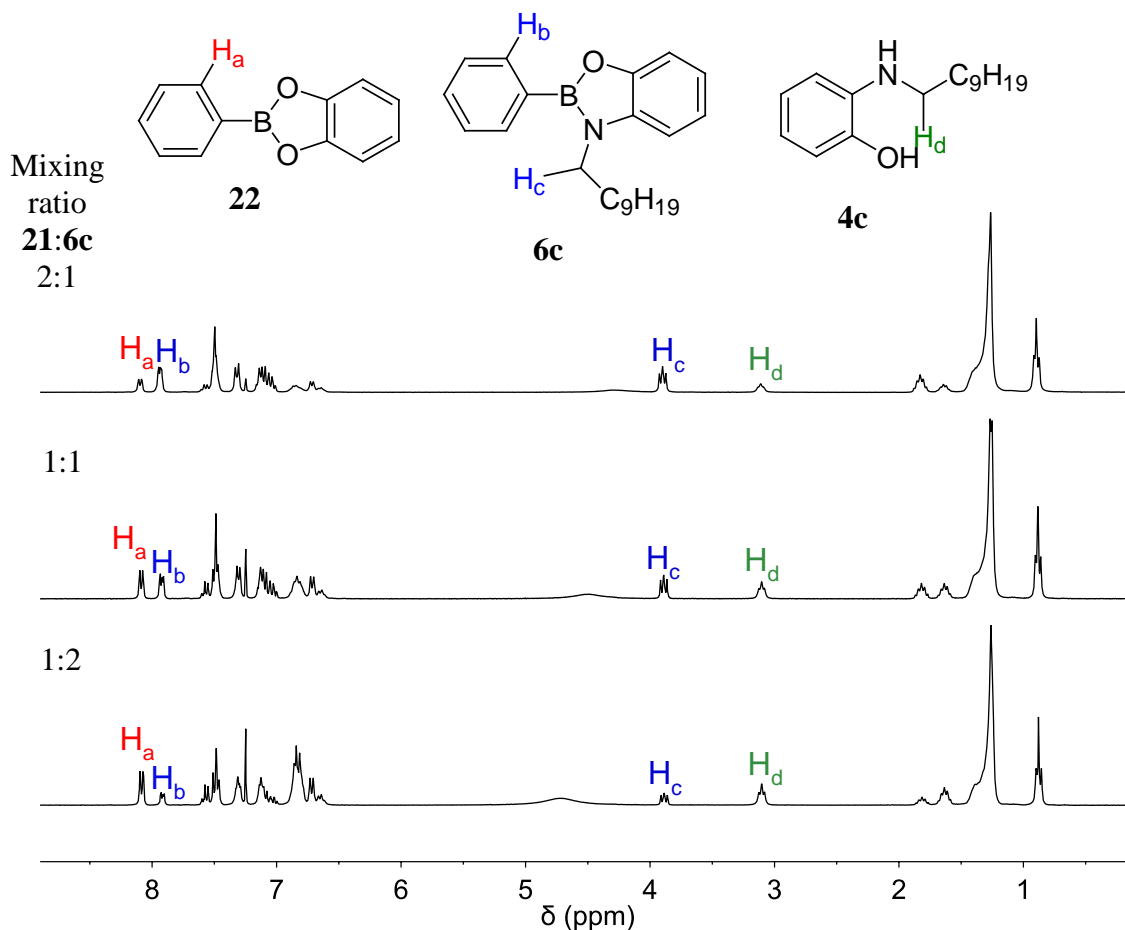


Figure 51. ^1H NMR spectra the for reaction of 3-decyl-2-phenyl-1,3,2-benzoxazaborole (**6c**) and catechol (**21**).

In total, six different experiments were conducted, three experiments involved increasing the concentration of **6c** while holding the concentration of **21** constant, and three experiments involved increasing the concentration of **21** while keeping the concentration of **6c** constant. The equilibrium constant (K_{eq}) for each of the above reactions was calculated using the integral values of protons H_a , H_b , H_c , and H_d (Tables 9 and 10). Between the six measurements and two sets of integrals 12 K_{eq} values were calculated.

$$K_{eq} = \frac{[22][4c]}{[6c][21]}$$

For the 1:2 (**6c:21**) ratio K_{eq} was calculated using the integral values [] of H_a (**22**) and H_b (**6b**).

	6c	21	22	4c
Initial	[6c]+[22]	2([6c]+[22])	0	0
Change	-[22]	-[22]	[22]	[22]
At Equilibrium	[6c]	2[6c]+[22]	[22]	[22]

For 1:2,

$$K_{eq} = \frac{[22]^2}{2[6c]^2 + [22][6c]}$$

For the 1:1 (**6c:21**) ratio K_{eq} was calculated using the integral values [] of H_a (**22**) and H_b (**6c**).

	6c	21	22	4c
Initial	[6c]+[22]	[6c]+[22]	0	0
Change	-[22]	-[22]	[22]	[22]
At Equilibrium	[6c]	[6c]	[22]	[22]

For 1:1,

$$K_{eq} = \frac{[22]^2}{[6c]^2}$$

For the 2:1 mixing (**6c:21**) ratio K_{eq} was calculated using the integral values [] of H_a (**22**) and H_b (**6b**).

	6c	21	22	4c
Initial	[6c]+[22]	([6c]+[22])/2	0	0
Change	-[22]	-[22]	[22]	[22]
At Equilibrium	[6c]	([6c]-[22])/2	[22]	[22]

$$K_{eq} = \frac{[22]^2}{([6c])([6c]-[22])/2}$$

For 2:1,

$$K_{eq} = \frac{[22]^2}{([6c]^2 - [6c][22])/2}$$

The Gibbs free energy (ΔG°) was calculated using the above determined K_{eq} .

$$\Delta G^\circ = -RT \ln K_{eq}$$

Where,

R = Universal gas constant, 8.314 J/mol K

T = Absolute temperature, 298.15 K

K_{eq} = Equilibrium constant

Table 9

Equilibrium constants, calculated using the integral values for protons H_a and H_b of 6c and 22.

Mixing ratio of 6c:21	[6c] ^a	[21] ^b	[22] ^a	[4c] ^b	<i>K</i> _{eq}	Δ <i>G</i> ^o (kJ/mol)
1:2 ^c	0.4	1.8	1	1	1.39	-0.821
1:1 ^c	1	1	1	1	1	0
2:1 ^c	2.18	0.59	1	1	0.78	0.620
2:1 ^d	1.64	0.325	0.99	0.99	1.84	-1.520
1:1 ^d	0.82	0.82	0.99	0.99	1.46	-0.944
1:2 ^d	0.33	1.64	0.98	0.98	1.77	-1.424

^aintegral values measured directly, ^bcalculated integral values, ^camount of **21** was held constant (0.05 mmol), and ^damount of **6c** was held constant (0.05 mmol).

Table 10

Equilibrium constants, calculated using the integral values for protons H_c and H_d of 6c and 4c.

Mixing ratio of 6c:21	[6c] ^a	[21] ^b	[22] ^a	[4c] ^b	<i>K</i> _{eq}	Δ <i>G</i> ^o (kJ/mol)
1:2 ^c	0.4	1.74	0.94	0.94	1.27	-0.596
1:1 ^c	0.98	0.98	0.94	0.94	0.92	0.208
2:1 ^c	2.27	0.68	0.91	0.91	0.54	1.537
2:1 ^d	3.35	0.765	1.82	1.82	1.29	-0.635
1:1 ^d	0.80	0.80	0.93	0.93	1.35	-0.748
1:2 ^d	0.32	1.58	0.94	0.94	1.75	-1.396

^aintegral values measured directly, ^bcalculated integral values, ^camount of **21** was held constant (0.05 mmol), and ^damount of **6c** was held constant (0.05 mmol).

The average K_{eq} of the above reaction is 1.28 ± 0.41 . The average Gibbs free energy (ΔG°) of the above reaction is -0.48 ± 0.92 kJ/mol. The high standard deviation associated with ΔG° is likely due to weighing errors when measuring small quantities of reactants. According to the small average ΔG° value, there is no significant difference in energy between benzodioxaborole **22** and benzoxazaborole **6c**.

The Gibbs free energy of above reaction was calculated computationally using DFT and B3LYP function with the 6-311++G(d,p) method in the gas phase at room temperature. The ΔG° was found to be -8 kJ/mol. The small calculated ΔG° value suggests that there is no significant difference in energy between 3-(decyl)benzoxazaborole (**6c**) and benzodioxaborole **22**.

$$\Delta G^\circ = (\text{Energy } \mathbf{22} + \text{Energy } \mathbf{4c}) - (\text{Energy } \mathbf{6c} + \text{Energy } \mathbf{21})$$

$$\Delta G^\circ = [(-638.126) + (-755.820)] - [(-1011.213) + (-382.730)]$$

$$\Delta G^\circ = -0.003 \text{ Hartrees}$$

$$\Delta G^\circ = -8 \text{ kJ/mol}$$

Similar results were obtained when mixing of 2-(4-bromophenyl)-3-butyl-1,3,2-benzoxazaborole **3** and catechol (**21**) (Figure 52). Different ratios (2:1, 1:1, and 1:2) of **9b:21** were mixed in two different series of experiments similar to that described in the previous section and proton NMR spectra were obtained (Figure 53).

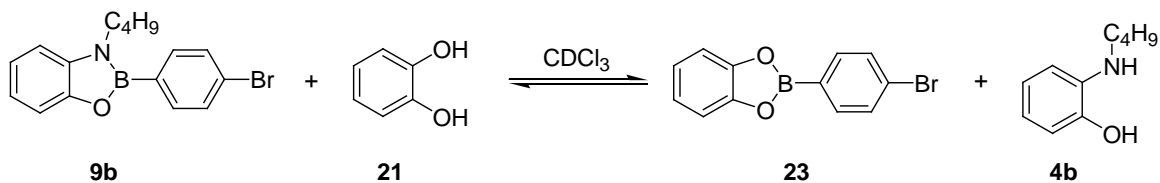


Figure 52. Exchange reaction of 2-(4-bromophenyl)-3-butyl-1,3,2-benzoxazaborole (**9b**) and catechol (**21**).

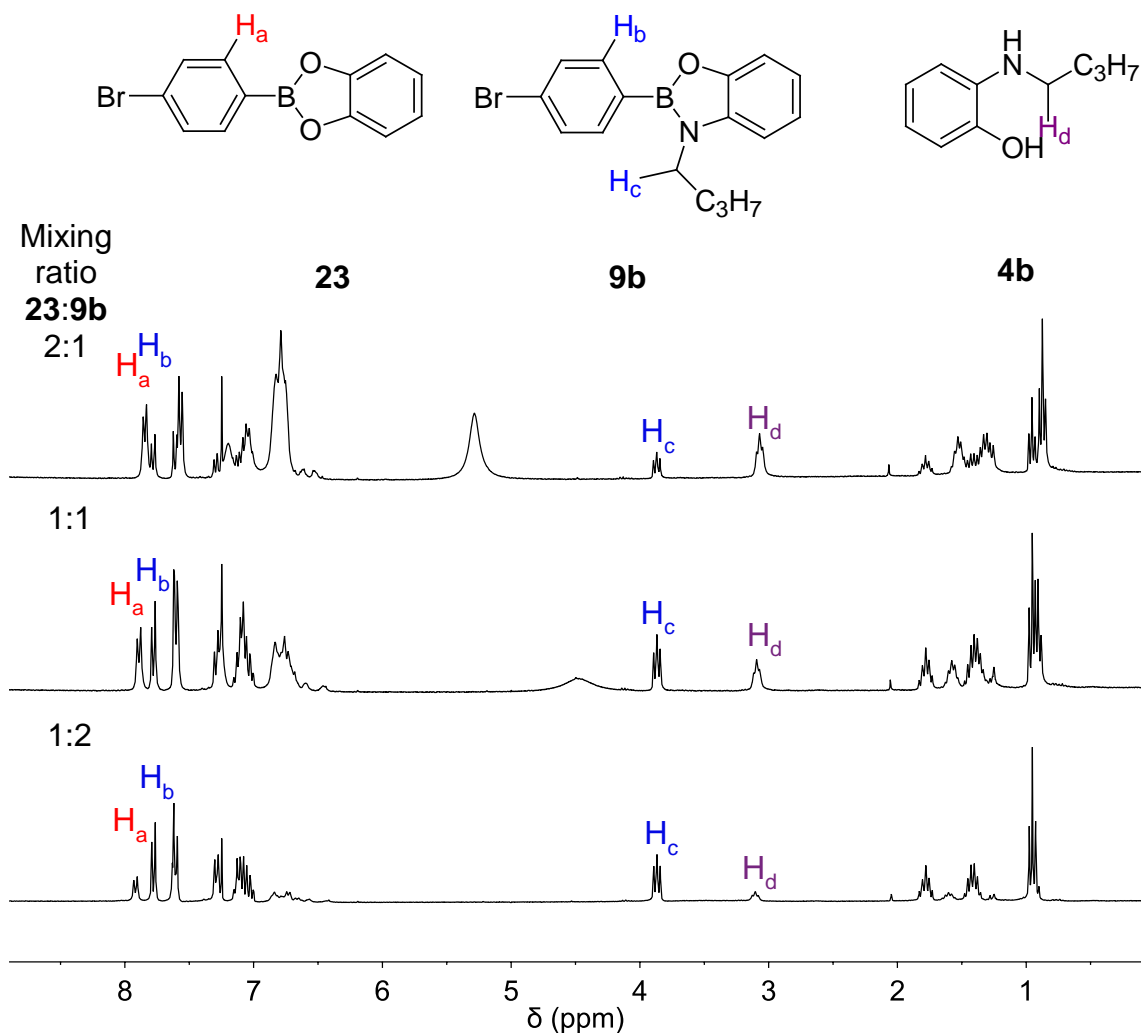


Figure 53. ^1H NMR spectra for the reaction of 2-(4-bromophenyl)-3-butyl-1,3,2-benzoxazaborole (**9b**) and catechol (**21**) in a 2:1, 1:1, and 1:2 ratio.

As can be seen from the relative proton signals near 8 ppm (H_a and H_b), oxazaborole and dioxaborole are both present which indicates that the starting materials underwent dynamic covalent exchange. When mixing benzoxazaboroles and catechol in a 1:1 ratio a near 1:1 mixture of benzoboroles **9b** and **23** is observed. In total six different experiments were conducted three experiments involved increasing the concentration of **9b** while holding the concentration of **21** constant and three experiments involved increasing the concentration of **21** while keeping the concentration of **9b** constant. The

equilibrium constant (K_{eq}) for each of the above reactions was calculated using the integral values of protons H_a, H_b, H_c, and H_d (Tables 11 and 12). Between the six measurements and two sets of integrals 11 K_{eq} values were calculated. It was not possible to integrate H_a and H_b accurately for the 2:1 mixture. K_{eq} and ΔG° were calculated similar to the previous method.

Table 11

*Equilibrium constants, calculated using the integral values for protons H_a and H_b of **9b** and **23**.*

Mixing ratio of 9b:21	[9b] ^a	[21] ^b	[23] ^a	[4b] ^b	K_{eq}	ΔG° (kJ/mol)
2:1 ^c						
1:1 ^d	0.84	0.84	0.99	0.99	1.39	-0.821
1:2 ^d	2.08	0.52	1.03	1.03	0.97	0.075
1:2 ^e	0.38	1.68	0.92	0.92	1.33	-0.711
1:1 ^e	1.27	1.27	1.41	1.41	1.23	-0.516
2:1 ^e	1.96	0.54	0.87	0.87	0.71	0.854

^aintegral values measured directly, ^bcalculated integral values, ^coverlapping signals prevented accurate measurement of integrals, ^damount of **9b** was held constant (0.05 mmol), and ^eamount of **21** was held constant (0.05 mmol).

Table 12

*Equilibrium constants, calculated using the integral values for protons H_c and H_d of **9b** and **4b**.*

Mixing ratio of 9b:21	[9b] ^a	[21] ^b	[23] ^b	[4b] ^a	K_{eq}	ΔG° (kJ/mol)
2:1 ^c	0.59	1.115	1.64	1.64	0.24	3.559
1:1 ^c	1.18	1.18	1.06	1.06	0.76	0.684
1:2 ^c	0.62	2.19	0.95	0.95	1.65	-1.249
1:2 ^d	0.38	1.47	0.71	0.71	0.90	0.262
1:1 ^d	1.26	1.26	0.99	0.99	0.62	1.192
2:1 ^d	1.93	0.74	0.45	0.45	0.14	4.903

^aintegral values measured directly, ^bcalculated integral values, ^camount of **9b** was held constant (0.05 mmol), and ^damount of **21** was held constant (0.05 mmol).

The average K_{eq} of the above reaction is 0.90 ± 0.47 . The average Gibbs free energy (ΔG°) of the above reaction is 0.75 ± 1.90 kJ/mol. Again, the high standard deviation associated with ΔG° is likely due to weighing errors when measuring small quantities of reactants. According to the small average ΔG° value, there is no significant difference in energy between **23** and **9b**.

The Gibbs free energy of above reaction was calculated computationally using DFT and B3LYP function with the 6-311++G (d,p) method in the gas phase at room temperature. The ΔG° was found to be -5 kJ/mol. The small calculated ΔG° supports that there is no significant difference in energy between **23** and **9b**.

$$\Delta G^\circ = (\text{Energy } \mathbf{23} + \text{Energy } \mathbf{4b}) - (\text{Energy } \mathbf{9b} + \text{Energy } \mathbf{21})$$

$$\Delta G^\circ = [(-3211.682) + (-520.030)] - [(-3348.980) + (-382.730)]$$

$$\Delta G^\circ = -0.002 \text{ Hartrees}$$

$$\Delta G^\circ = -5 \text{ kJ/mol}$$

3.3.3 Dynamic covalent exchange: the reaction of benzodioxaborole with 2-(butylamino)phenol. The reverse reaction was carried out starting with benzodioxaborole **23** and 2-(butylamino)phenol (**4b**), the products from the previous experiment. Again the reactants were mixed in different ratios (2:1, 1:1, and 1:2, respectively) in CDCl_3 (Figure 54). The mixtures reached equilibrium within five minutes.

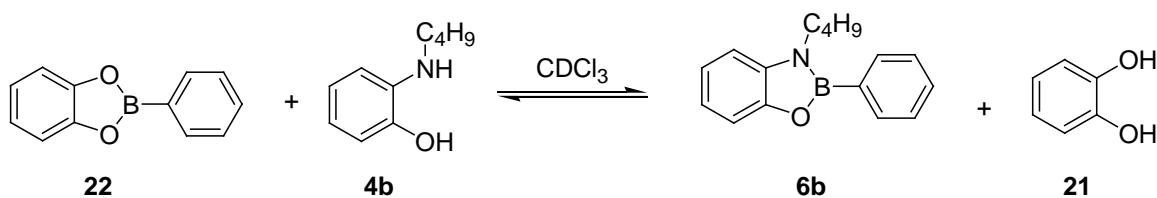


Figure 54. Exchange reaction of benzodioxaborole (**22**) and 2-(butylamino)phenol (**4b**).

The ratio of **6b**:**22** was determined by integrating the signals corresponding to the protons ortho to the boron atom of **6b** (H_b) and **22** (H_a) (Figure 55). The methylene signals H_c (**6b**) and H_d (**4b**) were also used to determine equilibrium data. When mixing benzodioxaborole **22** and 2-(butylamino)phenol (**4b**) in a 1:1 ratio a near 1:1 mixture of benzoboroles **6b** and **22** was observed.

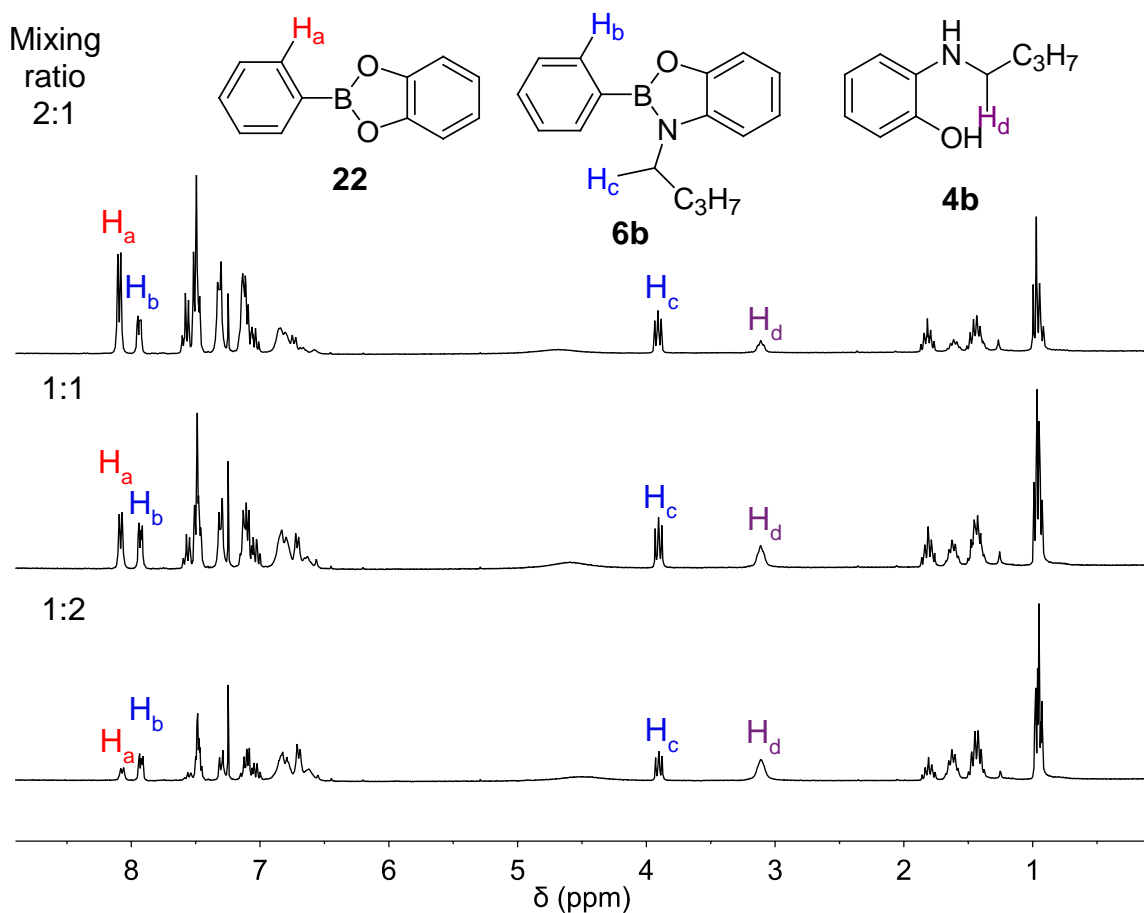


Figure 55. ^1H NMR spectra for the reaction of benzodioxaborole (**22**) and 2-(butylamino)phenol (**4b**) in a 2:1, 1:1, and 1:2 ratio.

In total six different experiments were conducted three experiments involved increasing the concentration of **22** while holding the concentration of **4b** constant and three experiments involved increasing the concentration of **4b** while keeping the concentration of **22** constant. The equilibrium constant (K_{eq}) for each of the above reactions was calculated using the integral values of protons H_a , H_b , H_c , and H_d (Tables 13 and 14). Between the six measurements and two sets of integrals 12 K_{eq} and ΔG° values were calculated similar to the previous method.

Table 13

*Equilibrium constants, calculated using the integral values for protons H_a and H_b of **22** and **6b**.*

Mixing ratio of 22:4b	[22] ^a	[4b] ^b	[6b] ^a	[21] ^b	<i>K</i> _{eq}	Δ <i>G</i> ^o (kJ/mol)
2:1 ^c	1.46	0.42	0.62	0.62	0.63	1.152
1:1 ^c	1.60	1.60	1.36	1.36	0.72	0.819
1:2 ^c	0.95	3.68	1.78	1.78	0.91	0.235
1:2 ^d	1.25	6.26	3.76	3.76	1.81	-1.480
1:1 ^d	1.14	1.14	0.73	0.73	0.41	2.224
2:1 ^d	1.10	0.40	0.30	0.30	0.20	3.990

^aintegral values measured directly, ^bcalculated integral values, ^camount of **22** was held constant (0.05 mmol), and ^damount of **4b** was held constant (0.05 mmol).

Table 14

*Equilibrium constants, calculated using the integral values for protons H_c and H_d of **6b** and **4b**.*

Mixing ratio of 22:4b	[22] ^a	[4b] ^b	[6b] ^a	[21] ^b	<i>K</i> _{eq}	Δ <i>G</i> ^o (kJ/mol)
2:1 ^c	1.28	0.33	0.62	0.62	0.91	0.234
1:1 ^c	1.52	1.52	1.37	1.37	0.81	0.522
1:2 ^c	0.895	3.66	1.87	1.87	1.07	-0.168
1:2 ^d	1.595	6.96	3.77	3.77	1.07	-0.168
1:1 ^d	1	1.14	1	1.14	1.30	-0.650
2:1 ^d	0.69	0.20	0.29	0.29	0.61	1.225

^aintegral values measured directly, ^bcalculated integral values, ^camount of **22** was held constant (0.05 mmol), and ^damount of **4b** was held constant (0.05 mmol).

The average K_{eq} of the above reaction is 0.87 ± 0.42 . The average Gibbs free energy (ΔG°) of the above reaction is 0.66 ± 1.42 kJ/mol. Again, the high standard deviation associated with ΔG° is likely due to weighing errors when measuring small quantities of reactants. According to the small average ΔG° value, there is no significant difference in energy between **6b** and **22**.

The Gibbs free energy of above reaction was calculated computationally using DFT and B3LYP function with the 6-311++G(d,p) method in gas the phase at room temperature. The ΔG° was found to be 8 kJ/mol. The small calculated ΔG° value suggests that there is no significant difference in energy between **6b** and **24**.

$$\Delta G^\circ = (\text{Energy } \mathbf{6b} + \text{Energy } \mathbf{21}) - (\text{Energy } \mathbf{22} + \text{Energy } \mathbf{4b})$$

$$\Delta G^\circ = [(-775.423) + (-382.730)] - [(-638.126) + (-520.030)]$$

$$\Delta G^\circ = 0.003 \text{ Hartrees}$$

$$\Delta G^\circ = 8 \text{ kJ/mol}$$

3.4 Conclusions

All of the above reactions achieved apparent equilibrium in short time under mild reaction conditions and they provide evidence of dynamic exchange between 3-(alkyl)benzoxazaboroles and dioxaboroles. The experimental data supports that the stability of 3-(alkyl)benzoxazaboroles does not depend on the length of the alkyl chain. Computational calculations supported this data by giving ΔG° of 0 kJ/mol for the 3-(alkyl)benzoxazaborole exchange reaction. The dynamic covalent exchange between benzoxazaborole **6c** and benzodioxaborole **22** gave average experimental K_{eq} of 1.28 ± 0.41 and average ΔG° value of -0.48 ± 0.92 kJ/mol. The computationally calculated ΔG° value for the same reaction was found to be 8 kJ/mol. The exchange reaction

between benzoxazaborole **9b** and catechol **21** gave average experimental K_{eq} of 0.90 ± 0.47 and average ΔG° value of -0.75 ± 1.90 kJ/mol. The computationally calculated ΔG° value for the same reaction was found to be 5 kJ/mol. The exchange reaction between benzodioxaborole **22** and catechol **4b** gave average experimental K_{eq} of 0.87 ± 0.42 and average ΔG° value of 0.66 ± 1.42 kJ/mol. The computationally calculated ΔG° value for the same reaction was found to be 8 kJ/mol. The experimental and computational ΔG° values suggests that benzoxazaborole and benzodioxaborole have similar stability.

3.5 Experimental Section

Chemicals and reagents. Starting materials **6b**, **4a**, **6c**, and **9b** were synthesized as described in chapter II. Benzodioxaborole **22** was synthesized by former group member Dulamini Ekanayake.⁴⁰ Catechol (**21**) was purchased from Alfa Aesar and used without further purification. The CDCl_3 was stored over 4 Å molecular sieves.

NMR spectroscopy. The ^1H spectra were collected on a JEOL Eclipse 300+ spectrometer. Chemical shifts are reported in δ (ppm) relative to the solvent signal (CHCl_3 : 7.26 for ^1H). The splitting patterns are designated as d (doublet), t (triplet), and m (multiplet).

Computational calculations. All computational calculations were performed with the Gaussian G09W suite of programs. Originally, the molecular structures were built within the GaussView 5.0 interface and the geometric optimization in the gas phase was carried out to obtain geometries with lowest energy by utilizing computationally low cost, Hartree-Fock (HF) level with a minimum basis set (3-21G). Then the optimized geometries were subjected to full convergence geometry optimization using density functional theory (DFT) and B3LYP function with the 6-311++G(d,p) basis set to obtain

a more accurate geometry. The molecules were then subjected to frequency calculations at the same level of theory.³⁵

3.5.1 Dynamic covalent exchange analysis of 3-butyl-2-phenyl-1,3,2-benzoxazaborole (6b) and 2-(ethylamino)phenol (4a). 3-(butyl)benzoxazaborole (**6b**) (12.5 mg, 0.05 mmol) and 2-(ethylamino)phenol (**4a**) (6.9 mg, 0.05 mmol), and CDCl₃ (0.7 ml) were combined in a NMR tube and the reaction progress was monitored using NMR spectroscopy. There was no difference in the spectra between the first measurement (soon after mixing) and after 24h. Partial ¹H NMR data (301 MHz, CDCl₃) δ 7.97-7.89 (m, 4H (**6a** & **6b**)), 4.04-3.85 (m, 4H (**6a** & **6b**)), 1.90-1.76 (m, 2H (**6b**)), 1.72-1.56 (m, 2H (**4b**)), 1.54-1.35 (m, 7H (**6a**, **6b** & **4b**)), 1.28 (t, $J = 7.1$ Hz, 3H (**4a**)) 1.03-0.89 (m, 6H (**4b** & **6b**)).

3.5.2 Dynamic covalent exchange analysis of 2-phenyl-3-decyl-1,3,2-benzoxazaborole (6c) and catechol (21). Benzoxazaborole **6a** catechol (**21**) and CDCl₃ (0.7 ml) were combined in a NMR tube as shown in Table 15 in six different experiments, three experiments (1-3) with an increasing amount of catechol (**21**) and other three experiments (4-6) with an increasing amount of **6c**.

Table 15

Amount of 3-decyl-2-phenyl-1,3,2-benzoxazaborole (6c) and catechol (21) used in each experiment.

Experiment number	Ratio	Amount of 6c (mg)	mmol	Amount of 21 (mg)	mmol
1	2:1	16.8	0.05	2.8	0.025
2	1:1	16.8	0.05	5.5	0.05
3	1:2	16.8	0.05	11.0	0.10
4	1:2	8.4	0.025	5.5	0.05
5	1:1	16.8	0.05	5.5	0.05
6	2:1	33.6	0.10	5.5	0.05

The ^1H NMR spectra were taken soon after mixing and after 24h. There was no change in the spectra between the first measurement and after 24h. Partial ^1H NMR data (301 MHz, CDCl_3) δ 8.08 (d, $J = 7.1$ Hz, 2H (**21**)), 7.91 (d, $J = 6.4$ Hz, 2H (**6c**)), 3.89 (t, 2H (**6c**)), 3.10 (t, $J = 7.3$ Hz, 2H (**4c**)).

3.5.3 Dynamic covalent exchange analysis of 3-butyl-2-(4-bromophenyl)-1,3,2-benzoxazaborole (9b) and catechol (21). Benzoxazaborole (**9b**) catechol (**21**) and CDCl_3 (0.7 ml) were combined in a NMR tube in six different experiments as shown in Table 16, three experiments (1-3) with an increasing amount of catechol (**21**) and other three experiments with an increasing amount of benzoxazaborole (**9b**)

Table 16

Amount of 2-(4-bromophenyl)-3-butyl-1,3,2-benzoxazaborole (9b) and catechol (21) used in each experiment.

Experiment number	Ratio	Amount of 9b (mg)	mmol	Amount of 21 (mg)	mmol
1	2:1	16.5	0.05	2.8	0.025
2	1:1	16.5	0.05	5.5	0.05
3	1:2	16.5	0.05	11.0	0.10
4	1:2	8.2	0.025	5.5	0.05
5	1:1	16.5	0.05	5.5	0.05
6	2:1	33.0	0.10	5.5	0.05

The ^1H NMR spectra was taken soon after mixing and after 24h. There was no difference in the spectra between the first measurement and after 24h. Partial ^1H NMR data (301 MHz, CDCl_3) δ 7.84 (d, $J = 7.8$ Hz, 2H (**25**)), 7.78 (d, $J = 8.1$ Hz, 2H (**9b**)), 3.87 (t, $J = 7.6$ Hz, 2H (**9b**)), 3.06 (t, $J = 7.5$ Hz, 2H (**4b**)).

3.5.4 Dynamic covalent exchange analysis of 2-phenyl-1,3,2-benzodioxaborole (22) and 2-(butylamino)phenol (4b). Benzodioxaborole (**22**) 2-(butylamino)phenol (**4b**) and CDCl_3 (0.7 ml) were combined in a NMR tube in six different experiments as shown in Table 17, three experiments (1-3) with an increasing amount of benzodioxaborole **22** and other three experiments with an increasing amount of 2-(butylamino)phenol (**4b**)

Table 17

Amount of 2-phenyl-1,3,2-benzodioxaborole (22) and 2-(butylamino)phenol (4b) used in each experiment.

Experiment number	Ratio	Amount of 22 (mg)	mmol	Amount of 4b (mg)	mmol
1	1:2	4.9	0.025	8.3	0.05
2	1:1	9.8	0.05	8.3	0.05
3	2:1	19.6	0.10	8.3	0.05
4	2:1	9.8	0.05	4.1	0.025
5	1:1	9.8	0.05	8.3	0.025
6	1:2	9.8	0.05	16.6	0.05

The ^1H NMR spectra were taken soon after mixing and after 24h. There was no change in the spectra after the first measurement and after 24h. Partial ^1H NMR data (301 MHz, CDCl_3) δ 8.07 (d, $J = 7.2$ Hz, 2H (**21**)), 7.92 (d, $J = 7.0$ Hz, 2H (**6b**)), 3.90 (t, 2H (**6b**)), 3.11 (t, 2H (**4b**)).

CHAPTER IV

Summary

The overall goal of this work is to synthesize and characterize benzoxazaborole-based materials. The direct synthesis of benzoxazaborole was impeded by the presence of water in DMSO-*d*₆ and slow removal of water in THF-*d*₈ by adding molecular sieves. The rapid formation of 3-(alkyl)benzoxazaboroles was observed in EtOAc and CDCl₃ at room temperature with phenylboronic acid derivatives and 2-(alkylamino)phenol. bis(Benzoxazaborole)s were synthesized via condensation reactions of 2-(alkylamino)phenol or 2-aminophenol and arylene diboronic acids. NMR characterization of both benzoxazaboroles and bis(benzoxazaborole)s confirmed the formation of products. In addition to NMR studies, other spectroscopic analysis such as UV-visible and fluorescence supported the formation of benzoxazaboroles and bis(benzoxazaborole)s and showed that these materials are blue emissive. Further structural information was obtained for bis(benzoxazaborole) **13a** and **15a** from X-ray crystallographic analysis.

Apart from the experimental studies, computational studies were carried out using density functional theory (DFT) and B3LYP function with the 6-311++G(d,p) basis set. The bond lengths were obtained from computationally optimized geometries, and were found to be comparable to X-ray structural data. All alkyl benzoxazaboroles and alkyl bis(benzoxazaborole)s gave a dihedral angle of 20-33° due to alkyl chain attached to the N atom. Absorption data obtained from computational calculations also confirmed that these materials are blue emissive.

Equilibrium studies of 3-(alkyl)benzoxazaborole and benzodioxaborole exchange reactions were carried out. Gibbs free energy values of exchange reactions were calculated both computationally and experimentally. The stability of 3-(alkyl)benzoxazaboroles is independent of the length of the alkyl chain. Both computational and experimental data showed that there is no significant difference in stability of benzoxazaborole and benzodioxaborole.

REFERENCES

- (1) Xu, R.; Pang, W.; Yu, J.; Huo, Q.; Chen, J. *Chemistry of Zeolites and Related Porous Materials: Synthesis and Structure*; John Wiley & Sons: Singapore, 2010.
- (2) Long, J. R.; Yaghi, O. M. The pervasive chemistry of metal–organic frameworks. *Chem. Soc. Rev.* **2009**, *38*, 1213–1214.
- (3) Zou, X.; Ren, H.; Zhu, G. Topology-directed design of porous organic frameworks and their advanced applications. *Chem. Commun.* **2013**, *49*, 3925–3936.
- (4) Valtchev, V.; Mintova, S.; Tsapatsis, M. *Ordered Porous Solids*, 1st ed.; Elsevier Science: Oxford, 2009.
- (5) Côté, A. P.; Benin, A. I.; Ockwig, N. W.; O’Keeffe, M.; Matzger, A. J.; Yaghi, O. M. Porous, Crystalline, Covalent Organic Frameworks. *Science* **2005**, *310*, 1166–1170.
- (6) Choi, Y. J.; Choi, J. H.; Choi, K. M.; Kang, J. K. Covalent organic frameworks for extremely high reversible CO₂ uptake capacity: a theoretical approach. *J. Mater. Chem.* **2011**, *21*, 1073–1078.
- (7) Vilela, F.; Zhang, K.; Antonietti, M. Conjugated porous polymers for energy applications. *Energy Environ. Sci.* **2012**, *5*, 7819–7832.
- (8) Tylianakis, E.; Klontzas, E.; Froudakis, G. E. Multi-scale theoretical investigation of hydrogen storage in covalent organic frameworks. *Nanoscale* **2011**, *3*, 856–869.
- (9) Kaur, P.; Hupp, J. T.; Nguyen, S. T. Porous Organic Polymers in Catalysis: Opportunities and Challenges. *ACS Catal.* **2011**, *1*, 819–835.
- (10) Kojima, T.; Kumaki, D.; Nishida, J.; Tokito, S.; Yamashita, Y. Organic field-effect transistors based on novel organic semiconductors containing diazaboroles. *J.*

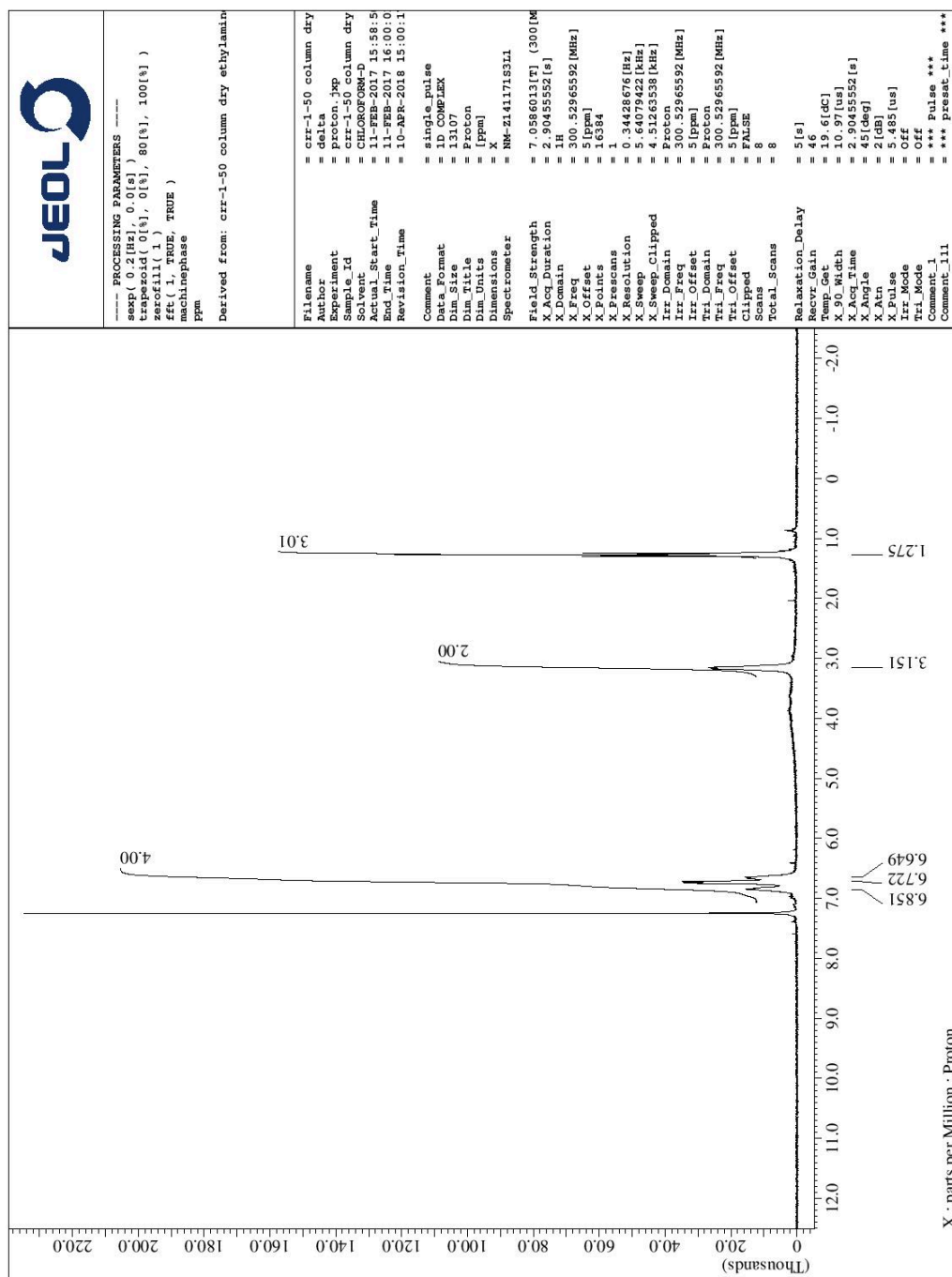
- Mater. Chem.* **2011**, *21*, 6607–6613.
- (11) El-Kaderi, H. M.; Hunt, J. R.; Mendoza-Cortés, J. L.; Côté, A. P.; Taylor, R. E.; O’Keeffe, M.; Yaghi, O. M. Designed Synthesis of 3D Covalent Organic Frameworks. *Science* **2007**, *316*, 268–272.
- (12) Kahveci, Z.; Sekizkardes, A. K.; Arvapally, R. K.; Wilder, L.; El-Kaderi, H. M. Highly Porous Photoluminescent Diazaborole-Linked Polymers: Synthesis, Characterization, and Application to Selective Gas Adsorption. *Polym. Chem.* **2017**, *8*, 2509–2515.
- (13) Jin, Y.; Wang, Q.; Taynton, P.; Zhang, W. Dynamic Covalent Chemistry Approaches Toward Macrocycles, Molecular Cages, and Polymers. *Acc. Chem. Res.* **2014**, *47*, 1575–1586.
- (14) Corbett, P. T.; Leclaire, J.; Vial, L.; West, K. R.; Wietor, J.-L.; Sanders, J. K. M.; Otto, S. Dynamic combinatorial chemistry. *Chem. Rev.* **2006**, *106*, 3652–3711.
- (15) Bapat, A. P.; Roy, D.; Ray, J. G.; Savin, D. a.; Sumerlin, B. S. Dynamic-covalent macromolecular stars with boronic ester linkages. *J. Am. Chem. Soc.* **2011**, *133*, 19832–19838.
- (16) Jin, Y.; Yu, C.; Denman, R. J.; Zhang, W. Recent Advances in Dynamic Covalent Chemistry. *Chem. Soc. Rev.* **2013**, *42*, 6634–6654.
- (17) Rowan, S. J.; Cantrill, S. J.; Cousins, G. R. L.; Sanders, J. K. M.; Stoddart, J. F. Dynamic Covalent Chemistry. *Angew. Chem. Int. Ed. Engl.* **2002**, *41*, 898–952.
- (18) Vougioukalakis, G. C.; Grubbs, R. H. Ruthenium-Based Heterocyclic Carbene-Coordinated Olefin Metathesis Catalysts. *Chem. Rev.* **2010**, *110*, 1746–1787.
- (19) Zhang, W.; Moore, J. S. Shape-Persistent Macrocycles: Structures and Synthetic

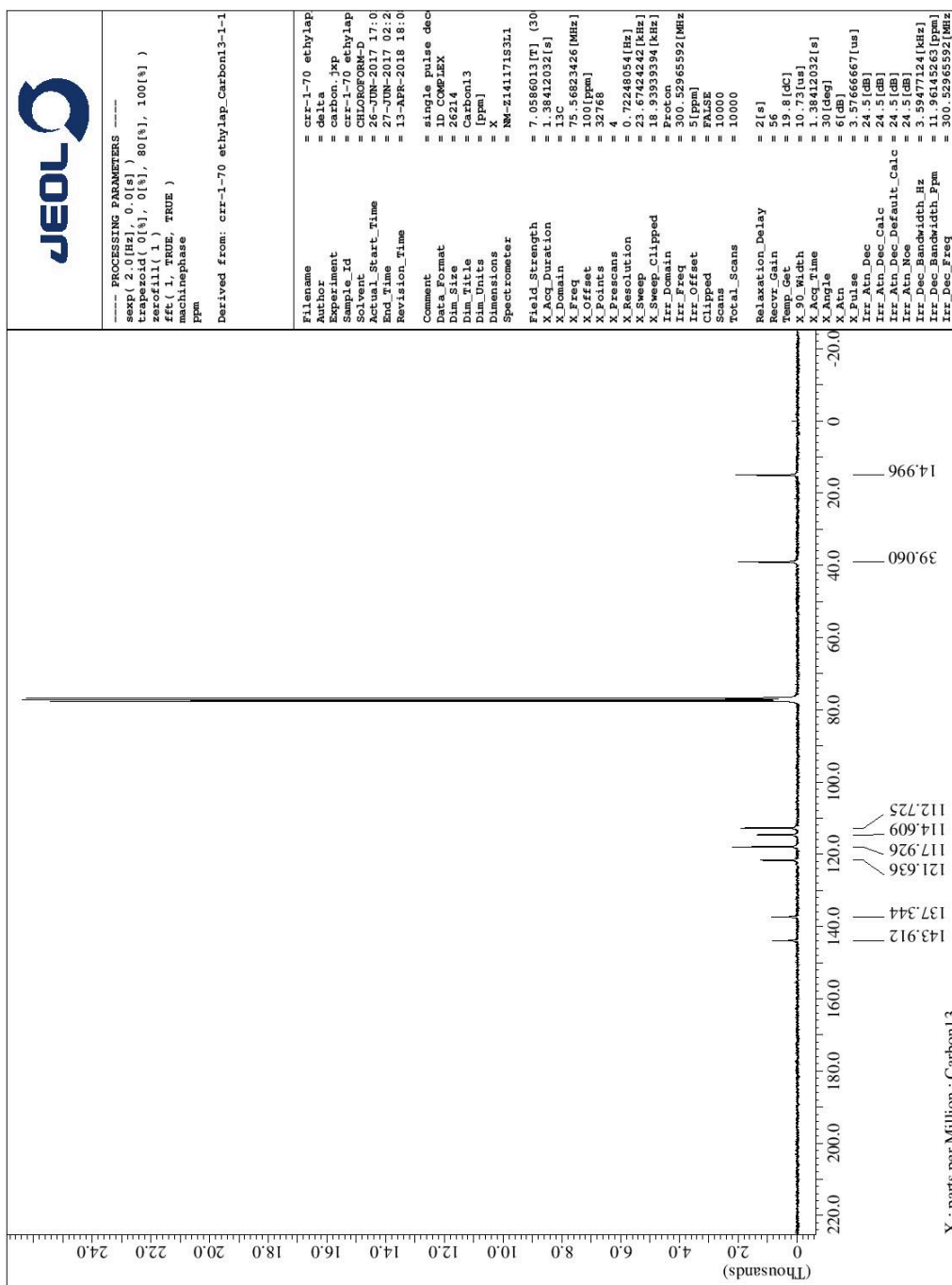
- Approaches from Arylene and Ethynylene Building Blocks. *Angew. Chem. Int. Ed.* **2006**, *45*, 4416–4439.
- (20) Belowich, M. E.; Stoddart, J. F. Dynamic imine chemistry. *Chem. Soc. Rev.* **2012**, *41*, 2003–2024.
- (21) Rue, N. M.; Sun, J.; Warmuth, R. Polyimine container molecules and nanocapsules. *Isr. J. Chem.* **2011**, *51*, 743–768.
- (22) Li, J.; Carnall, J. M. A.; Stuart, M. C. A.; Otto, S. Hydrogel Formation upon Photoinduced Covalent Capture of Macrocyclic Stacks from Dynamic Combinatorial Libraries. *Angew. Chemie Int. Ed.* **2011**, *50*, 8384–8386.
- (23) Hall, D. G. Structure, Properties, and Preparation of Boronic Acid Derivatives. Overview of Their Reactions and Applications. In *Boronic Acids: Preparation and Applications in Organic Synthesis and Medicine*; Hall, D. G., Ed.; Wiley-VCH Verlag GmbH & Co. KGaA: Weinheim, FRG, 2006; pp 1–99.
- (24) Dewar, M. J. S.; Kubba, V. P.; Pettit, R. New heteroaromatic compounds. II. Boron compounds isoconjugate with indole, 2,3-benzofuran, and thianaphthene. *J. Chem. Soc.* **1958**, 3076–3079.
- (25) Sugihara, J. M.; Bowman, C. M. Cyclic Benzenboronate Esters. *J. Am. Chem. Soc.* **1958**, *80*, 2443–2446.
- (26) Steinberg, H; Brotherton, R. J. Direct Preparation of Some Cyclic Boron-Nitrogen Compounds from Alkoxyboranes. *J. Org. Chem* **1961**, *26*, 4632–4634.
- (27) Barba, V.; Rodríguez, A.; Ochoa, M. E.; Santillan, R.; Farfán, N. Bisoxazaborolidines and boron complexes derived from tetradentate ligands: synthesis and spectroscopic studies. *Inorg. Chim. Acta* **2004**, *357*, 2593–2601.

- (28) George, S. Synthesis and Characterization of Benzoxazaboroles. M.S. Thesis, Sam Houston State University, 2016.
- (29) Spitler, E. L.; Dichtel, W. R. Lewis acid-catalysed formation of two-dimensional phthalocyanine covalent organic frameworks. *Nat. Chem.* **2010**, *2*, 672–677.
- (30) Lokugama, S. Synthesis of Diazaborole Linked Oligomers using Aryl Boronic Acid Derivatives. M.S. Thesis, Sam Houston State University, 2015.
- (31) Kalgutkar, A. S.; Kozak, K. R.; Crews, B. C.; Hochgesang, G. P.; Marnett, L. J. Covalent modification of cyclooxygenase-2 (COX-2) by 2-acetoxyphenyl alkyl sulfides, a new class of selective COX-2 inactivators. *J. Med. Chem.* **1998**, *41*, 4800–4818.
- (32) Kombala, C. Investigation of Boronate Ester Equilibria Towards Macrocyclic Synthesis. M.S. Thesis, Sam Houston State University, 2015.
- (33) Goldberg, A. R.; Northrop, B. H. Spectroscopic and Computational Investigations of the Thermodynamics of Boronate Ester and Diazaborole Self-Assembly. *J. Org. Chem.* **2016**, *81*, 969–980.
- (34) Abeysinghe, J. Diazaboroles: Experimental Investigations of their Dynamic Covalent Nature and Computational Chemistry. M.S. Thesis, Sam Houston State University, 2016.
- (35) Einstein. *Handbook of*; 2001.
- (36) Davies, G. H. M.; Molander, G. A. Synthesis of Functionalized 1,3,2-Benzodiazaborole Cores Using Bench-Stable Components. *J. Org. Chem.* **2016**, *81*, 3771–3779.
- (37) Smith, M. K.; Powers-Riggs, N. E.; Northrop, B. H. Discrete, soluble covalent

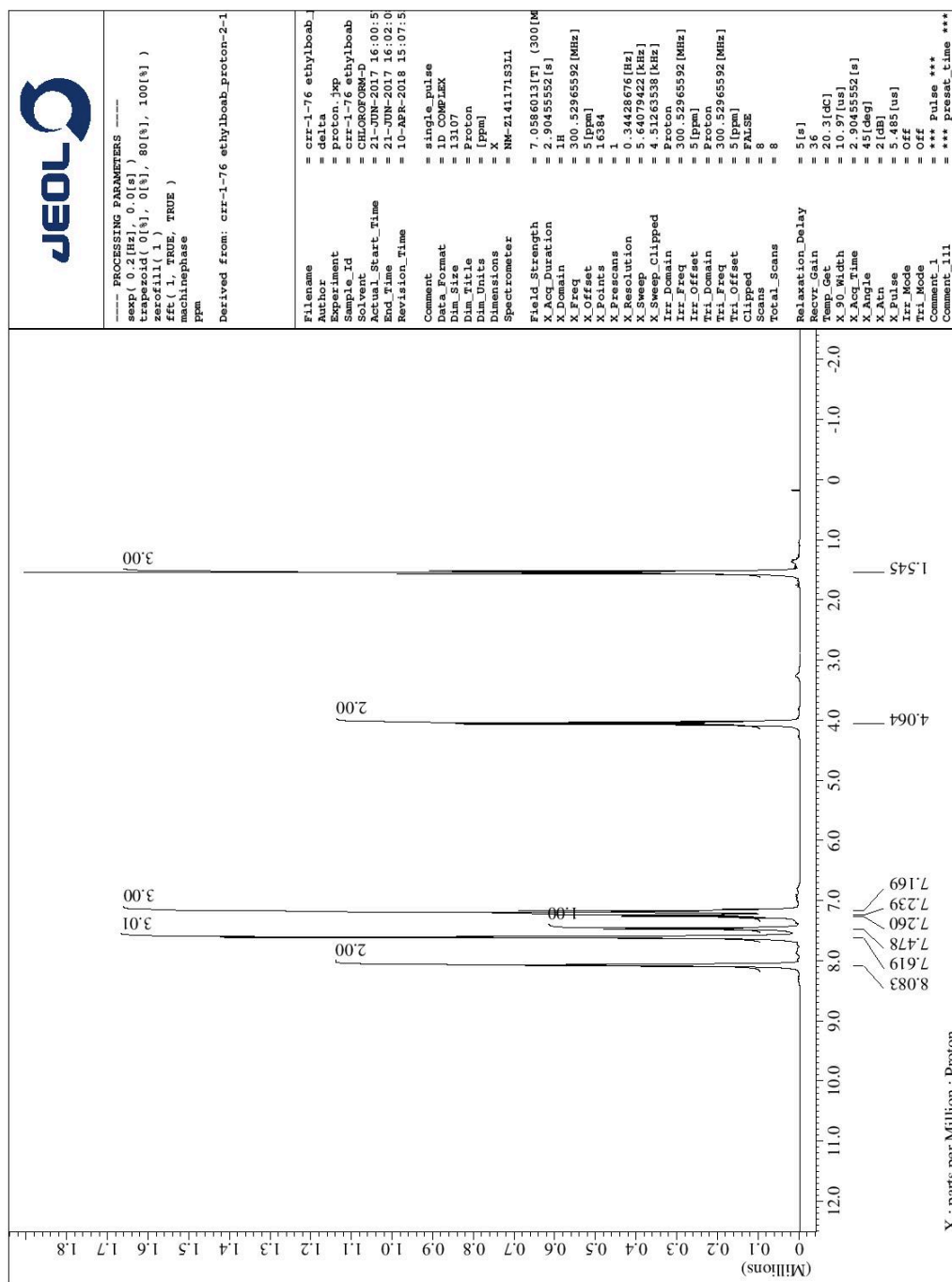
- organic boronate ester rectangles. *Chem. Commun.*, **2013**, *49*, 6167–6169.
- (38) Maruyama, S.; Kawanishi, Y. Syntheses and Emission Properties of Novel Violet-Blue Emissive Aromatic bis(diazaborole)s. *J. Mater. Chem.* **2002**, *12*, 2245–2249.
- (39) Rambo, B. M.; Lavigne, J. J.; Carolina, S.; March, R. V.; Re, V.; Recci, M.; May, V. Defining Self-Assembling Linear Oligo(dioxaborole)s. *Chem. Mater.* **2007**, *19*, 3732–3739.
- (40) Ekanayake, D. I. Effect of Boron Trifluoride on the Esterification of Boronate Esters. M.S. Thesis, Sam Houston State University, 2017.

APPENDIX A – NMR spectra for the synthesized compounds

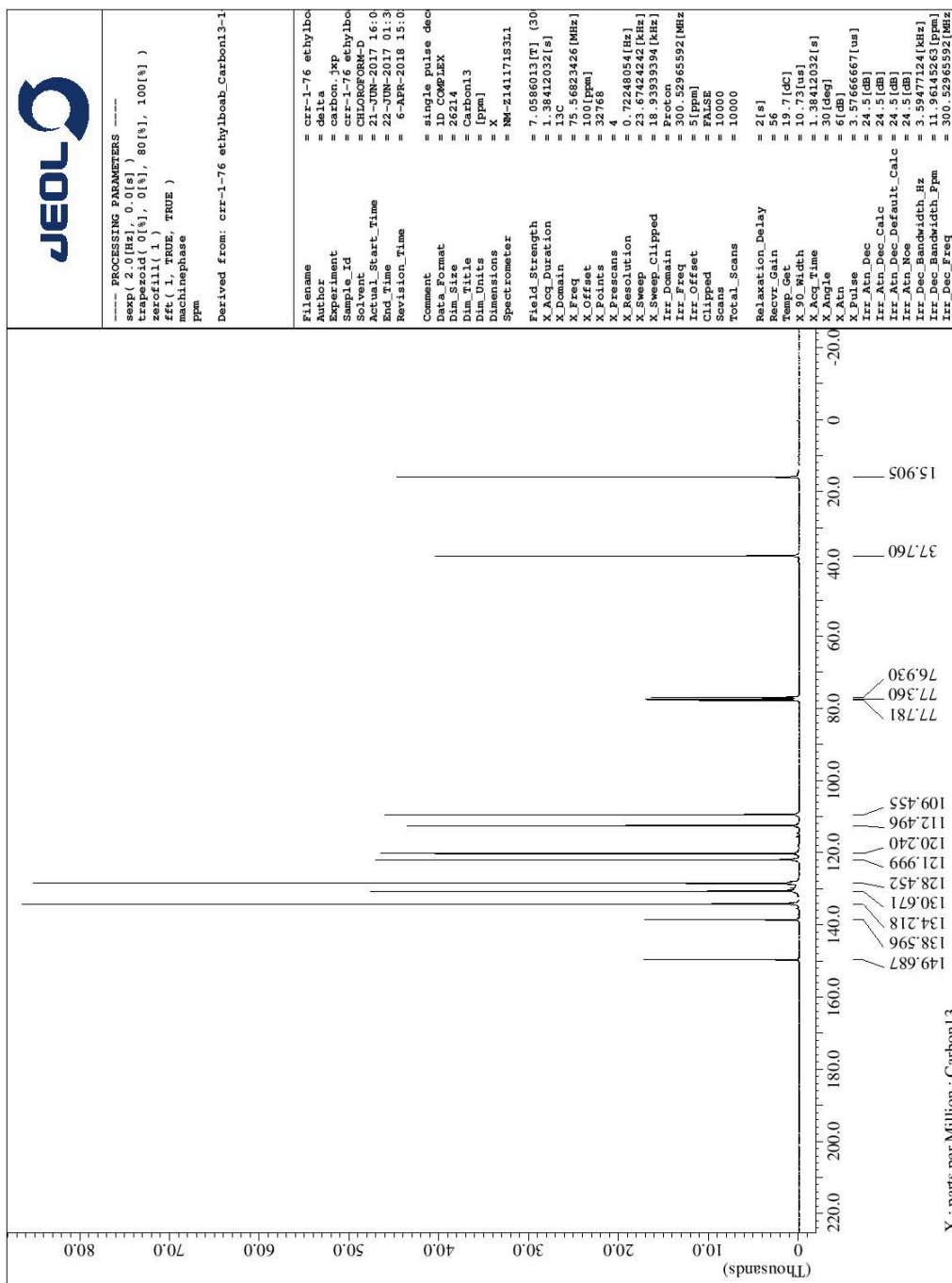
¹H NMR spectrum of 2-(ethylamino)phenol (**4a**) in CDCl₃.



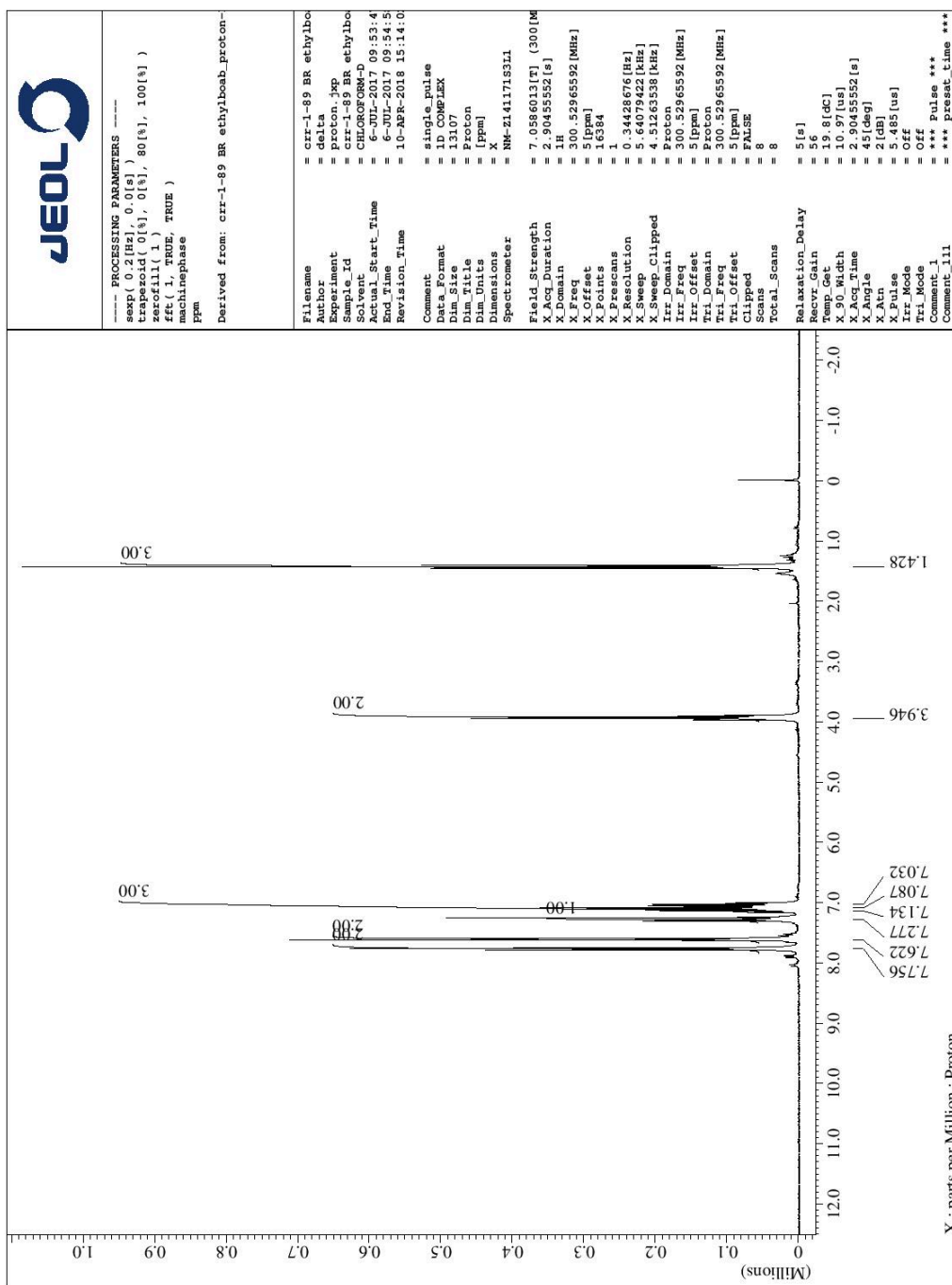
^{13}C NMR spectrum of 2-(ethylamino)phenol (**4a**) in CDCl_3 .



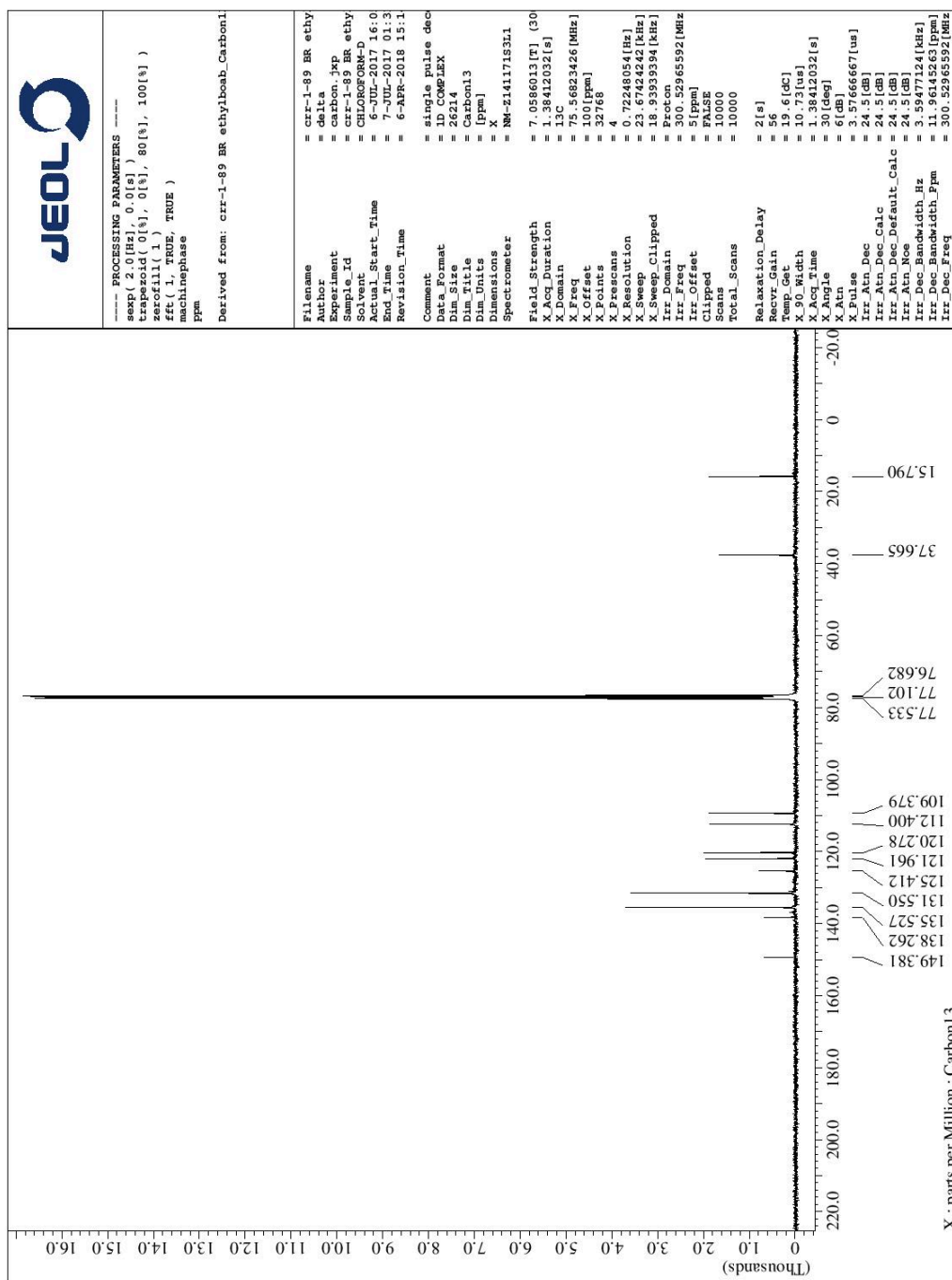
¹H NMR spectrum of 3-(ethyl)benzoxazaborole (**6a**) in CDCl₃.



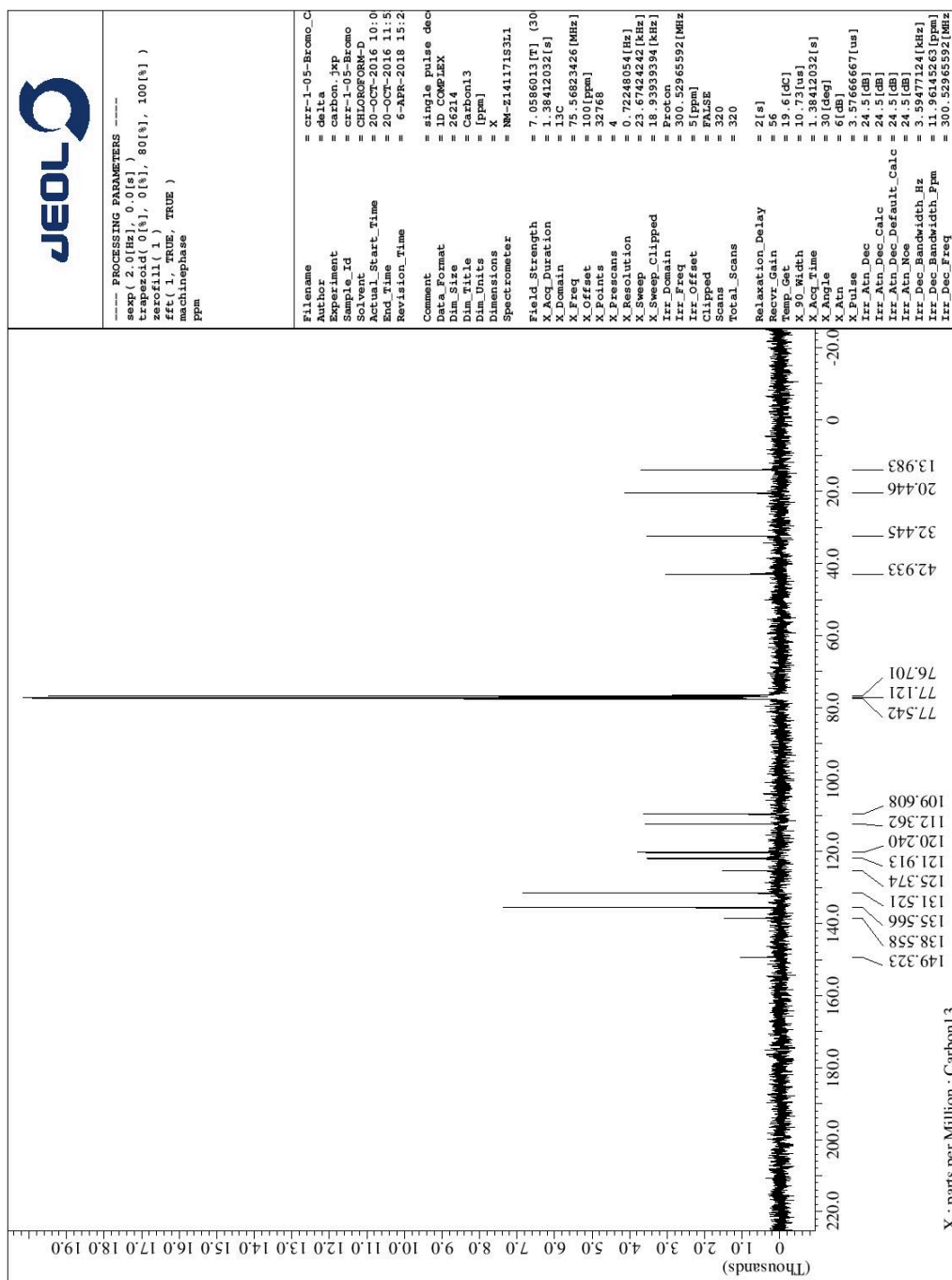
¹³C NMR spectrum of 3-(ethyl)benzoxazaborole (**6a**) in CDCl₃.



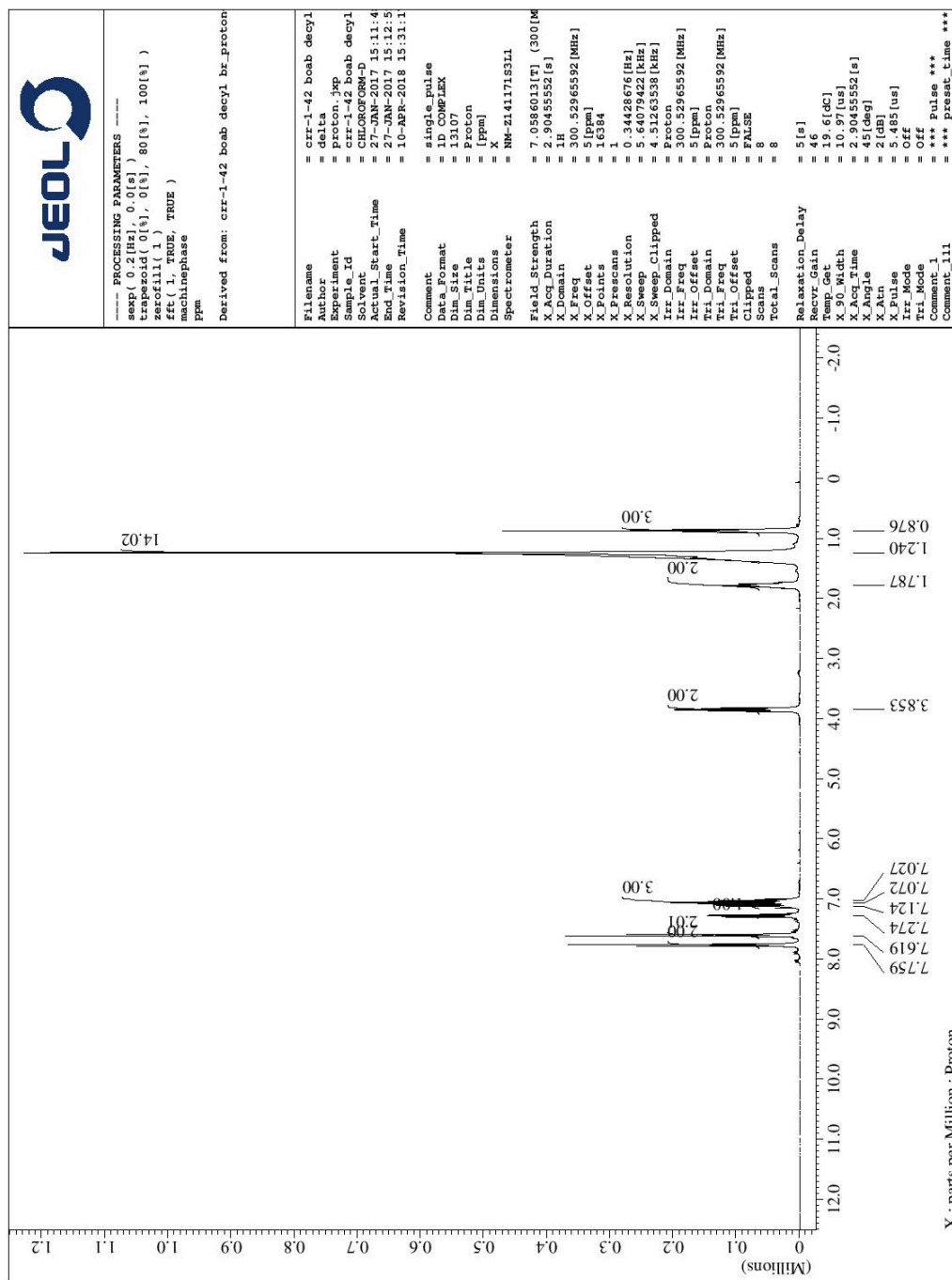
^1H NMR spectrum of 2-(4-bromophenyl)-3-(ethyl)benzoxazaborole (**9a**) in CDCl_3 .



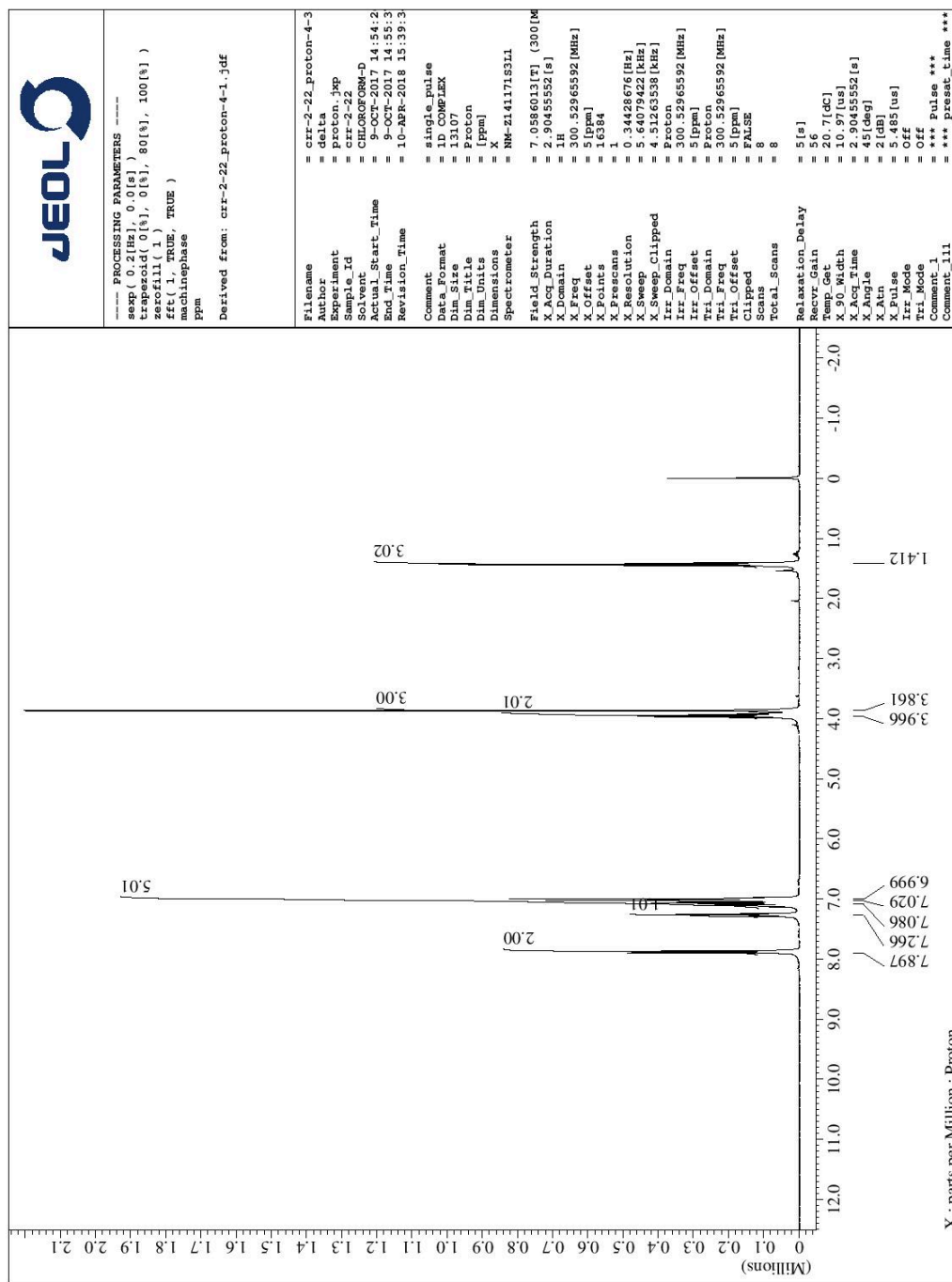
^{13}C NMR spectrum of 2-(4-bromophenyl)-3-(ethyl)benzoxaborole (**9a**) in CDCl_3 .



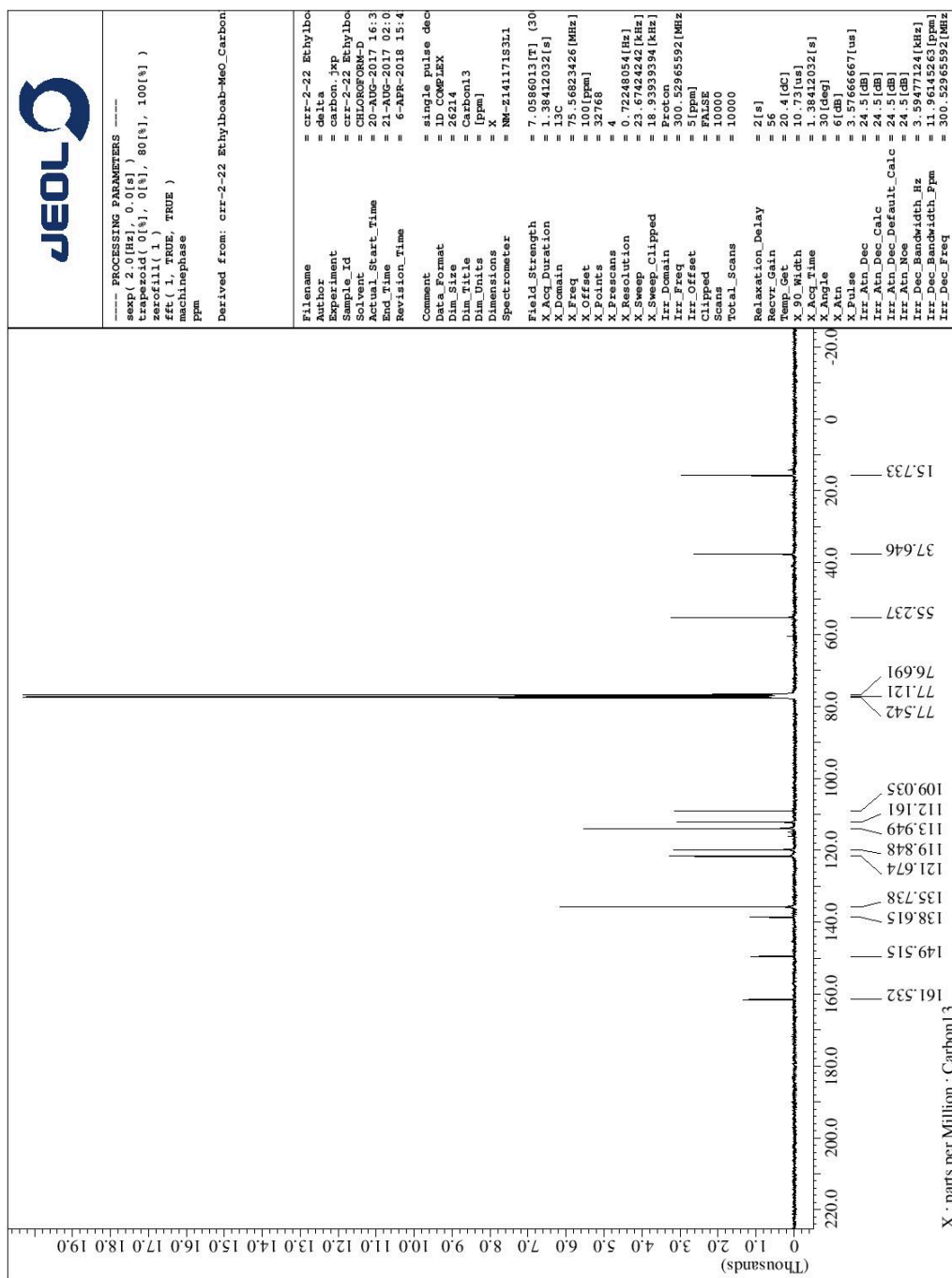
^{13}C NMR spectrum of 2-(4-bromophenyl)-3-(butyl)benzoxazaborole (**9b**) in CDCl_3 .



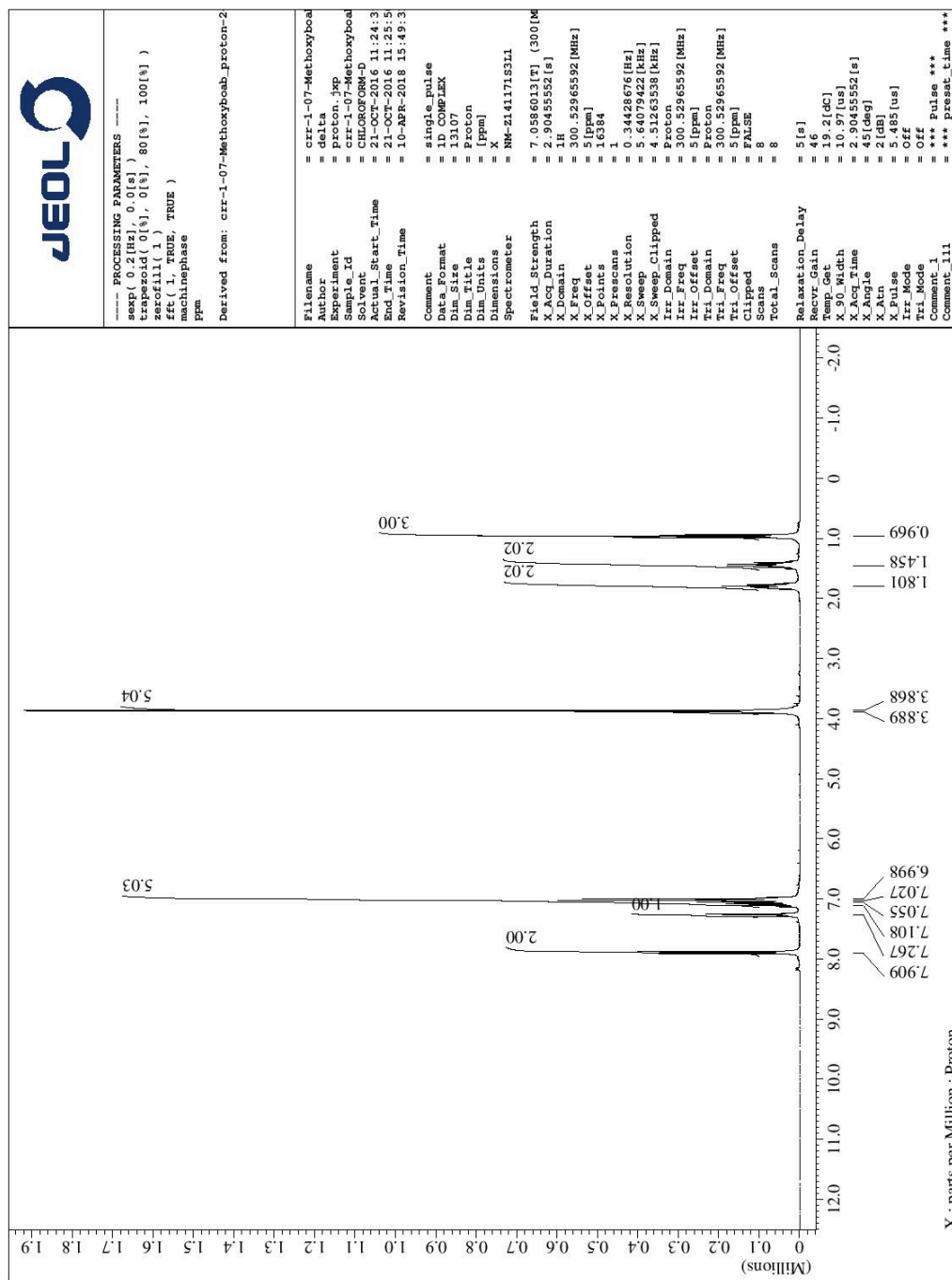
^1H NMR spectrum of 2-(4-bromophenyl)-3-(decyl)benzoxazaborole (**9c**) in CDCl_3 .



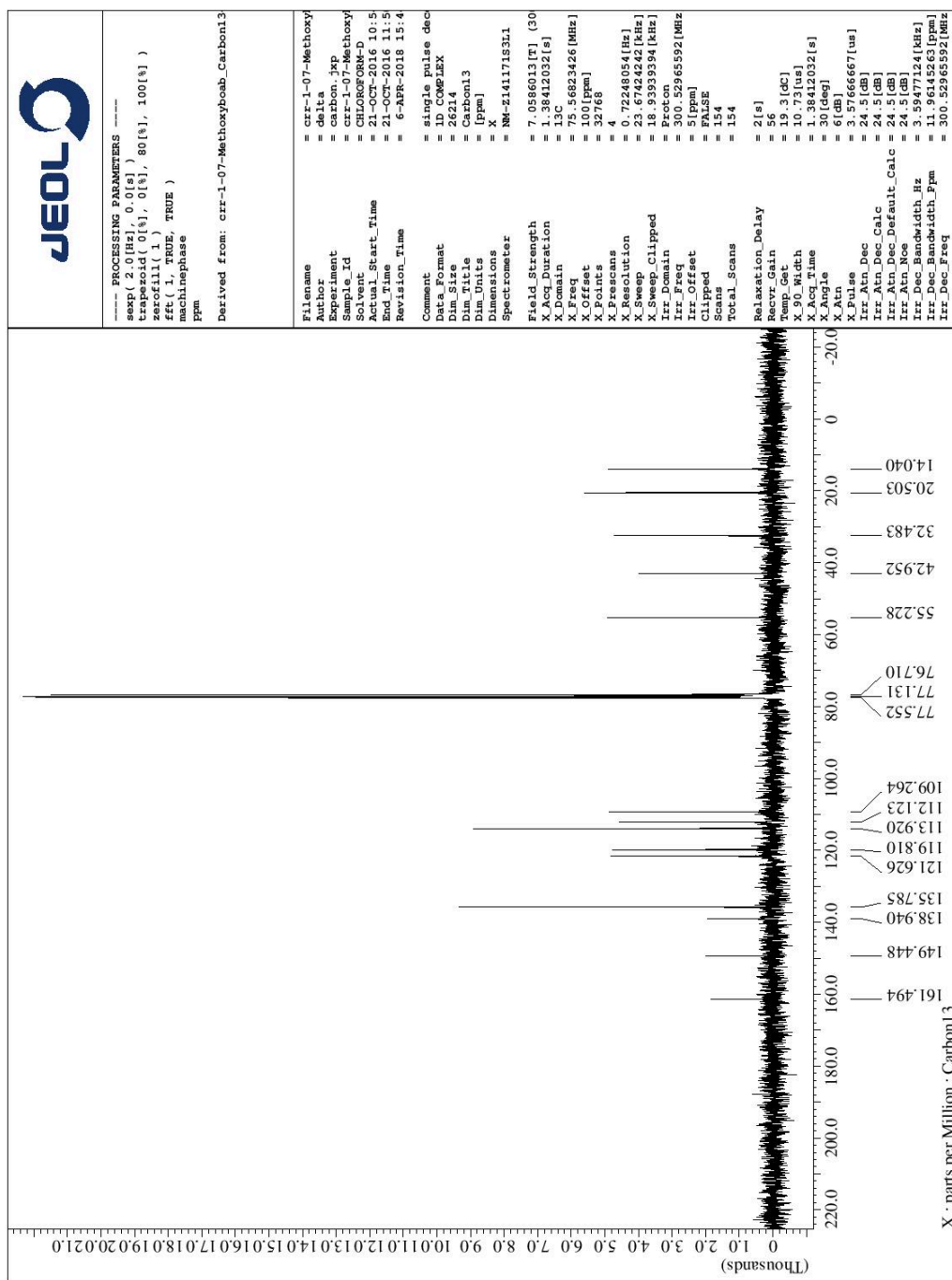
^1H NMR spectrum of 3-(ethyl)-2-(4-methoxyphenyl)-benzoxazaborole (**10a**) in CDCl_3 .



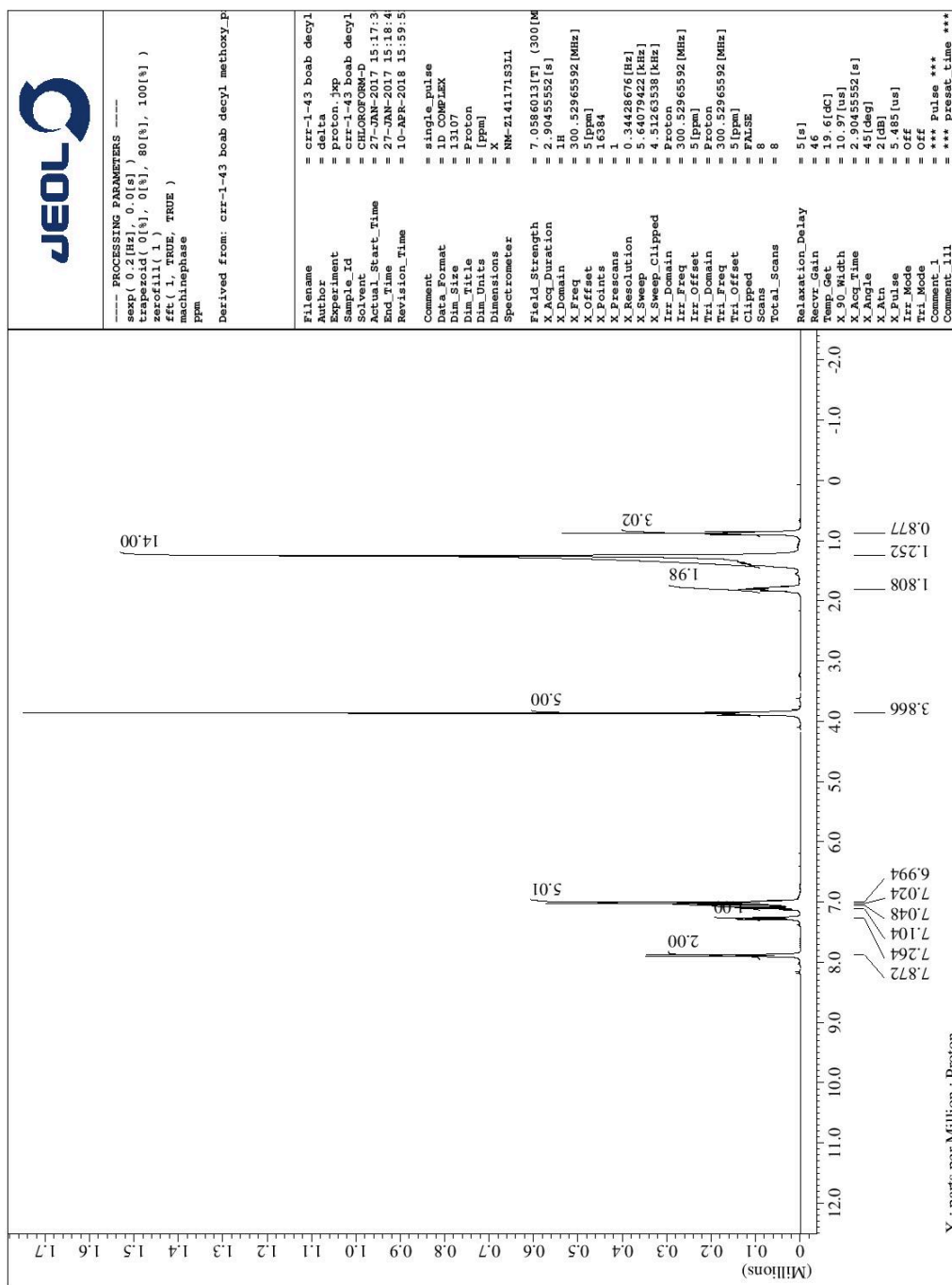
^{13}C NMR spectrum of 3-(ethyl)-2-(4-methoxyphenyl)-benzoxazaborole (**10a**) in CDCl_3 .



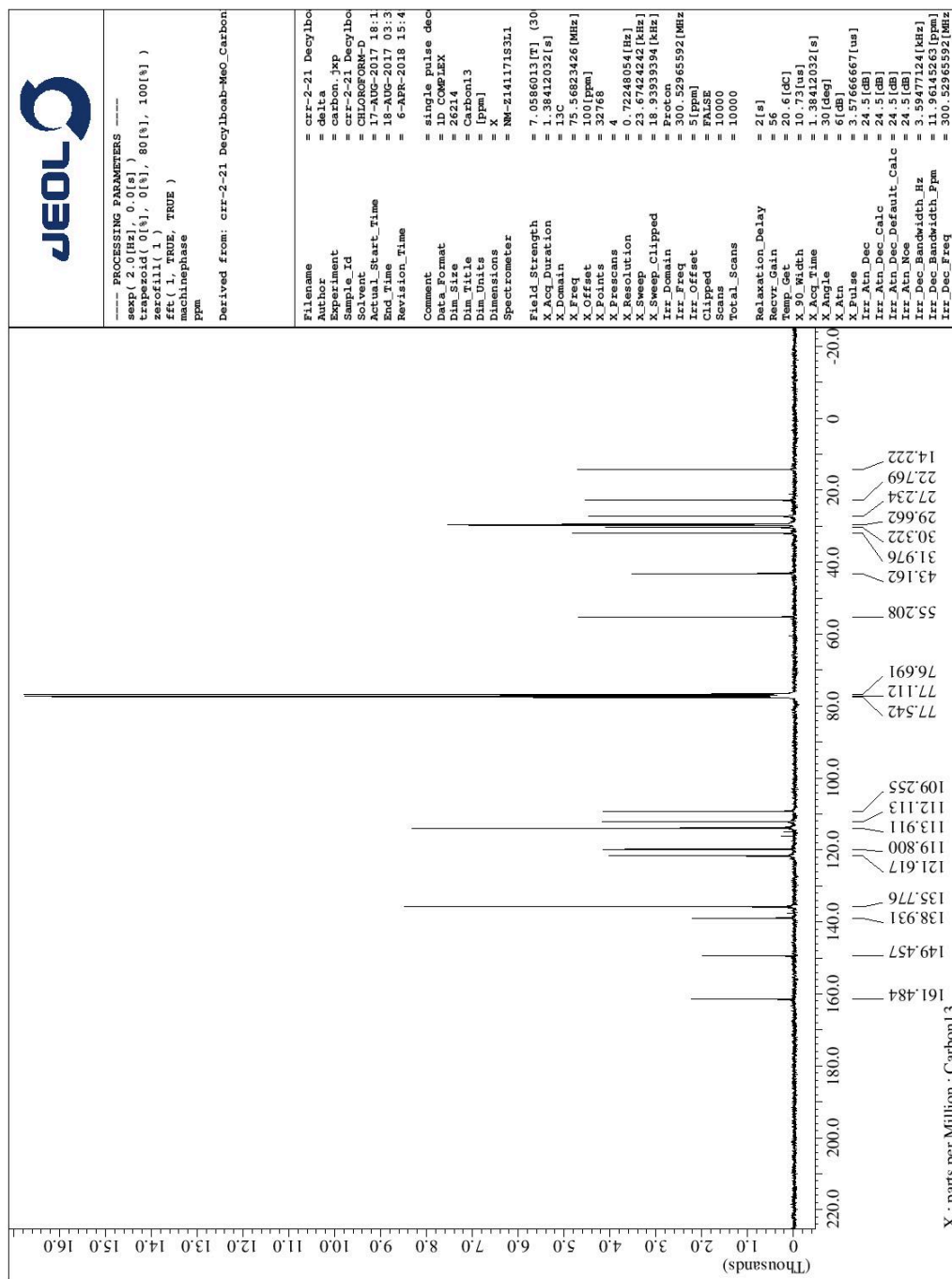
^1H NMR spectrum of 3-(butyl)-2-(4-methoxyphenyl)-benzoxazaborole (**10b**) in CDCl_3 .



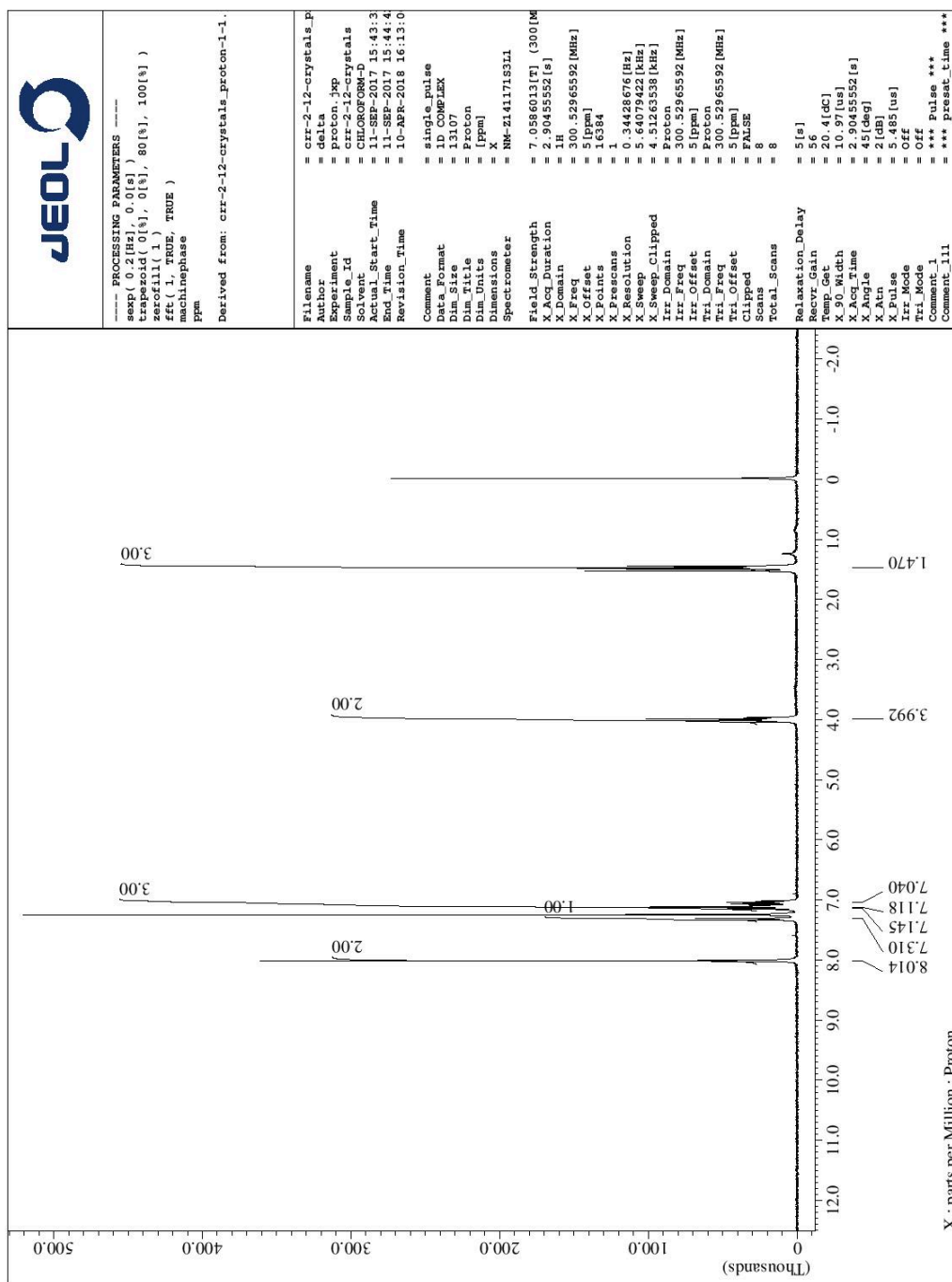
^{13}C NMR spectrum of 3-(butyl)-2-(4-methoxyphenyl)-benzoxazaborole (**10b**) in CDCl_3 .



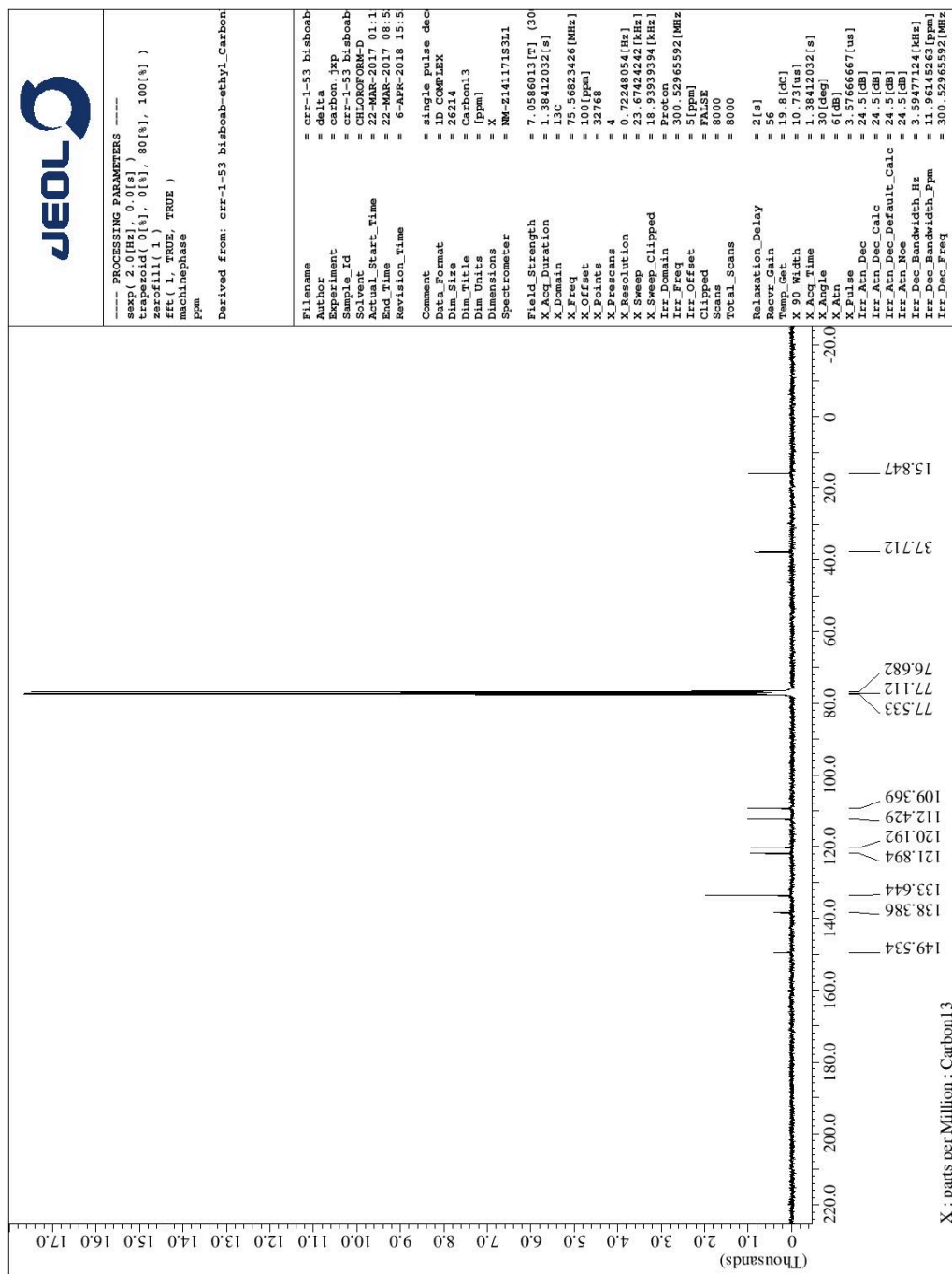
^1H NMR spectrum of 3-(decyl)-2-(4-methoxyphenyl)-benzoxazaborole (**10c**) in CDCl_3 .



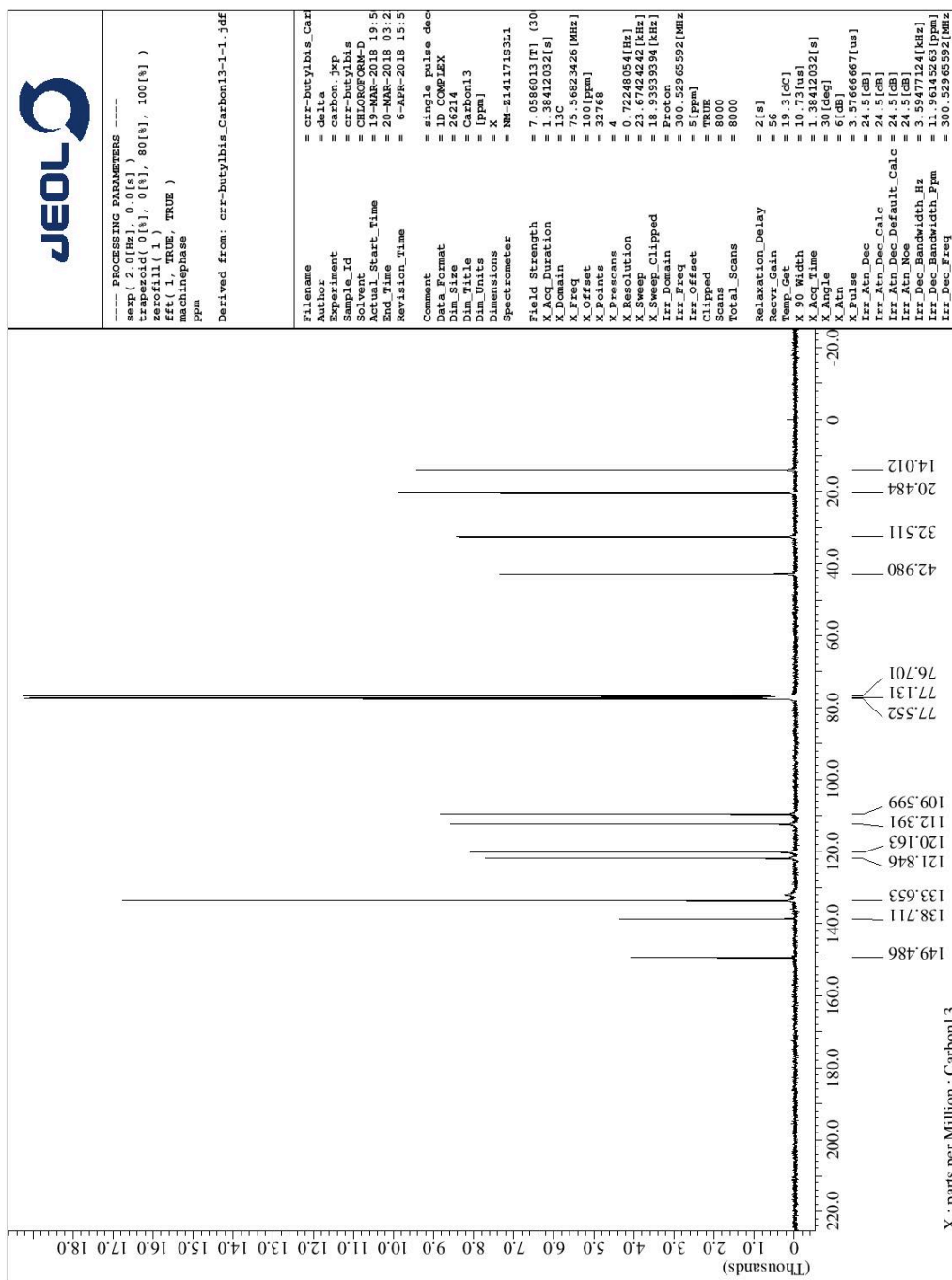
^{13}C NMR spectrum of 3-(decyl)-2-(4-methoxyphenyl)-benzoxazaborole (**10c**) in CDCl_3 .



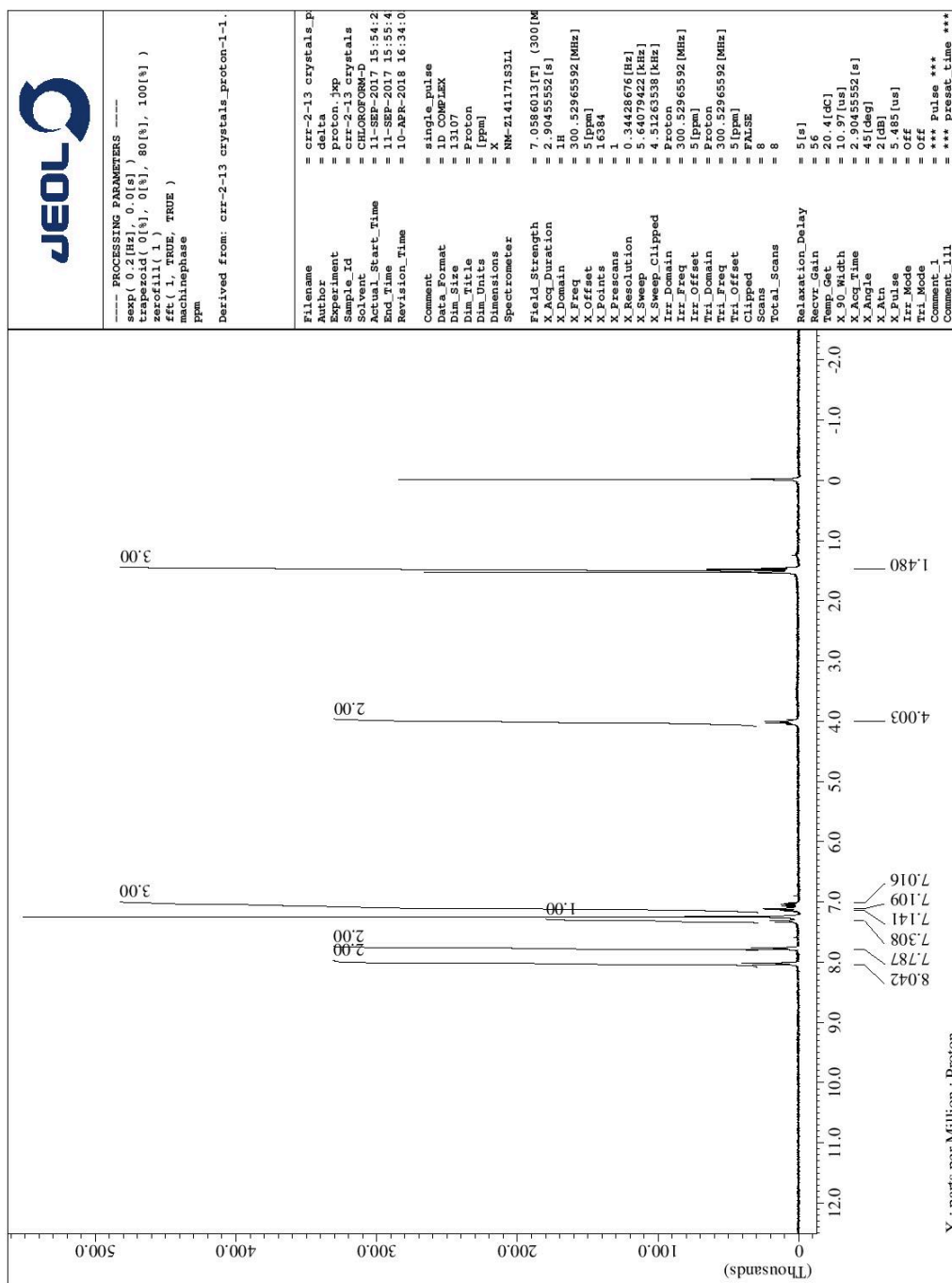
^1H NMR spectrum of 1,4-phenylene-bis-[3-(ethyl)benzoxazaborole] (**13a**) in CDCl_3 .



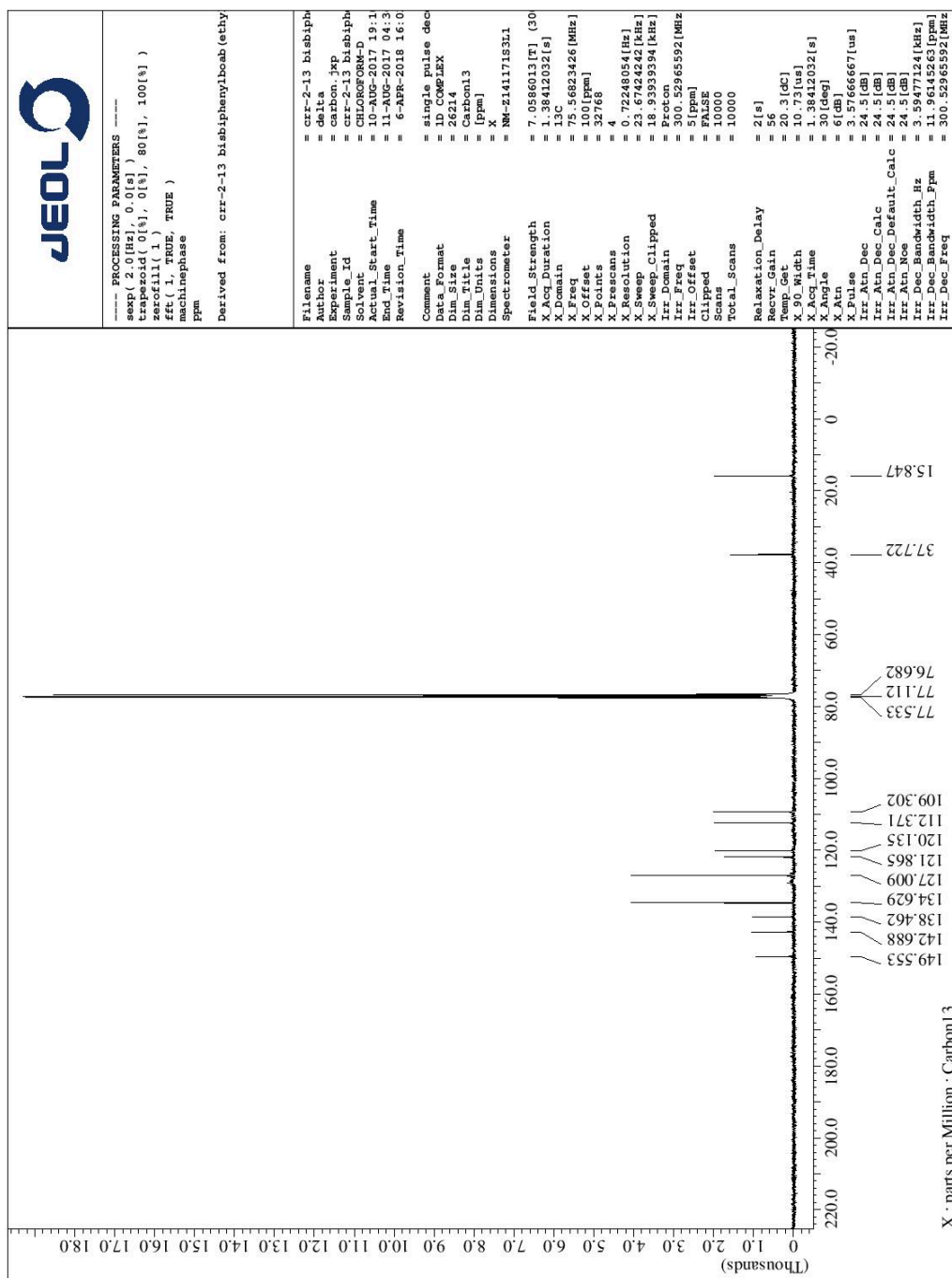
^{13}C NMR spectrum of 1,4-phenylene-bis-[3-(ethyl)benzoxazaborole] (**13a**) in CDCl_3 .



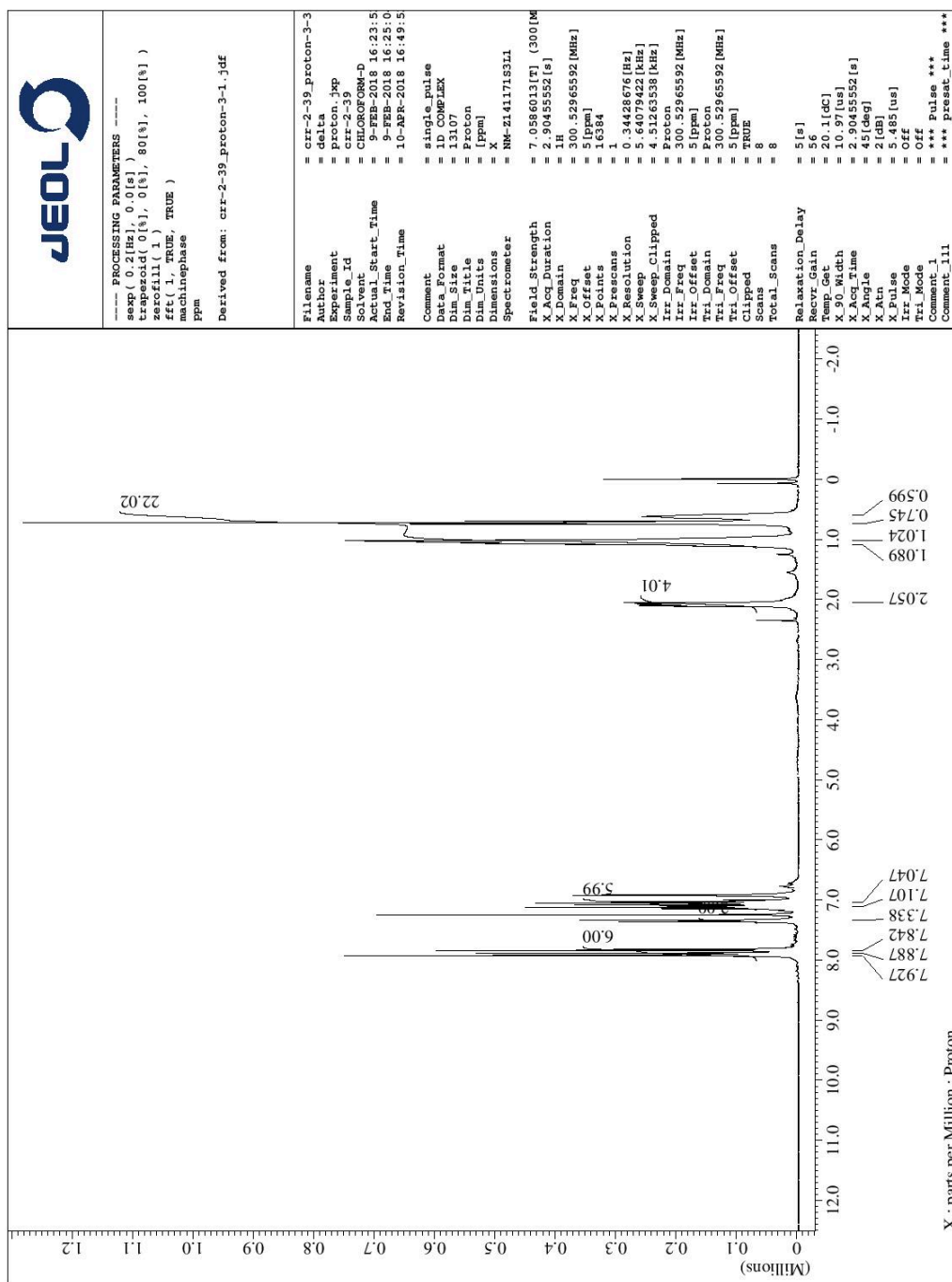
^{13}C NMR spectrum of 1,4-phenylene-bis-[3-(butyl)benzoxazaborole] (**13b**) in CDCl_3 .



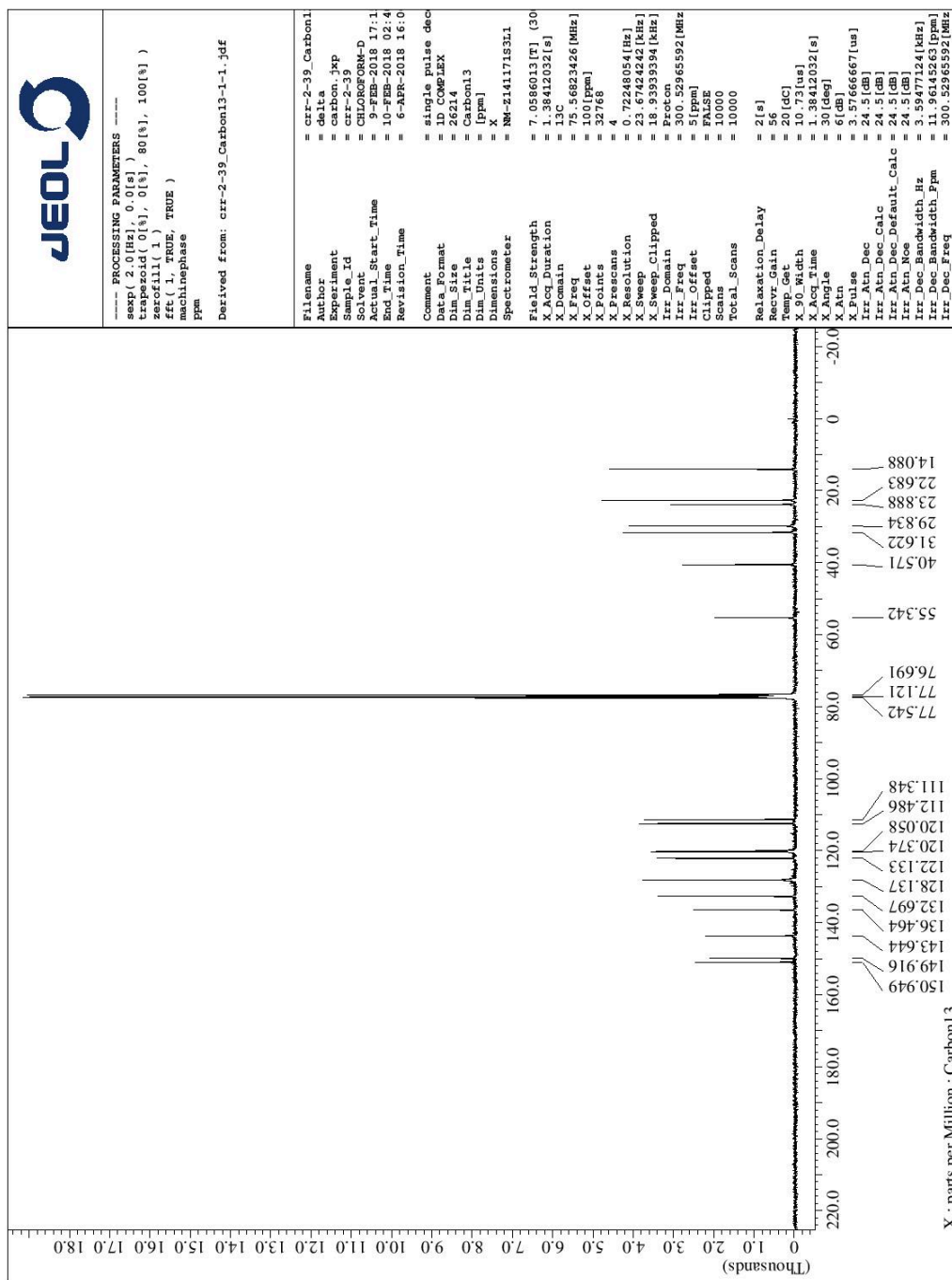
¹H NMR spectrum of biphenyl-4,4'-bis-[3-(ethyl)benzoxazaborole] (**15a**) in CDCl₃.



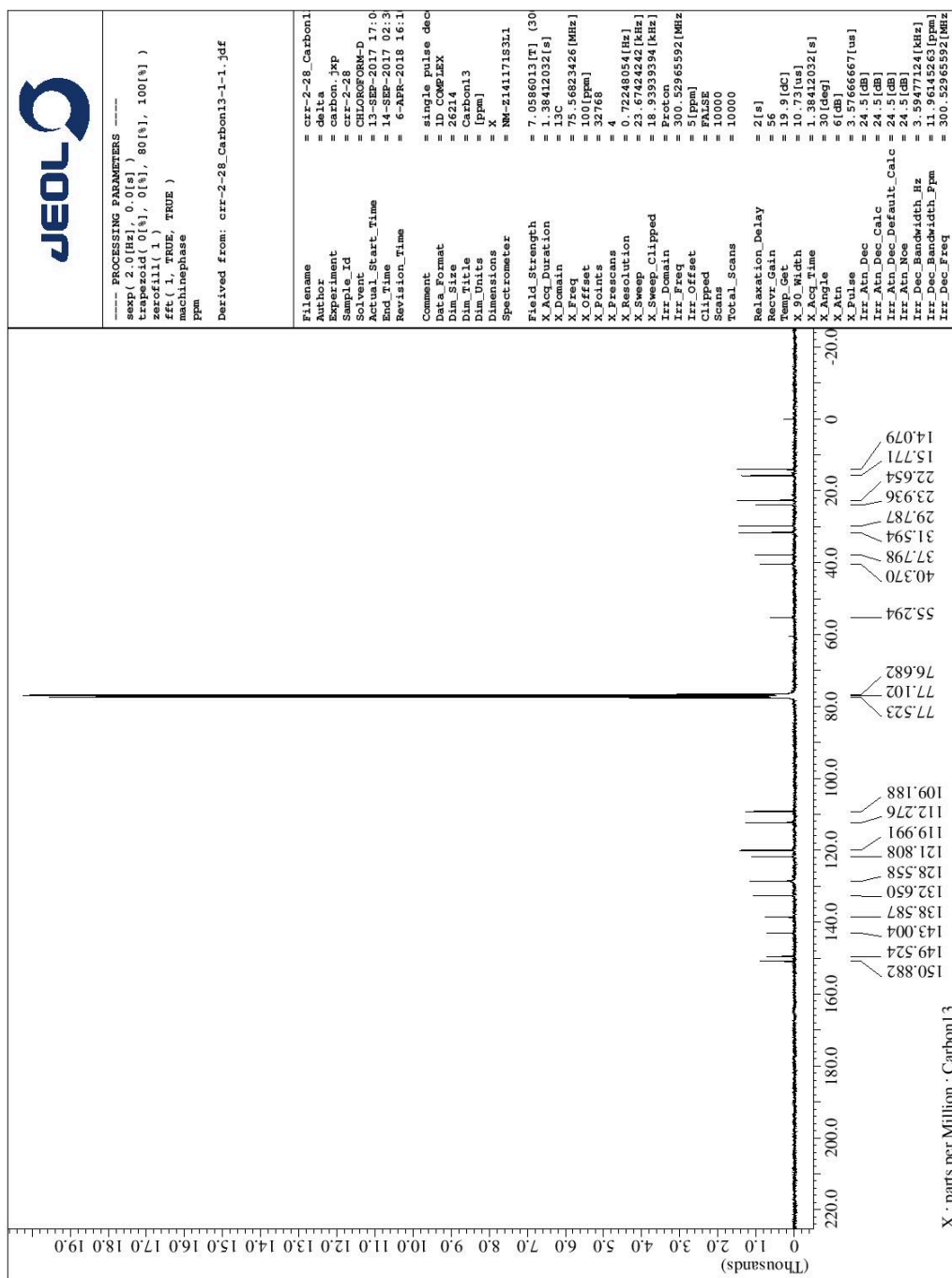
^{13}C NMR spectrum of biphenyl-4,4'-bis-[3-(ethyl)benzoxazaborole] (**15a**) in CDCl_3 .



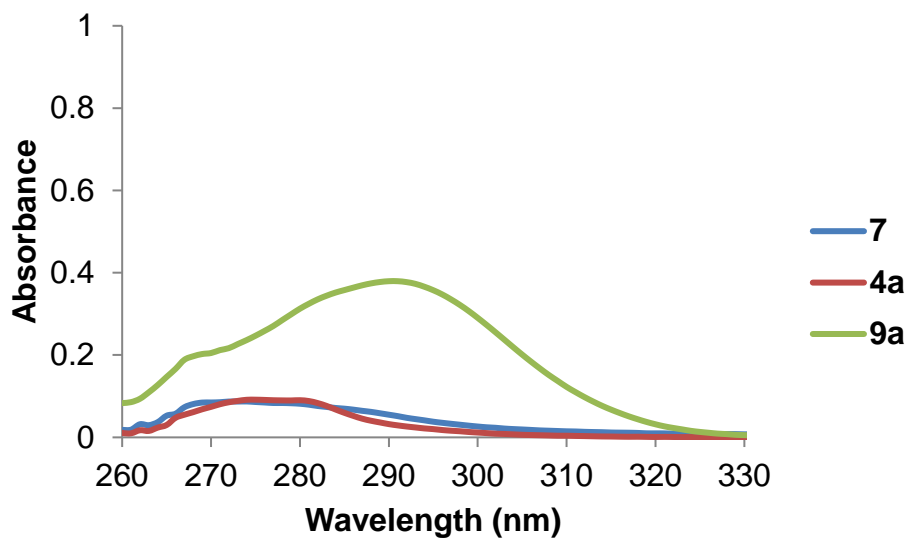
^1H NMR spectrum of 9,9-dihexylfluorene-2,7-bis(benzoxazaborole) (**17**) in CDCl_3 .



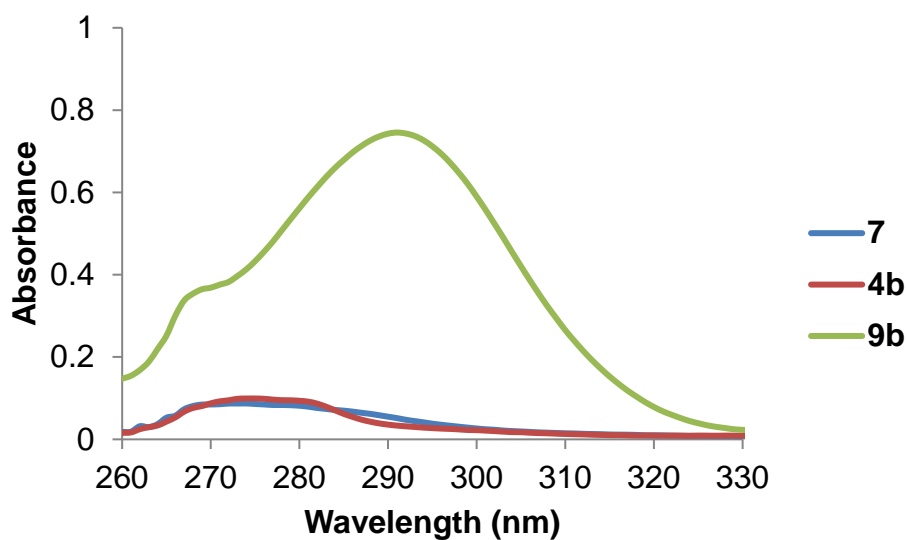
^{13}C NMR spectrum of 9,9-dihexylfluorene-2,7-bis(benzoxazaborole) (**17**) in CDCl_3 .



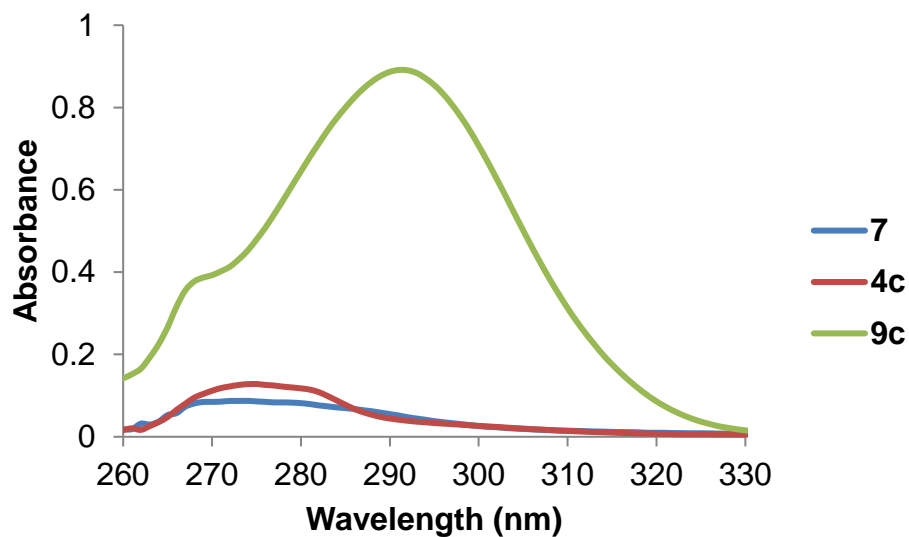
^{13}C NMR spectrum of 9,9-dihexylfluorene-2,7-bis-[3-(ethyl)benzoxaborole] (**17a**) in CDCl_3 .

APPENDIX B – UV-vis spectra for the synthesized compounds

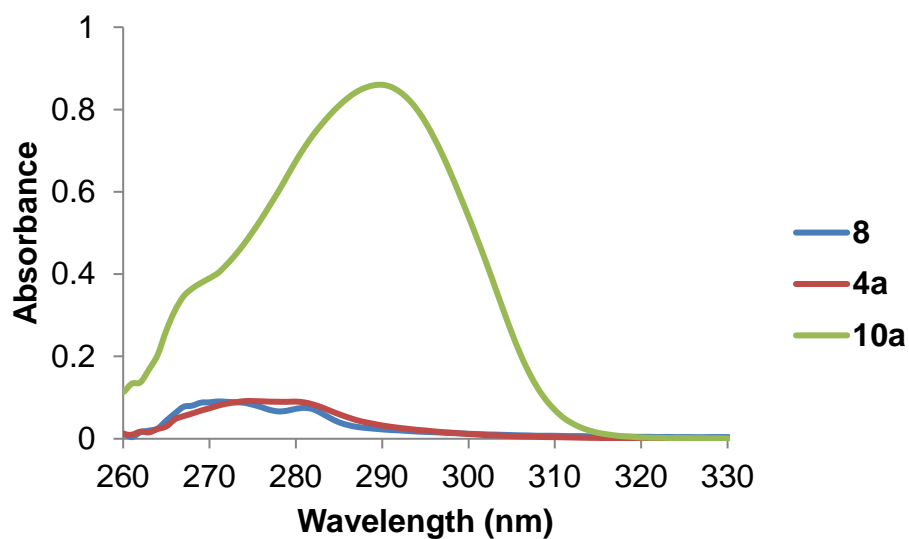
UV-vis spectra of 2-(4-bromophenyl)-3-(ethyl)benzoxazaborole (**9a**), 2-(ethylamino)phenol (**4a**) and 4-bromophenylboronic acid (**7**) in CHCl_3 .



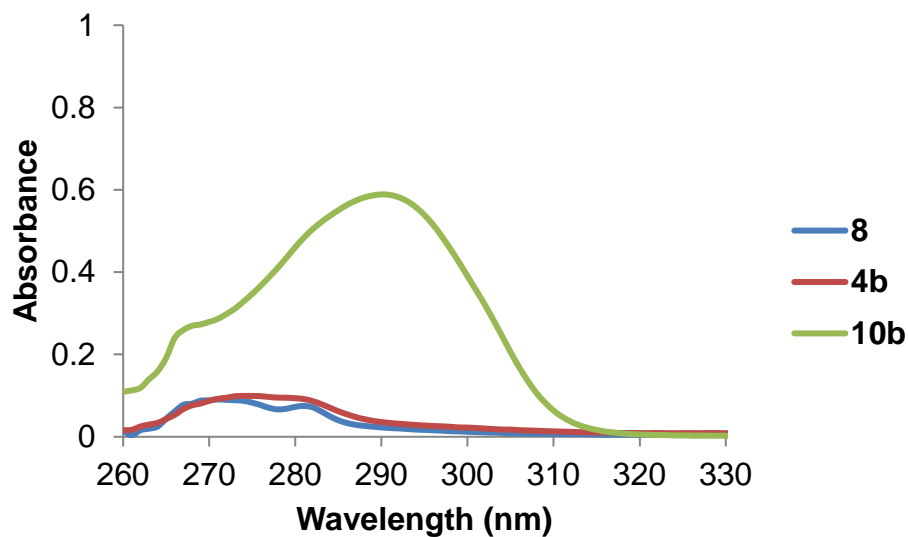
UV-vis spectra of 2-(4-bromophenyl)-3-(butyl)benzoxazaborole (**9b**), 2-(butylamino)phenol (**4b**) and 4-bromophenylboronic acid (**7**) in CHCl_3 .



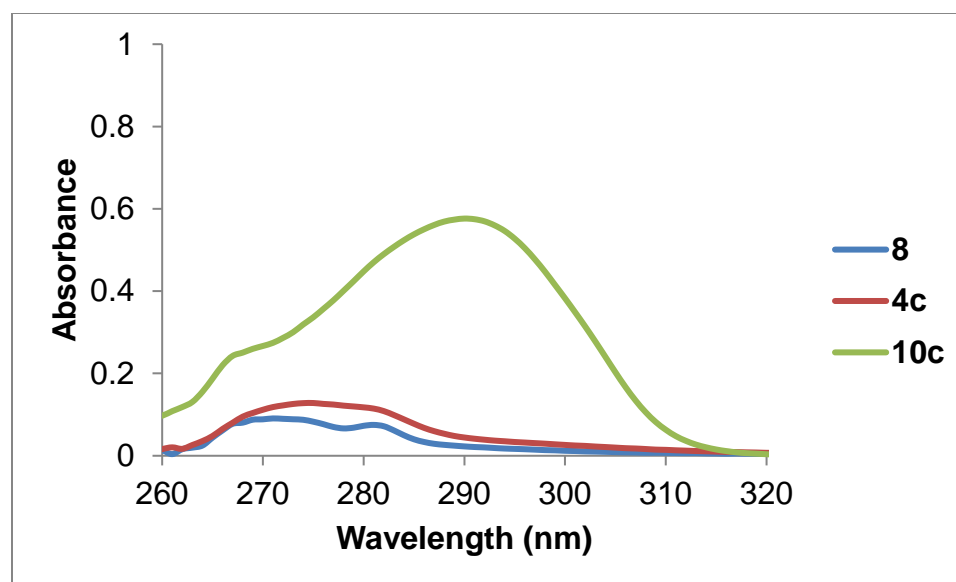
UV-vis spectra of 2-(4-bromophenyl)-3-(decyl)benzoxazaborole (**9c**), 2-(decylamino)phenol (**4c**) and 4-bromophenylboronic acid (**7**) in CHCl₃.



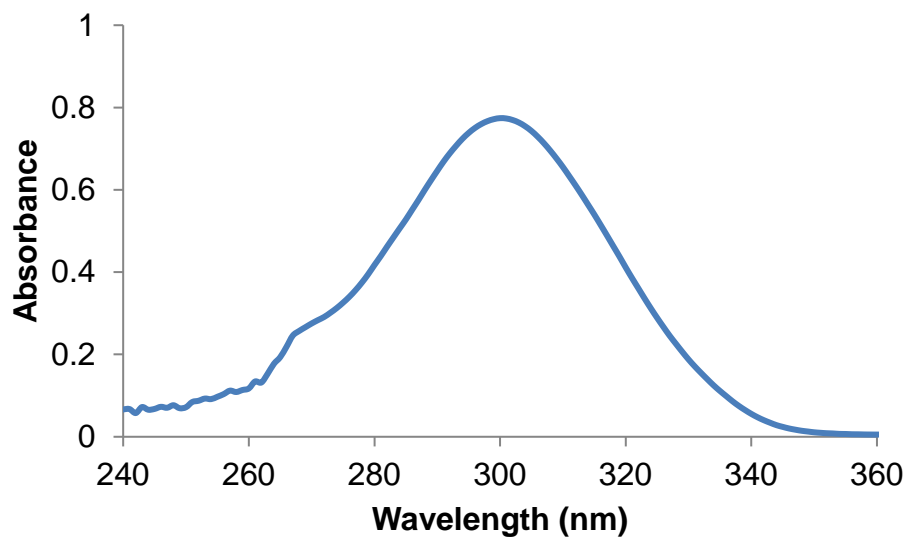
UV-vis spectra of 3-(ethyl)-2-(4-methoxyphenyl)-benzoxazaborole (**10a**), 2-(ethylamino)phenol (**4a**) and 4-methoxyphenylboronic acid (**8**) in CHCl₃.



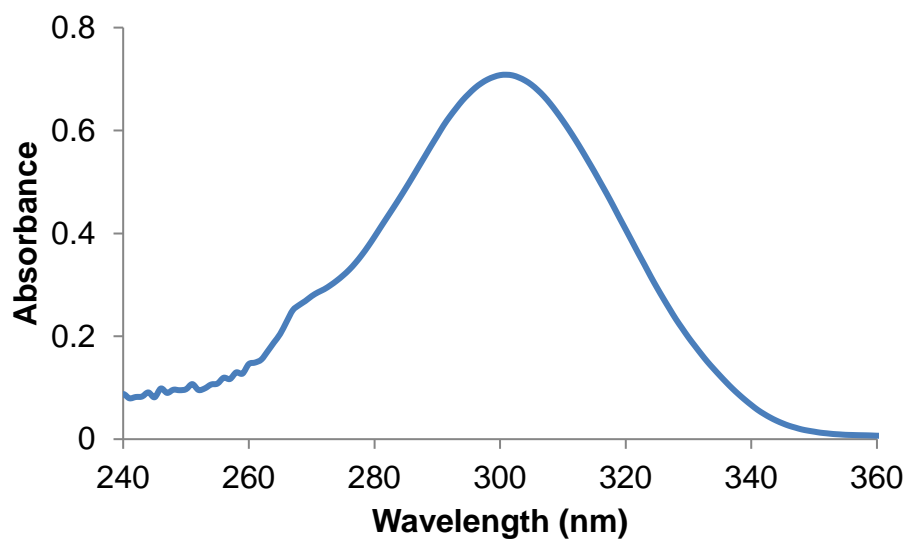
UV-vis spectra of 3-(butyl)-2-(4-methoxyphenyl)-benzoxazaborole (**10b**) 2-(butylamino)phenol (**4b**) and 4-methoxyphenylboronic acid (**8**) in CHCl₃.



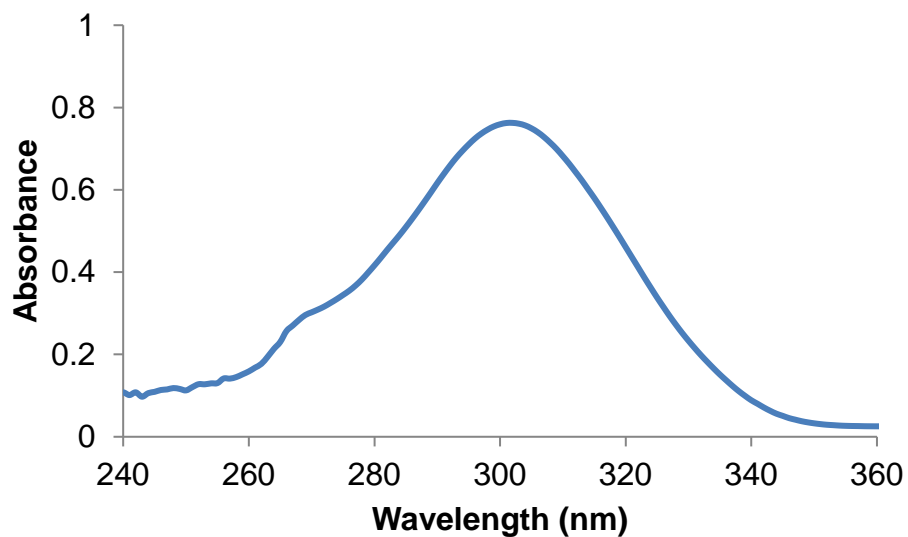
UV-vis spectra of 3-(decyl)-2-(4-methoxyphenyl)-benzoxazaborole (**10b**) 2-(decylamino)phenol (**4b**) and 4-methoxyphenylboronic acid (**8**) in CHCl₃.



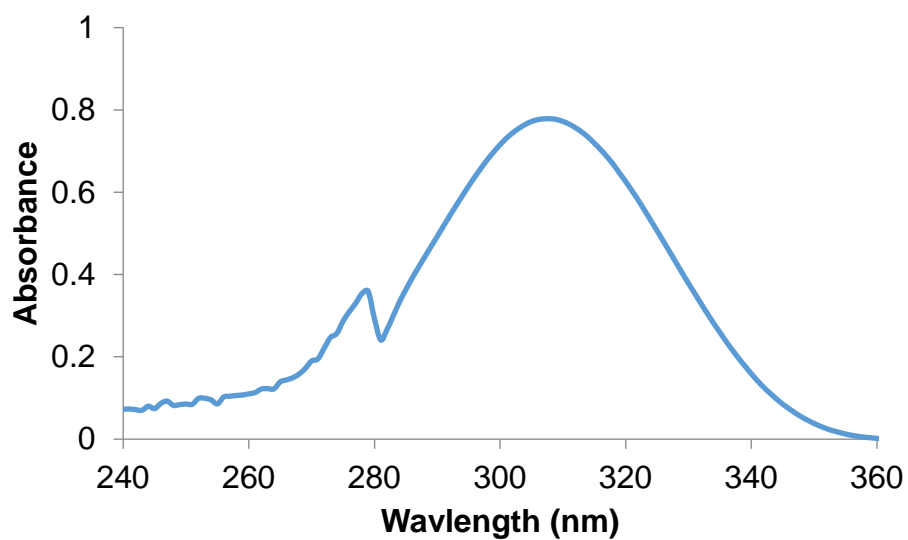
UV-vis spectrum of 1,4-phenylene-bis-[3-(ethyl)benzoxazaborole] (**13a**) in CHCl_3 .



UV-vis spectrum of 1,4-phenylene-bis-[3-(butyl)benzoxazaborole] (**13b**) in CHCl_3 .

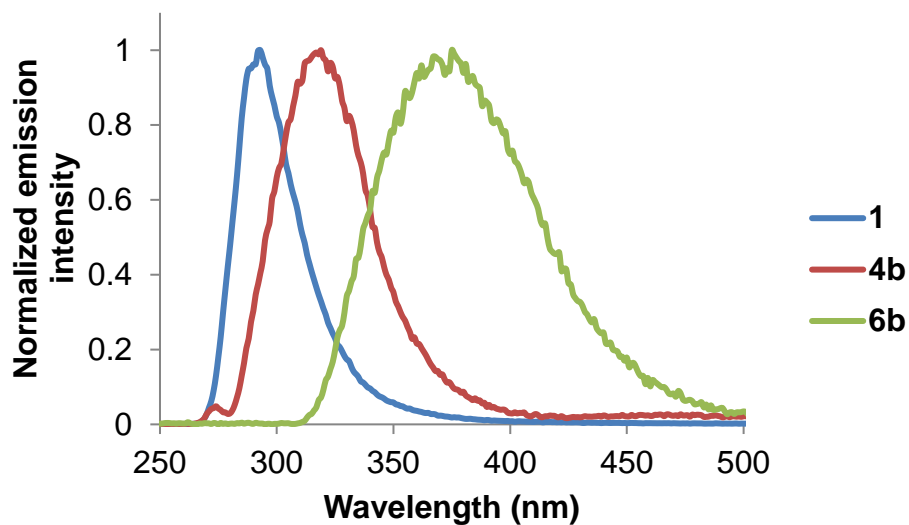


UV-vis spectrum of 1,4-phenylene-bis-[3-(decyl)benzoxazaborole] (**13c**) in CHCl_3 .

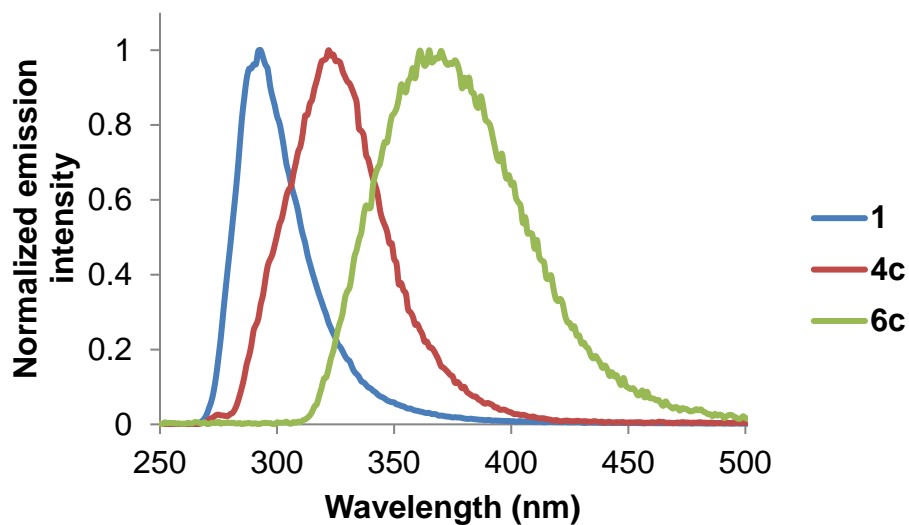


UV-vis spectrum of biphenyl-4,4'-bis-[3-(ethyl)benzoxazaborole] (**15a**) in CHCl_3 .

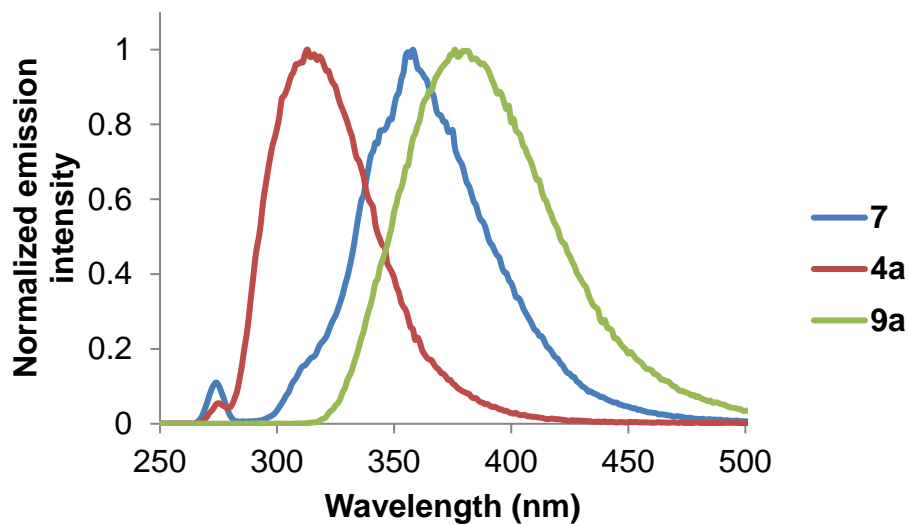
APPENDIX C – Emission spectra for the synthesized compounds



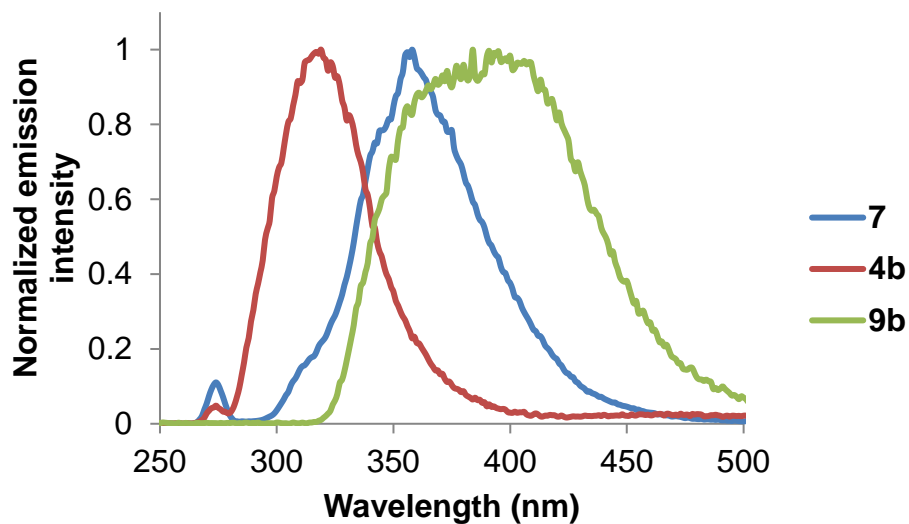
Normalized emission spectra of 3-(butyl)benzoxazaborole (**6b**), 2-(butylamino)phenol (**4b**) and phenylboronic acid (**1**) in CHCl₃.



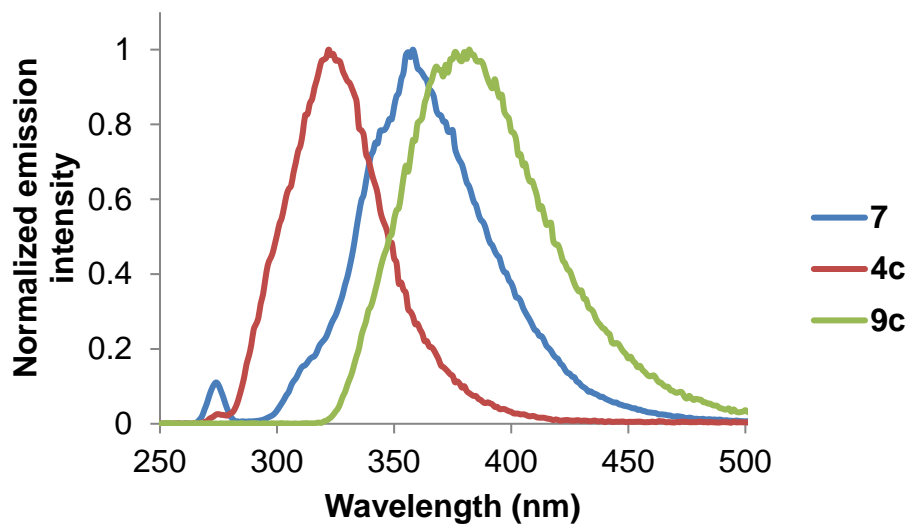
Normalized emission spectra of 3-(decyl)benzoxazaborole (**6c**), 2-(decylamino)phenol (**4c**) and phenylboronic acid (**1**) in CHCl₃.



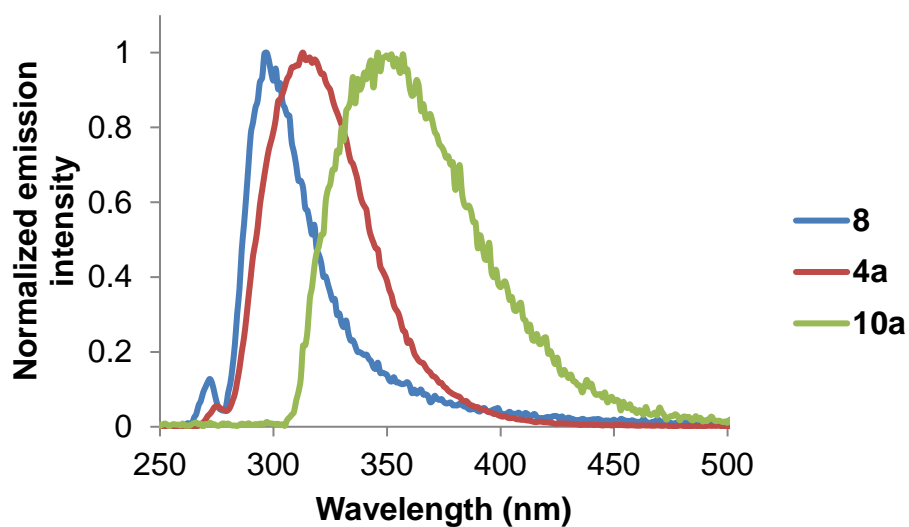
Normalized emission spectrum of 2-(4-bromophenyl)-3-(ethyl)benzoxazaborole (**9a**) in CHCl_3 .



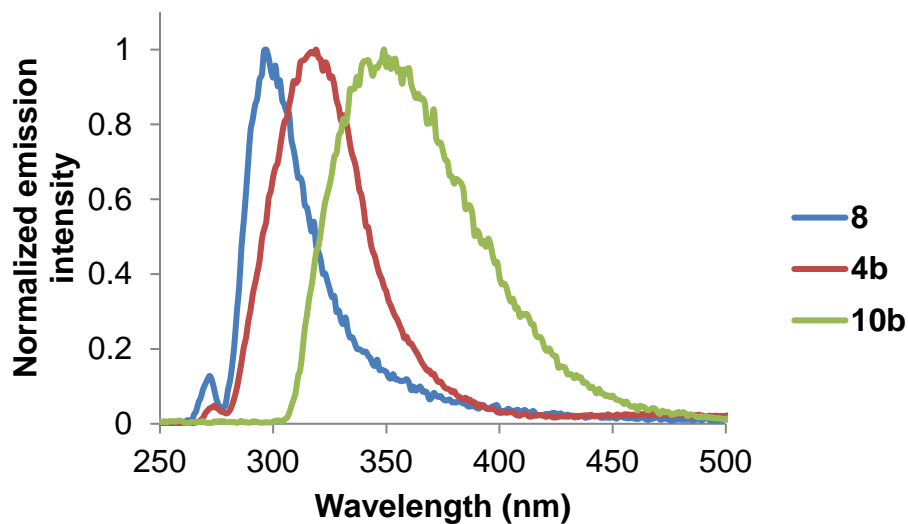
Normalized emission spectrum of 2-(4-bromophenyl)-3-(butyl)benzoxazaborole (**9b**) in CHCl_3 .



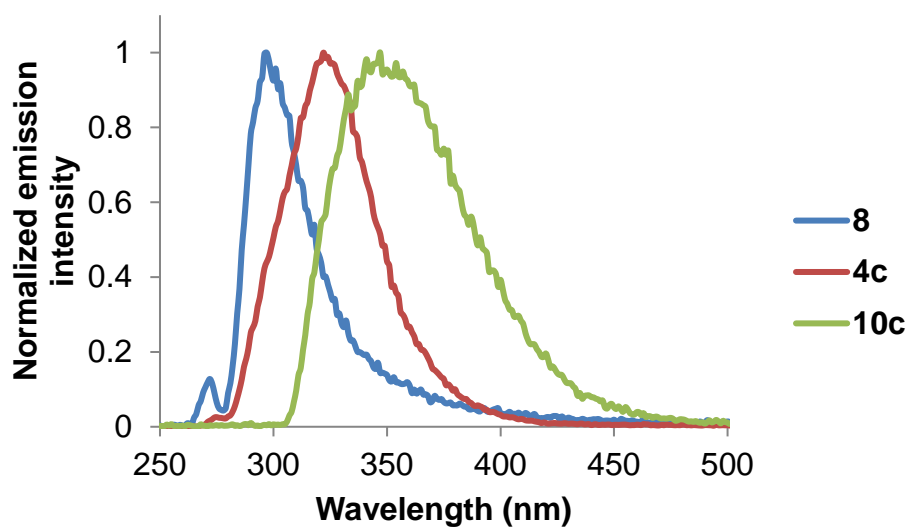
Normalized emission spectrum of 2-(4-bromophenyl)-3-(decyl)benzoxazaborole (**9c**) in CHCl_3 .



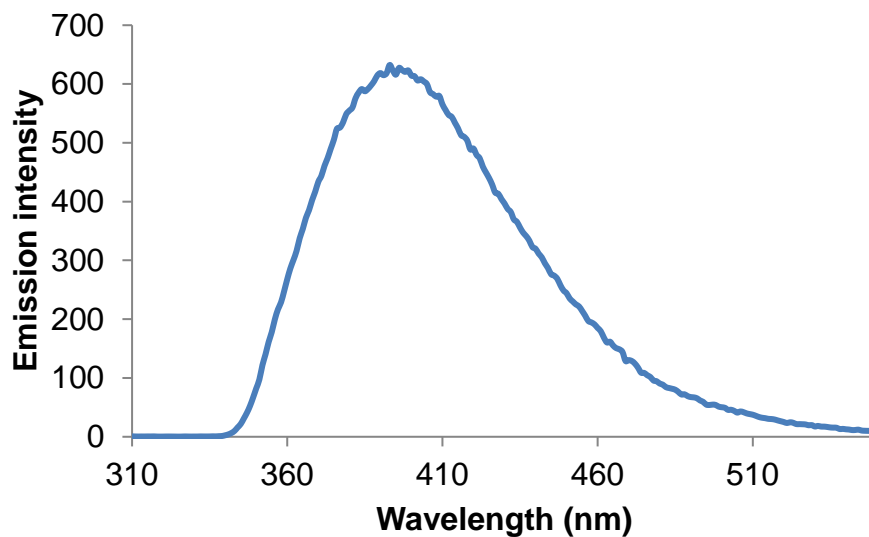
Normalized emission spectra of 3-(ethyl)-2-(4-methoxyphenyl)-benzoxazaborole (**10a**), 2-(ethylamino)phenol (**4a**) and 4-methoxyphenylboronic acid (**8**) in CHCl_3 .



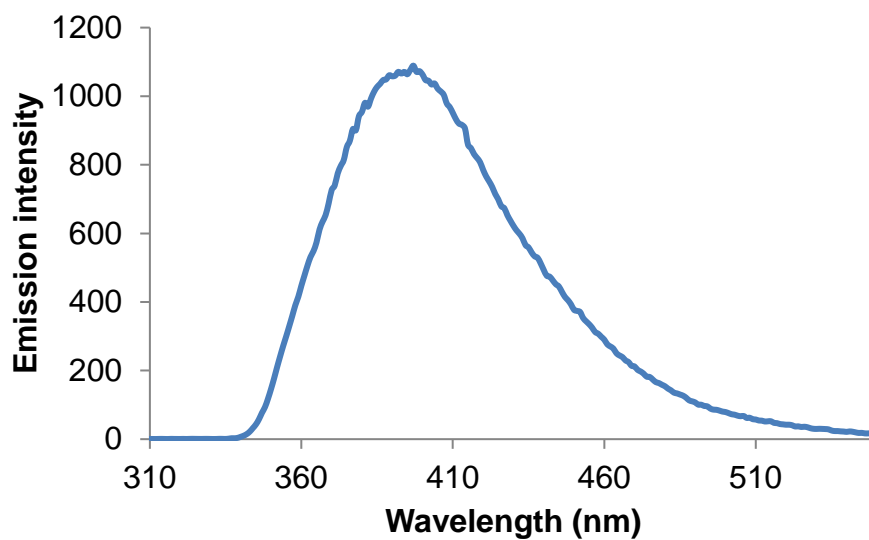
Normalized emission spectra of 3-(butyl)-2-(4-methoxyphenyl)-benzoxazaborole (**10b**)
2-(butylamino)phenol (**4b**) and 4-methoxyphenylboronic acid (**8**) in CHCl₃.



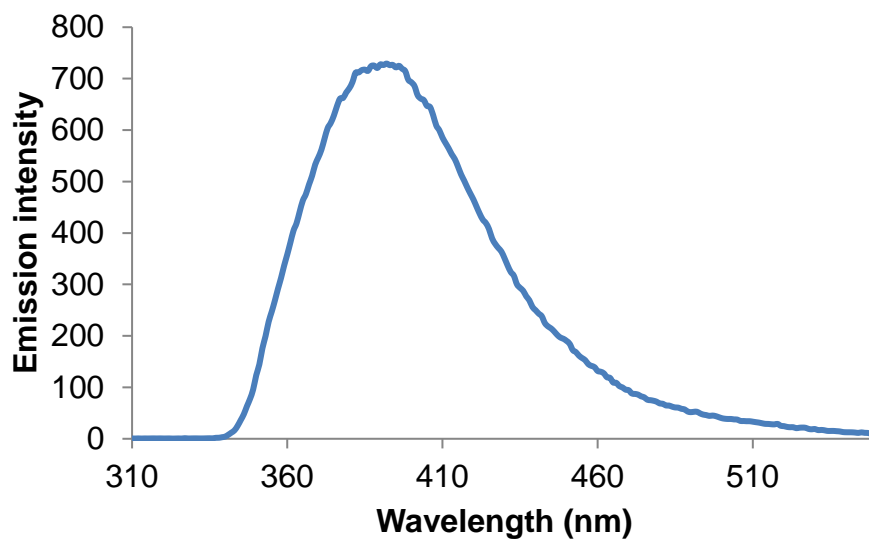
Normalized emission spectra of 3-(decyl)-2-(4-methoxyphenyl)-benzoxazaborole (**10c**)
2-(decylamino)phenol (**4c**) and 4-methoxyphenylboronic acid (**8**) in CHCl₃.



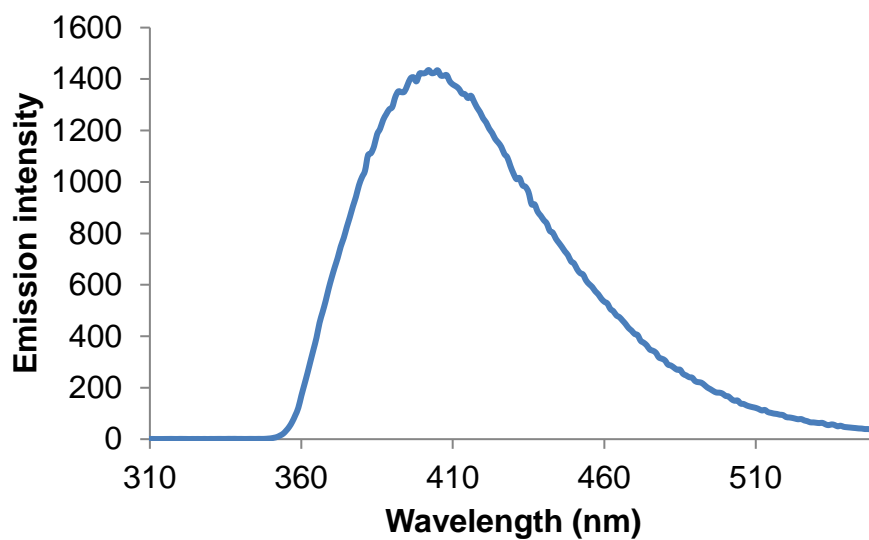
Emission spectrum of 1,4-phenylene-bis-[3-(ethyl)benzoxazaborole] (**13a**) in CHCl_3 .



Emission spectrum of 1,4-phenylene-bis-[3-(butyl)benzoxazaborole] (**13b**) in CHCl_3 .

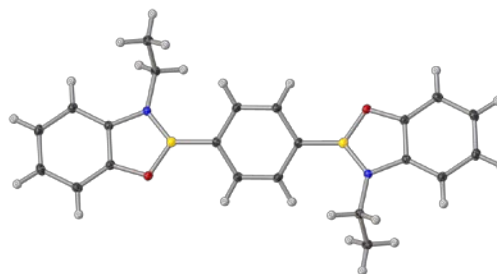


Emission spectrum of 1,4-phenylene-bis-[3-(decyl)benzoxazaborole] (**13c**) in CHCl_3 .



Emission spectrum of biphenyl-4,4'-bis-[3-(ethyl)benzoxazaborole] (**15a**) in CHCl_3 .

APPENDIX D – X-ray crystallographic data.

X-ray crystal structure of bis(benzoxazaborole) **13a**Table 1 Crystal data and structure refinement for **13a**.

Identification code	pbeb
Empirical formula	C ₂₂ H ₂₂ B ₂ N ₂ O ₂
Formula weight	368.03
Temperature/K	100(2)
Crystal system	monoclinic
Space group	P2 ₁ /c
a/Å	5.2985(11)
b/Å	13.201(3)
c/Å	13.070(3)
α/°	90
β/°	100.456(8)
γ/°	90
Volume/Å ³	899.0(3)
Z	2
ρ _{calc} /cm ³	1.360
μ/mm ⁻¹	0.085
F(000)	388.0
Crystal size/mm ³	0.240 × 0.200 × 0.150
Radiation	MoKα (λ = 0.71073)
2θ range for data collection/°	6.172 to 61.132
Index ranges	-7 ≤ h ≤ 7, -18 ≤ k ≤ 18, -18 ≤ l ≤ 18
Reflections collected	13901
Independent reflections	2766 [R _{int} = 0.0435, R _{sigma} = 0.0352]
Data/restraints/parameters	2766/0/136
Goodness-of-fit on F ²	1.007
Final R indexes [I >= 2σ (I)]	R ₁ = 0.0437, wR ₂ = 0.1119

(continued)

Final R indexes [all data] $R_1 = 0.0559$, $wR_2 = 0.1189$
 Largest diff. peak/hole / e \AA^{-3} 0.53/-0.20

Table 2 Fractional Atomic Coordinates ($\times 10^4$) and Equivalent Isotropic Displacement Parameters ($\text{\AA}^2 \times 10^3$) for **13a**. U_{eq} is defined as 1/3 of the trace of the orthogonalised U_{ij} tensor.

Atom	x	y	z	U(eq)
C1	11345(2)	2632.4(8)	3542.4(8)	10.4(2)
C2	12881(2)	2239.6(8)	2885.3(8)	12.5(2)
C3	14724(2)	1524.4(8)	3300.2(9)	13.9(2)
C4	14973(2)	1196.3(8)	4322.8(9)	14.7(2)
C5	13375(2)	1573.5(8)	4975.3(8)	13.8(2)
C6	11601(2)	2294.3(8)	4568.3(8)	11.2(2)
C7	6740.9(19)	4290.5(8)	4689.9(8)	10.6(2)
C8	5481(2)	4088.4(8)	5519.8(8)	12.1(2)
C9	6229(2)	5222.3(8)	4181.9(8)	12.8(2)
C10	8631(2)	3853.9(8)	2384.3(8)	12.2(2)
C11	10431(2)	4686.9(9)	2160.7(9)	16.1(2)
B1	8654(2)	3515.6(9)	4369.5(9)	11.1(2)
N1	9467.2(17)	3384.3(6)	3398.2(7)	10.17(18)
O1	9956.7(15)	2810.1(6)	5082.0(6)	12.09(17)

Table 3 Anisotropic Displacement Parameters ($\text{\AA}^2 \times 10^3$) for **13a**. The Anisotropic displacement factor exponent takes the form: $-2\pi^2[h^2a^2U_{11}+2hka^*b^*U_{12}+\dots]$.

Atom	U ₁₁	U ₂₂	U ₃₃	U ₂₃	U ₁₃	U ₁₂
C1	10.5(5)	8.7(4)	12.1(5)	-0.8(3)	2.2(4)	-0.6(3)
C2	14.1(5)	11.4(5)	12.7(5)	-0.9(3)	4.4(4)	0.3(4)
C3	14.1(5)	11.5(5)	17.4(5)	-2.6(4)	5.8(4)	0.8(4)
C4	14.6(5)	10.8(5)	18.4(5)	0.0(4)	2.1(4)	2.5(4)
C5	16.5(5)	11.6(5)	13.0(5)	0.9(4)	2.3(4)	0.8(4)
C6	12.6(5)	9.9(4)	11.7(5)	-1.6(3)	3.7(4)	-0.4(3)
C7	10.0(4)	10.8(4)	11.1(4)	-2.1(3)	2.6(3)	-0.9(3)
C8	14.4(5)	10.1(4)	12.4(4)	0.1(4)	4.0(4)	0.3(4)
C9	14.5(5)	12.5(5)	12.6(5)	-0.6(4)	6.0(4)	0.0(4)
C10	12.1(5)	14.0(5)	10.3(4)	0.6(3)	1.3(4)	1.2(4)

(continued)

C11	16.1(5)	16.6(5)	16.8(5)	4.6(4)	6.4(4)	2.1(4)
B1	11.6(5)	10.6(5)	11.3(5)	-1.1(4)	2.3(4)	-1.0(4)
N1	10.5(4)	9.9(4)	10.3(4)	0.3(3)	2.3(3)	1.3(3)
O1	14.2(4)	11.8(3)	11.2(3)	-0.5(3)	4.9(3)	2.0(3)

Table 4 Bond Lengths for **13a**.

Atom	Atom	Length/Å	Atom	Atom	Length/Å
C1	C2	1.3868(14)	C7	C8	1.3985(14)
C1	N1	1.3937(13)	C7	C9	1.4007(15)
C1	C6	1.3961(14)	C7	B1	1.5502(15)
C2	C3	1.3951(15)	C8	C9 ¹	1.3892(15)
C3	C4	1.3882(16)	C10	N1	1.4573(13)
C4	C5	1.3980(15)	C10	C11	1.5187(15)
C5	C6	1.3751(15)	B1	O1	1.4063(14)
C6	O1	1.3731(12)	B1	N1	1.4234(14)

¹1-X,1-Y,1-ZTable 5 Bond Angles for **13a**.

Atom	Atom	Atom	Angle/°	Atom	Atom	Atom	Angle/°
C2	C1	N1	131.87(10)	C9	C7	B1	122.08(9)
C2	C1	C6	120.64(10)	C9 ¹	C8	C7	121.35(10)
N1	C1	C6	107.46(9)	C8 ¹	C9	C7	121.47(9)
C1	C2	C3	117.41(10)	N1	C10	C11	112.64(9)
C4	C3	C2	121.53(10)	O1	B1	N1	108.56(9)
C3	C4	C5	120.92(10)	O1	B1	C7	121.64(9)
C6	C5	C4	117.24(10)	N1	B1	C7	129.79(10)
O1	C6	C5	127.14(9)	C1	N1	B1	106.87(8)
O1	C6	C1	110.58(9)	C1	N1	C10	121.19(9)
C5	C6	C1	122.22(10)	B1	N1	C10	131.90(9)
C8	C7	C9	117.17(9)	C6	O1	B1	106.46(8)
C8	C7	B1	120.74(9)				

¹1-X,1-Y,1-Z

Table 6 Torsion Angles for **13a**.

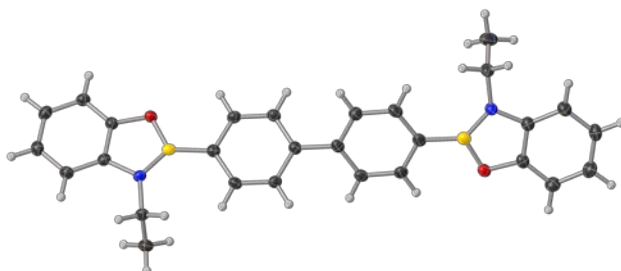
A	B	C	D	Angle/°	A	B	C	D	Angle/°
N1	C1	C2	C3	175.74(10)	C8	C7	B1	N1	156.52(11)
C6	C1	C2	C3	-1.95(15)	C9	C7	B1	N1	-24.62(17)
C1	C2	C3	C4	1.65(16)	C2	C1	N1	B1	-176.08(11)
C2	C3	C4	C5	0.04(17)	C6	C1	N1	B1	1.83(11)
C3	C4	C5	C6	-1.42(16)	C2	C1	N1	C10	5.78(17)
C4	C5	C6	O1	-175.73(10)	C6	C1	N1	C10	-176.31(9)
C4	C5	C6	C1	1.12(16)	O1	B1	N1	C1	-2.71(11)
C2	C1	C6	O1	177.90(9)	C7	B1	N1	C1	175.72(10)
N1	C1	C6	O1	-0.30(12)	O1	B1	N1	C10	175.15(10)
C2	C1	C6	C5	0.59(16)	C7	B1	N1	C10	-6.42(19)
N1	C1	C6	C5	-177.61(9)	C11	C10	N1	C1	-81.58(12)
C9	C7	C8	C9 ¹	0.82(17)	C11	C10	N1	B1	100.82(13)
B1	C7	C8	C9 ¹	179.73(10)	C5	C6	O1	B1	175.76(11)
C8	C7	C9	C8 ¹	-0.82(17)	C1	C6	O1	B1	-1.38(11)
B1	C7	C9	C8 ¹	-179.72(10)	N1	B1	O1	C6	2.51(11)
C8	C7	B1	O1	-25.23(15)	C7	B1	O1	C6	-176.07(9)
C9	C7	B1	O1	153.63(10)					

¹1-X,1-Y,1-ZTable 7 Hydrogen Atom Coordinates ($\text{\AA} \times 10^4$) and Isotropic Displacement Parameters ($\text{\AA}^2 \times 10^3$) for **13a**.

Atom	x	y	z	U(eq)
H2	12686.93	2449.36	2180.07	15
H3	15833.7	1255.67	2873.05	17
H4	16247.57	708.68	4582.75	18
H5	13509.29	1341.33	5671.08	17
H10A	6893.2	4141.71	2354.09	15
H10B	8517.23	3328.23	1837.61	15
H11A	10444.38	5235.86	2666.39	24
H11B	9842.99	4950.03	1456.64	24
H11C	12169.16	4412.47	2214.67	24

(continued)

H8	5780(30) 3450(11)	5884(12) 17(4)
H9	7110(30) 5405(12)	3634(12) 19(4)

X-ray crystal structure of bis(benzoxazaborole) **15a**Table 1 Crystal data and structure refinement for **15a**.

Identification code	bpebp
Empirical formula	C ₂₈ H ₂₆ B ₂ N ₂ O ₂
Formula weight	444.13
Temperature/K	100(2)
Crystal system	triclinic
Space group	P-1
a/Å	9.215(2)
b/Å	9.338(2)
c/Å	14.013(3)
α/°	79.618(5)
β/°	89.669(6)
γ/°	78.376(6)
Volume/Å ³	1161.3(5)
Z	2
ρ _{calc} /cm ³	1.270
μ/mm ⁻¹	0.078
F(000)	468.0
Crystal size/mm ³	0.260 × 0.110 × 0.050
Radiation	MoKα (λ = 0.71075)
2θ range for data collection/°	6.106 to 54.936
Index ranges	-11 ≤ h ≤ 10, -12 ≤ k ≤ 12, -18 ≤ l ≤ 18
Reflections collected	17549
Independent reflections	5204 [R _{int} = 0.0374, R _{sigma} = 0.0360]
Data/restraints/parameters	5204/236/340

(continued)

Goodness-of-fit on F^2	1.072
Final R indexes [$I \geq 2\sigma(I)$]	$R_1 = 0.0416$, $wR_2 = 0.0994$
Final R indexes [all data]	$R_1 = 0.0544$, $wR_2 = 0.1055$
Largest diff. peak/hole / $e \text{ \AA}^{-3}$	0.27/-0.18

Table 2 Fractional Atomic Coordinates ($\times 10^4$) and Equivalent Isotropic Displacement Parameters ($\text{\AA}^2 \times 10^3$) for **15a**. U_{eq} is defined as 1/3 of of the trace of the orthogonalised U_{ij} tensor.

Atom	x	y	z	U(eq)
C7	4970.2(14)	12056.6(14)	2350.5(9)	23.9(3)
C8	4696.1(14)	10830.2(14)	1977.9(9)	26.3(3)
C9	4107.4(14)	9715.7(14)	2544.5(9)	24.8(3)
C10	3754.0(13)	9771.2(13)	3517.8(9)	21.8(3)
C11	3995.5(14)	11001.9(13)	3894.1(9)	23.1(3)
C12	4603.2(14)	12106.8(14)	3325.7(9)	23.9(3)
C13	3174.6(13)	8538.5(13)	4126.1(9)	20.7(3)
C14	3782.3(13)	7048.8(14)	4076.7(9)	22.4(3)
C15	3225.8(13)	5900.8(13)	4633.8(9)	22.0(3)
C16	2040.6(13)	6169.8(13)	5260.3(9)	20.6(3)
C17	1457.8(14)	7669.0(13)	5309.7(9)	22.4(3)
C18	2005.9(14)	8826.0(13)	4756.1(9)	22.1(3)
C19	1550.3(13)	2375.3(13)	6395.0(9)	20.3(3)
C20	1981.8(14)	847.8(13)	6616.6(9)	22.6(3)
C21	1075.0(14)	83.9(14)	7232.7(9)	24.8(3)
C22	-191.7(14)	843.9(14)	7608.2(9)	25.0(3)
C23	-604.8(14)	2402.6(14)	7395.4(9)	22.7(3)
C24	289.5(13)	3162.9(13)	6779.0(9)	20.1(3)
N1	6285.4(11)	13548.5(13)	816.2(9)	21.2(3)
O1	5814(3)	14520(3)	2220.6(18)	22.6(4)
C1	6530(4)	15437(3)	1583(2)	21.6(4)
C2	6858(6)	16760(3)	1720(2)	27.5(6)
C3	7549(7)	17538(5)	964(4)	30.5(7)
C4	7881(2)	16985(2)	111.4(17)	30.2(5)
C5	7515(2)	15644(2)	-31.2(13)	27.6(4)
C6	6822.7(18)	14877.7(19)	720.2(13)	22.8(4)
C25	6445.2(17)	12696.1(18)	26.3(11)	26.5(4)
C26	7974(2)	11695(2)	33.7(13)	38.9(5)

(continued)				
N1A	6817(5)	13273(6)	1099(4)	26
O1A	5662(13)	14699(15)	2158(8)	26
C1A	6467(18)	15544(14)	1533(10)	26
C2A	6810(20)	16896(16)	1581(12)	26
C3A	7730(30)	17470(20)	879(17)	26
C4A	8295(11)	16701(9)	148(8)	26
C5A	8035(9)	15286(8)	146(6)	26
C6A	7177(10)	14690(8)	870(6)	26
C25A	7396(7)	12111(7)	546(4)	26
C26A	6613(9)	12192(9)	-398(5)	37
C27	-954.2(14)	5825.7(14)	6714.3(10)	24.2(3)
C28	-524.2(16)	6341.1(15)	7624.5(10)	29.7(3)
B1	5691.7(17)	13319.0(16)	1779.8(11)	25.5(3)
B2	1481.0(15)	4806.8(15)	5838.1(10)	20.2(3)
N2	222.0(11)	4686.3(11)	6427.5(7)	20.3(2)
O2	2284.6(9)	3351.7(9)	5816.8(6)	21.6(2)

Table 3 Anisotropic Displacement Parameters ($\text{\AA}^2 \times 10^3$) for bpebp. The Anisotropic displacement factor exponent takes the form: $-2\pi^2[h^2a^*U_{11}+2hka^*b^*U_{12}+\dots]$.

Atom	U ₁₁	U ₂₂	U ₃₃	U ₂₃	U ₁₃	U ₁₂
C7	20.5(6)	21.0(6)	26.2(6)	-1.0(5)	4.8(5)	1.8(5)
C8	27.6(7)	28.4(7)	20.9(6)	-2.8(5)	4.8(5)	-2.5(5)
C9	26.0(7)	24.6(6)	23.7(6)	-4.3(5)	2.1(5)	-4.8(5)
C10	18.3(6)	21.5(6)	22.0(6)	-0.2(5)	1.6(5)	0.9(5)
C11	22.8(6)	21.8(6)	21.5(6)	-2.6(5)	3.5(5)	1.4(5)
C12	23.1(6)	18.6(6)	27.7(7)	-4.6(5)	3.7(5)	1.4(5)
C13	20.4(6)	21.4(6)	18.2(6)	-0.8(5)	-0.7(5)	-2.0(5)
C14	18.8(6)	23.4(6)	23.3(6)	-4.0(5)	3.2(5)	-0.6(5)
C15	20.2(6)	19.1(6)	24.5(6)	-3.9(5)	-0.3(5)	1.0(5)
C16	20.8(6)	21.3(6)	18.0(6)	-2.3(5)	-1.9(5)	-1.2(5)
C17	22.5(6)	23.3(6)	19.6(6)	-3.4(5)	3.5(5)	-0.8(5)
C18	24.6(6)	18.2(6)	21.3(6)	-2.9(5)	1.0(5)	0.1(5)
C19	20.9(6)	21.7(6)	18.1(6)	-3.5(5)	-0.2(5)	-3.7(5)
C20	22.1(6)	21.3(6)	22.8(6)	-4.6(5)	-0.5(5)	0.2(5)
C21	29.2(7)	19.0(6)	25.5(6)	-3.2(5)	-3.4(5)	-4.1(5)
C22	26.2(7)	25.7(6)	24.0(6)	-2.4(5)	0.2(5)	-9.1(5)

(continued)						
C23	20.0(6)	25.5(6)	22.7(6)	-5.8(5)	1.4(5)	-3.5(5)
C24	21.2(6)	19.3(6)	19.2(6)	-4.1(5)	-2.4(5)	-1.9(5)
N1	22.3(7)	22.8(7)	19.5(7)	-4.7(5)	2.2(5)	-6.0(5)
O1	24.4(9)	23.1(10)	18.4(7)	-1.4(6)	1.6(6)	-2.7(7)
C1	19.1(8)	23.5(9)	18.9(8)	1.9(7)	-3.0(6)	-1.9(7)
C2	31.1(10)	30.0(12)	22.3(14)	-6.3(11)	-3.5(12)	-6.6(10)
C3	32(3)	28.4(11)	34.0(16)	-5.4(8)	-4.0(10)	-11.6(14)
C4	28.3(12)	31.0(11)	31.0(9)	0.7(9)	2.4(10)	-11.2(8)
C5	28.8(10)	29.8(9)	23.7(9)	-2.8(7)	3.2(7)	-6.4(7)
C6	20.4(10)	24.8(8)	22.4(9)	-2.6(7)	-0.8(7)	-4.3(7)
C25	34.9(9)	28.5(8)	18.7(8)	-6.2(7)	4.5(7)	-11.0(7)
C26	53.1(12)	32.1(9)	27.1(9)	-6.8(8)	8.6(8)	2.3(9)
C27	21.3(6)	20.4(6)	29.6(7)	-6.3(5)	5.0(5)	0.1(5)
C28	34.4(8)	27.3(7)	28.4(7)	-9.4(6)	9.3(6)	-4.8(6)
B1	24.9(7)	22.2(7)	26.4(7)	-2.6(6)	4.7(6)	0.1(6)
B2	21.1(7)	19.7(6)	17.9(6)	-4.0(5)	-0.7(5)	0.6(5)
N2	21.1(5)	17.2(5)	21.2(5)	-4.0(4)	1.1(4)	-0.4(4)
O2	22.6(4)	19.3(4)	20.9(4)	-2.2(3)	4.3(3)	-0.9(3)

Table 4 Bond Lengths for **15a**.

Atom	Atom	Length/Å	Atom	Atom	Length/Å
C7	C8	1.4077(18)	O1	C1	1.382(2)
C7	C12	1.4126(18)	O1	B1	1.397(3)
C7	B1	1.5625(19)	C1	C2	1.376(3)
C8	C9	1.3902(18)	C1	C6	1.405(3)
C9	C10	1.4080(17)	C2	C3	1.398(3)
C10	C11	1.4040(18)	C3	C4	1.394(3)
C10	C13	1.4918(17)	C4	C5	1.408(2)
C11	C12	1.3943(18)	C5	C6	1.390(2)
C13	C18	1.4033(17)	C25	C26	1.525(2)
C13	C14	1.4050(17)	N1A	B1	1.405(6)
C14	C15	1.3917(18)	N1A	C6A	1.410(7)
C15	C16	1.4088(17)	N1A	C25A	1.458(6)
C16	C17	1.4088(17)	O1A	C1A	1.385(8)
C16	B2	1.5587(19)	O1A	B1	1.475(14)

						(continued)
C17	C18	1.3919(17)	C1A	C2A	1.377(8)	
C19	C20	1.3792(17)	C1A	C6A	1.406(8)	
C19	O2	1.3864(15)	C2A	C3A	1.398(8)	
C19	C24	1.4041(17)	C3A	C4A	1.391(8)	
C20	C21	1.4008(18)	C4A	C5A	1.390(8)	
C21	C22	1.3917(18)	C5A	C6A	1.388(7)	
C22	C23	1.4050(18)	C25A	C26A	1.494(7)	
C23	C24	1.3914(17)	C27	N2	1.4673(15)	
C24	N2	1.4080(15)	C27	C28	1.5230(18)	
N1	C6	1.411(2)	B2	O2	1.4159(15)	
N1	B1	1.450(2)	B2	N2	1.4314(17)	
N1	C25	1.466(2)				

Table 5 Bond Angles for **15a**.

Atom	Atom	Atom	Angle/°	Atom	Atom	Atom	Angle/°
C8	C7	C12	116.71(12)	C1	C2	C3	117.2(2)
C8	C7	B1	124.97(12)	C4	C3	C2	120.9(2)
C12	C7	B1	118.29(12)	C3	C4	C5	121.7(2)
C9	C8	C7	121.65(12)	C6	C5	C4	117.29(17)
C8	C9	C10	121.21(12)	C5	C6	C1	120.12(18)
C11	C10	C9	117.78(11)	C5	C6	N1	132.33(17)
C11	C10	C13	121.71(11)	C1	C6	N1	107.55(17)
C9	C10	C13	120.50(11)	N1	C25	C26	112.68(12)
C12	C11	C10	120.73(12)	B1	N1A	C6A	108.8(5)
C11	C12	C7	121.91(12)	B1	N1A	C25A	129.1(5)
C18	C13	C14	118.04(11)	C6A	N1A	C25A	121.2(6)
C18	C13	C10	121.36(11)	C1A	O1A	B1	106.9(8)
C14	C13	C10	120.59(11)	C2A	C1A	O1A	129.9(9)
C15	C14	C13	120.53(11)	C2A	C1A	C6A	120.0(8)
C14	C15	C16	122.19(11)	O1A	C1A	C6A	109.3(8)
C17	C16	C15	116.49(11)	C1A	C2A	C3A	118.1(9)
C17	C16	B2	125.37(11)	C4A	C3A	C2A	121.6(10)
C15	C16	B2	118.15(11)	C5A	C4A	C3A	119.9(8)
C18	C17	C16	121.81(11)	C6A	C5A	C4A	118.4(7)
C17	C18	C13	120.93(11)	C5A	C6A	C1A	121.1(7)

(continued)							
C20	C19	O2	126.82(11)	C5A	C6A	N1A	131.4(7)
C20	C19	C24	122.80(11)	C1A	C6A	N1A	107.5(7)
O2	C19	C24	110.33(10)	N1A	C25A	C26A	116.5(5)
C19	C20	C21	116.93(11)	N2	C27	C28	112.29(11)
C22	C21	C20	121.07(12)	O1	B1	N1	108.75(15)
C21	C22	C23	121.59(12)	N1A	B1	O1A	105.2(5)
C24	C23	C22	117.42(11)	O1	B1	C7	118.79(15)
C23	C24	C19	120.16(11)	N1A	B1	C7	130.9(2)
C23	C24	N2	132.56(11)	N1	B1	C7	132.45(13)
C19	C24	N2	107.27(11)	O1A	B1	C7	120.6(4)
C6	N1	B1	106.04(13)	O2	B2	N2	108.05(11)
C6	N1	C25	120.20(14)	O2	B2	C16	119.50(11)
B1	N1	C25	133.73(13)	N2	B2	C16	132.44(11)
C1	O1	B1	107.1(2)	C24	N2	B2	107.36(10)
C2	C1	O1	126.6(2)	C24	N2	C27	121.21(10)
C2	C1	C6	122.9(2)	B2	N2	C27	131.37(10)
O1	C1	C6	110.5(2)	C19	O2	B2	106.97(9)

Table 6 Torsion Angles for **15a**.

A	B	C	D	Angle/°	A	B	C	D	Angle/°
C12	C7	C8	C9	-0.64(19)	O1A	C1A	C2A	C3A	176(2)
B1	C7	C8	C9	177.19(12)	C6A	C1A	C2A	C3A	8(3)
C7	C8	C9	C10	0.3(2)	C1A	C2A	C3A	C4A	0(4)
C8	C9	C10	C11	0.92(18)	C2A	C3A	C4A	C5A	-5(4)
C8	C9	C10	C13	-177.77(11)	C3A	C4A	C5A	C6A	2(2)
C9	C10	C11	C12	-1.70(18)	C4A	C5A	C6A	C1A	6.1(14)
C13	C10	C11	C12	176.97(11)	C4A	C5A	C6A	N1A	-174.7(9)
C10	C11	C12	C7	1.36(19)	C2A	C1A	C6A	C5A	-11(2)
C8	C7	C12	C11	-0.16(18)	O1A	C1A	C6A	C5A	178.6(12)
B1	C7	C12	C11	-178.14(11)	C2A	C1A	C6A	N1A	169.4(16)
C11	C10	C13	C18	43.26(17)	O1A	C1A	C6A	N1A	-0.8(12)
C9	C10	C13	C18	-138.10(13)	B1	N1A	C6A	C5A	-169.0(9)
C11	C10	C13	C14	-137.23(13)	C25A	N1A	C6A	C5A	1.2(12)
C9	C10	C13	C14	41.40(17)	B1	N1A	C6A	C1A	10.3(9)
C18	C13	C14	C15	0.49(18)	C25A	N1A	C6A	C1A	-179.5(7)

(continued)

C10	C13	C14	C15	-179.03(11)	B1	N1A	C25A	C26A	87.4(7)
C13	C14	C15	C16	0.34(19)	C6A	N1A	C25A	C26A	-80.6(8)
C14	C15	C16	C17	-1.11(18)	C1	O1	B1	N1	-3.0(2)
C14	C15	C16	B2	178.88(11)	C1	O1	B1	C7	177.91(19)
C15	C16	C17	C18	1.09(18)	C6A	N1A	B1	O1A	-15.1(8)
B2	C16	C17	C18	-178.90(12)	C25A	N1A	B1	O1A	175.7(3)
C16	C17	C18	C13	-0.30(19)	C6A	N1A	B1	C7	-174.0(4)
C14	C13	C18	C17	-0.51(18)	C25A	N1A	B1	C7	16.8(5)
C10	C13	C18	C17	179.01(11)	C6	N1	B1	O1	2.69(18)
O2	C19	C20	C21	178.92(11)	C25	N1	B1	O1	-179.47(6)
C24	C19	C20	C21	1.73(18)	C6	N1	B1	C7	-178.43(14)
C19	C20	C21	C22	-0.67(18)	C25	N1	B1	C7	-0.6(2)
C20	C21	C22	C23	-0.72(19)	C1A	O1A	B1	N1A	14.5(11)
C21	C22	C23	C24	1.06(19)	C1A	O1A	B1	C7	176.0(8)
C22	C23	C24	C19	-0.04(18)	C8	C7	B1	O1	176.09(15)
C22	C23	C24	N2	-179.13(12)	C12	C7	B1	O1	-6.1(2)
C20	C19	C24	C23	-1.40(18)	C8	C7	B1	N1A	-36.1(3)
O2	C19	C24	C23	-179.00(10)	C12	C7	B1	N1A	141.7(3)
C20	C19	C24	N2	177.90(11)	C8	C7	B1	N1	-2.7(2)
O2	C19	C24	N2	0.30(13)	C12	C7	B1	N1	175.09(13)
B1	O1	C1	C2	178.8(4)	C8	C7	B1	O1A	167.8(6)
B1	O1	C1	C6	2.2(3)	C12	C7	B1	O1A	-14.5(6)
O1	C1	C2	C3	-178.0(5)	C17	C16	B2	O2	-171.97(11)
C6	C1	C2	C3	-1.8(7)	C15	C16	B2	O2	8.04(17)
C1	C2	C3	C4	0.2(9)	C17	C16	B2	N2	8.8(2)
C2	C3	C4	C5	1.1(8)	C15	C16	B2	N2	-171.17(13)
C3	C4	C5	C6	-0.8(4)	C23	C24	N2	B2	178.12(13)
C4	C5	C6	C1	-0.8(3)	C19	C24	N2	B2	-1.05(13)
C4	C5	C6	N1	178.48(15)	C23	C24	N2	C27	0.8(2)
C2	C1	C6	C5	2.1(5)	C19	C24	N2	C27	-178.41(10)
O1	C1	C6	C5	178.9(2)	O2	B2	N2	C24	1.42(13)
C2	C1	C6	N1	-177.3(3)	C16	B2	N2	C24	-179.30(13)
O1	C1	C6	N1	-0.6(3)	O2	B2	N2	C27	178.41(11)
B1	N1	C6	C5	179.39(17)	C16	B2	N2	C27	-2.3(2)
C25	N1	C6	C5	1.2(2)	C28	C27	N2	C24	90.02(14)
B1	N1	C6	C1	-1.3(2)	C28	C27	N2	B2	-86.62(16)
C25	N1	C6	C1	-179.49(17)	C20	C19	O2	B2	-176.89(12)

(continued)

C6	N1	C25	C26	82.08(16)	C24	C19	O2	B2	0.59(13)
B1	N1	C25	C26	-95.52(17)	N2	B2	O2	C19	-1.23(13)
B1	O1A	C1A	C2A	-177.4(19)	C16	B2	O2	C19	179.38(10)
B1	O1A	C1A	C6A	-8.5(13)					

Table 7 Hydrogen Atom Coordinates ($\text{\AA} \times 10^4$) and Isotropic Displacement Parameters ($\text{\AA}^2 \times 10^3$) for **15a**.

Atom	<i>x</i>	<i>y</i>	<i>z</i>	U(eq)
H8	4919.11	10762.44	1322.79	32
H9	3940.38	8901.82	2270.01	30
H11	3742.19	11082.68	4543.11	28
H12	4775.28	12917	3602.32	29
H14	4579.56	6823.28	3659.83	27
H15	3659.46	4902.65	4590.04	26
H17	669.08	7896.57	5732.35	27
H18	1582.85	9824.39	4805.49	27
H20	2853.68	337.3	6363.06	27
H21	1328.98	-969.98	7396.87	30
H22	-791.63	295.43	8018.26	30
H23	-1461.5	2917.45	7662.15	27
H2	6624.87	17130.53	2302.49	33
H3	7795.57	18454.36	1033.36	37
H4	8365.89	17526.97	-386.28	36
H5	7733.23	15278.16	-616.92	33
H25A	6266.08	13394.87	-602.36	32
H25B	5683.77	12076.31	82.73	32
H26A	8729.59	12307.15	-58.45	58
H26B	8012.88	11127.03	-492.89	58
H26C	8163.32	11007.77	657.28	58
H2A	6440.18	17426.9	2078.47	31
H3A	7983.45	18398.58	901.27	31
H4A	8855.17	17144.71	-349.6	31
H5A	8433.81	14740.44	-338.21	31
H25C	7371.36	11137.4	957.68	31
H25D	8448.52	12137.66	415.54	31
H26D	5558.92	12206.62	-288.76	55

(continued)

H26E	7045.08	11321.87	-681.83	55
H26F	6719.84	13099.4	-844.01	55
H27A	-1864.81	5418.9	6832.58	29
H27B	-1177.61	6690.68	6175.44	29
H28A	-299.87	5488.19	8160.13	45
H28B	-1347.93	7082.36	7797.15	45
H28C	352.05	6784.49	7502.03	45

Table 8 Atomic Occupancy for **15a**.

Atom	Occupancy	Atom	Occupancy	Atom	Occupancy
N1	0.8	O1	0.8	C1	0.8
C2	0.8	H2	0.8	C3	0.8
H3	0.8	C4	0.8	H4	0.8
C5	0.8	H5	0.8	C6	0.8
C25	0.8	H25A	0.8	H25B	0.8
C26	0.8	H26A	0.8	H26B	0.8
H26C	0.8	N1A	0.2	O1A	0.2
C1A	0.2	C2A	0.2	H2A	0.2
C3A	0.2	H3A	0.2	C4A	0.2
H4A	0.2	C5A	0.2	H5A	0.2
C6A	0.2	C25A	0.2	H25C	0.2
H25D	0.2	C26A	0.2	H26D	0.2
H26E	0.2	H26F	0.2		

VITA

EDUCATION

Master of Science in Chemistry 08/2016 – Present
Sam Houston State University, Texas, USA

- Expected graduation: Summer 2018
- Thesis title: “Synthesis, Characterization, and Computational Studies of *N*-alkylbenzoxazaboroles”
- Advisor: Dr. Dustin E. Gross
- Current GPA: 3.78 out of 4.00

Master of Science in Analytical Chemistry 05/2013 – 06/2015
Post Graduate Institute of Science, University of Peradeniya, Sri Lanka

- Thesis title: “Desalination Applications of Murunkan Clay - A Laboratory Simulated Study”
- Advisors: Prof. A. D. L. C. Perera & Dr. Nilwala Kottegoda
- GPA: 3.60 out of 4.00

Bachelor of Science in Applied Sciences (Major-Chemistry) 08/2008 – 11/2012
University of Peradeniya, Sri Lanka

- Final year project: “Analysis of Operational Equipment Efficiency in GlaxoSmithKline Pharmaceuticals”
- Advisors: Dr. W. A. M. Daundasekera & Mr. Asanga Ramyajith
- GPA 3.30 out of 4.00 (Second Class Upper Division)

CONFERENCE AND SYMPOSIUM PRESENTATIONS

Rathnayaka, R. M. C.; Gross, D. E. “Synthesis and spectroscopic studies of benzoxazaboroles” Poster presented at The 73rd Southwest Regional Meeting of the ACS, Lubbock, October 29-November 01, 2017.

Rathnayaka, R. M. C.; George, S.; Gross, D. E. “Synthesis and stability analysis of alkylbenzoxazaboroles” Poster presented at The 120th annual meeting of Texas Academy of Science Meeting, University of Mary Hardin-Baylor, March 04, 2017.

Rathnayaka, R. M. C.; Kottegoda, N; Perera, A. D. L. C. “Desalination Ability of Murunkan Clay” Oral presentation, International Symposium on CHALLENGES AHEAD Water Quality and Human Health, Postgraduate Institute of Science (PGIS) University of Peradeniya - Sri Lanka, June 27 & 28, 2014.

TEACHING AND MENTORING

Graduate Teaching Assistant

09/2016 - Present

Department of Chemistry, Sam Houston State University

Responsibilities: Graded exams, quizzes, and homework problem sets; supervised students in the laboratory and graded lab reports. (12 sections, 16 students each)

2016 (fall)	Organic chemistry I, laboratory	Dr. D. E. Gross
2017 (spring)	Organic chemistry II, laboratory	Dr. B. E. Arney
2017 (fall)	Organic chemistry I, laboratory	Dr. B. E. Arney
2018 (spring)	General chemistry II, laboratory	Dr. A. Villalta C.

Temporary Demonstrator in Chemistry

09/2013 – 02/2016

Department of Chemistry, University of Peradeniya, Sri Lanka

Responsibilities: Prepared chemicals for labs; graded exams and homework problem sets; supervised students in the laboratory and graded lab reports; carried out demonstrations for high school students at Science Education Resource Center.

2013	Physical chemistry laboratory	Prof. A. D. L. C. Perera
2013	General chemistry laboratory	Dr. R. J. K. U. Ranatunga
2014	Industrial chemistry laboratory	Dr. A. C. A. Jayasundara
2015	Industrial chemistry laboratory	Dr. A. C. A. Jayasundara
2016	Environmental chemistry laboratory	Dr. A. C. A. Jayasundara

AWARDS AND MEMBERSHIPS

- College of Science and Engineering Technology Special Graduate Scholarship – Spring 2018, Sam Houston State University, TX, USA
- College of Science and Engineering Technology Special Graduate Scholarship – Fall 2017, Sam Houston State University, TX, USA
- Graduate Studies Scholarship – Fall 2017, Sam Houston State University, TX, USA
- Research Scholarship – Part of a grant awarded to D.E. Gross, Summer 2017, Sam Houston State University, TX, USA
- Member of Texas Academy of Science

SKILLS AND COMPETENCIES

- Lab techniques and instrumentation – Organic synthesis and characterization, Varian NMR, UV-vis and fluorescence spectroscopy, gel permeation chromatography, infrared spectroscopy, atomic absorption spectroscopy.
- Chemical laboratory safety

- Software: Microsoft Office, ChemDraw, Scifinder, MestreNova, Mendeley, DELTA